Synthesis of Novel Cyclopentadienyl Cobalt(I)-Complexes and their Application in [2+2+2] Cycloaddition Reactions

Dissertation
to obtain the academic degree
„Doktor der Naturwissenschaften“ (Dr. rer. nat.)
submitted at the
Mathematisch-Naturwissenschaftlichen Fakultät
an der Universität Rostock

submitted by
MSc. Indre Thiel
born on November 27th 1987 in Düsseldorf

Rostock, September 13th 2013

urn:nbn:de:gbv:28-diss2014-0044-1

The work of this thesis was conducted between January 2011 and October 2013 under the supervision of Dr. Marko Hapke and Professor Dr. Uwe Rosenthal at the Leibniz-Institut für Katalyse an der Universität Rostock.

Referees:

1st Referee: Professor Dr. Uwe Rosenthal, Leibniz-Institut für Katalyse e.V. and der Universität Rostock

2nd Referee: Professor Dr. Matthias Tamm, Technische Universität Braunschweig

Thesis Submission: September 13th 2013

PhD Defense: December 3rd 2013

Acknowledgement

Writing a dissertation takes all kinds of support. Therefore I would like to express my sincere gratitude to all those who made it possible and generously gave their time and expertise.

First and foremost I am deeply indebted to my supervisor **Dr. Marko Hapke** for making me part of his group and providing me with this interesting research project but also giving me the space to pursue my own ideas. His endless believe in me made it possible to push through all the rough stretches that are part of research.

My sincere appreciation for many helpful and complaisant discussions and continuous guidance goes to **Professor Dr. Uwe Rosenthal**.

A huge "Thank you" goes to my **group members** and **former group members** Fabian Fischer, Phillip Jungk, Dr. Karolin Kral and Dr. Nico Weding. I could not have wished for a better group to share all my experimental successes as well as failures with. Working with you guys never seemed quite as much work than rather great times spend with friends! I will miss you!

For creating a warm and welcoming working atmosphere I want to thank the entire **Rosenthal group:** Kai Altenburger, Dr. Perdita Arndt, Lisanne Becker, Dr. Torsten Beweries, Laura Dura, Christian Godemann, Marc Gongoll, Martin Hähnel, Dr. Sven Hansen, Dr. Katharina Kaleta, Dr. Marcus Klahn, Dr. Monty Kessler, Dr. Bernd H. Müller, Dr. Normen Peulecke, Kathleen Schubert, Johannes Thomas and Ute von Zweydorf.

Special thanks are directed towards **Dr. Guido Walther**, not only because his help with the *in situ* NMR spectroscopy was essential but also for inspiring as well as diverting conversations.

Without the **Analytical Department** this dissertation would not have been possible. Therefore I want to thank PD Dr. Wolfgang Baumann for all the extraordinary NMR measurements. Susann Buchholz, Kathrin Fiedler, Sigrun Rossmeisl, Susanne Schareina and Dr. Christine Fischer I owe thanks for all the chiral HPLC and mass spectroscopic analyses. I am indebted to Dr. Anke Spannenberg, who was able to determine all X-ray structures even if challenged with infinitely tiny crystals. And last but not least I am grateful to Astrid Lehmann

and Anja Simmula for all elemental analyses. I would also like to recognize the help and interest extended to me along the way by all those that have not been mentioned explicitly.

Finally I do owe more gratitude than I can express to both my **parents**, who supported me throughout everything and continuously encouraged me to pursue my own path and ideas. Thank you for always being there for me!

All my **friends** I have to acknowledge for the good times and great memories outside the institute!

And last but not least I am grateful to the **Fonds der Chemischen Industrie** for all the financial support throughout my dissertation in the form of a Kekulé scholarship.

Aspects of this thesis have already been published:

1. I. Thiel, H. Jiao, A. Spannenberg, M. Hapke, *Chem. Eur. J.* **2013**, *19*, 2548-2554.
2. I. Thiel, M. Hapke, *Angew. Chem.* **2013**, *125*, 6030-6032; *Angew. Chem. Int. Ed.* **2013**, *52*, 5916–5918.
3. I. Thiel, M. Lamác, H. Jiao, A. Spannenberg, M. Hapke, *Organometallics* **2013**, *32,* 11, 3415–3418.
4. I. Thiel, A. Spannenberg, M. Hapke, *ChemCatChem* **2013**, *5*, 2865–2868.
5. I. Thiel, M. Hapke, *J. Mol. Catal. A: Chem* **2014**, DOI:10.1016/j.molcata.2013.12.002.

Presentations at national and international conferences:

Oral Presentations:

1. I. Thiel, *CO_2 – Vom Schornstein in den Kolben*, 3. Mainzer Wissenschaftsgespräche, Mainz, Germany, September 30th - October 1st 2011 (invited speaker)
2. I. Thiel, M. Hapke, *Activity versus Stability – A Compromise*, 15th Nordic Symposium on Catalysis, Mariehamn, Åland, Finland, June 10th - 12th 2012, O52
3. I. Thiel, M. Hapke, *Two Sides of the (Cobalt-) Medal: Activity vs. Stability*, CaSus Workshop, Rostock, Germany, September 16th - 18th 2013, T15
4. I. Thiel, M. Hapke, *Two Sides of the (Cobalt-) Medal*, YoungChem 2013, Poznan, Poland, October 9th - 13th 2013

Poster Presentations:

1. I. Thiel, N. Weding, M. Hapke, *Neue Übergangsmetallkomplexe in der Katalyse von [2+2+2]-Cycloadditionsreaktionen*, HTI (7. Tagung Hochschule trifft Industrie – Ein Dialog), Schlangenbad, Germany, September 14th - 16th 2011, P2 (invitation)
2. I. Thiel, M. Hapke, *New Transition Metal Complexes for [2+2+2] Cycloaddition Reactions*, 15th JCF Frühjahrssymposium, Rostock, Germany, March 18th - 21th 2012, P185

3. I. Thiel, M. Hapke, *Ligand Influence on the Stability and Activity of Novel Cobalt Complexes for [2+2+2] Cycloaddition Reactions*, International Conference Catalysis in Organic Synthesis, Moscow, Russia, September 15th - 20th 2012, P255

4. I. Thiel, M. Hapke, *Ligand Influence on the Stability and Activity of Novel Cobalt Complexes for [2+2+2] Cycloaddition Reactions*, Frontiers of Organometallic Chemistry (Post-Conference Symposium), St. Petersburg, Russia, September 21st - 22nd 2012, P83

5. I. Thiel, M. Hapke, *Ligand Influence on the Stability and Activity of Novel Cobalt Complexes for [2+2+2] Cycloaddition Reactions*, ORCHEM, Weimar, Germany, September 24th - 26th 2012, P9

"The most exciting phrase to hear in science,

the one that heralds the most discoveries

is not 'Eureka!' but 'That's funny...'."

Isaac Asimov (1920-1992)

Table of Contents

Abbreviations

BINAP	2,2'-bis(diphenylphosphino)-1,1'-binaphthyl	min	minute
		mL	milliliter
bs	broad singlet	mmol	millimol
calc.	calculated	mp	melting point
CI	chemical ionization	MS	mass spectroscopy
cod	1,5-cyclooctadiene	MW	microwave
coe	*cis*-cyclooctene	m/z	mass/charge
Cp	cyclopentadienyl	NHC	*N*-heterocyclic carbene
Cp*	pentamethylcyclopentadienyl	NMR	nuclear magnetic resonance
δ	chemical shift		
d	doublet	Ph	phenyl
dd	doublet of doublets	PHOX	2-[2-(diphenylphosphino)phenyl]-4-isopropyl-2-oxazoline
DFT	density functional theory		
DMF	dimethylformamid		
DMSO	dimethylsulfoxide	*N*-PINAP	4-[2-(diphenylphosphino)-1-naphthalenyl]-N-(1-phenylethyl)-1-phthalazinamine
equiv.	equivalent		
Et	ethyl		
g	gram		
GC	gas chromatography	*O*-PINAP	1-[2-(diphenylphosphino)-1-naphthalenyl]-4-(1-phenylethoxy)-phthalazine
EA	elemental analysis		
ee	enantiomeric excess		
EI	electron ionization		
ESI	electrospray ionization	*o*- / *m*- / *p*-	ortho / meta / para
h	hour	q	quartet
HRMS	high resolution mass spectroscopy	quin	quintet
		QUINAP	1-(2-diphenylphosphino-1-naphthyl)isoquinoline
Hz	hertz		
i-Pr	*iso*-propyl	s	singlet
J	coupling constant	sep	septet
m	multiplet	t / *t*	triplet / *tert*-
Me	methyl	THF	tetrahydrofuran
mg	milligram	UV-VIS	ultraviolet / visible light

1. INTRODUCTION

The term “catalysis” – derived from the greek “katalusis” or rather “kataluein”, meaning the ability to dissolve [1] – has been first introduced by Berzelius in 1836. He recognized the broad phenomenon of catalysis – homo- and heterogeneous – in the ever-growing amount of published experimental data and wrote:

“It is, then, proved that several simple or compound bodies, soluble and insoluble, have the property of exercising on other bodies an action very different from chemical affinity. By means of this action they produce, in these bodies, decomposition of their elements and different recombinations of these same elements to which they remain indifferent.” [2]

The basic chemical definition of a catalyst was therefore coined as a substance, which is capable to speed up chemical reactions by its mere presence without undergoing chemical changes itself, when over half a century later, Ostwald combined catalysis with chemical thermodynamics and kinetics in one principle.

Catalysis has played a central role in the chemical industry from its beginning in the late eighteenth century. While homogeneous catalysts have been used by civilization for thousands of years for processes such as fermentation without any deeper knowledge of the exact molecular aspects, the majority of chemists were applying heterogeneous catalysts for instance various hot metal wires trying to develop novel processes. The most prominent example here would be the Haber-Bosch synthesis of ammonia. [3]

Nowadays, most industrial processes are catalyst-assisted such as the purification of gasoline and the synthesis of pharmaceuticals, natural substances or polymers. Catalysis is publicly often associated with environmental science and green chemistry due to catalytic converters in cars regarding emission control of exhaust fumes or emission filters of industrial plants. Because of the ever-growing importance of catalysis for the chemical industry to generate complex molecules in a simple, atom-economic manner, academic research has been focusing increasingly on the study of fundamental mechanisms involved in catalytic processes at an atomic level. These studies have become possible since analytical techniques have largely improved and become more sensitive towards short-lived species. [4] The field of catalysis has been steadily growing, offering new ideas and concepts for the development of novel catalytic systems concerning basic laboratory scale reactions as well as up-scaled industrial processes.

1.1 Benzene and Pyridine as Motives in Natural Substances – Synthetic Approaches

Natural substances have inspired various chemists to imitate or slightly modify nature's prototypes to develop novel pharmaceuticals such as antitumor agents but also to produce dietary supplements in larger quantaties than could ever be extracted from plants. Many of these natural substances contain (modified) benzene or pyridine moieties as their core structure. [5] However, the de novo biosynthesis of pyridine derivatives such as nicotinic acid (vitamin B3) or vitamin B6 still remains unclear in spite of their simple structure. Several pathways for the synthesis of nicotinic acid are discussed, for example the transformation of tryptophan via the intermediates kynurenine, 3-hydroxyanthranilic acid and quinolinic acid in chicks, mammals and certain bacteria or the conversion of glyceraldehyde-3-phosphate and aspartate in *Escherischia coli*. [6] In case of vitamin B6 it is believed that there are at least two different biosynthetic pathways in microorganisms. Several intermediates were identified like glycolaldehyde, but the entire biosynthesis is still not fully understood. [7]

In order to obtain easy access to these molecules chemists have derived several ways to generate (annulated) benzene or pyridine rings synthetically. Pyridine in its unsubstituted form is industrially produced by the Chichibabin process from acrolein (formed by a Knoevenagel condensation from acetaldehyde and formaldehyde), acetaldehyde and ammonia. [8] Over 100 years ago Hantzsch reported on the synthesis of dihydropyridines, which can be easily oxidized to substituted pyridines. [9] The Bohlmann-Rahtz pyridine synthesis is another alternative to yield substituted pyridine derivatives. It consists of a two-step process involving an initial Michael addition of, for example, ethyl β-aminocrotonate and an ethynyl carbonyl compound. The aminodienone intermediate can be isolated and transformed through cyclodehydration at elevated temperatures to the respective pyridine. [10]

Nowadays a larger focus on the reduction of accumulating waste, milder reaction conditions and especially atom-economy dominates the design of new reactions. The concept of tandem ring-closing olefin metathesis and dehydration is a very effective way to synthesize substituted benzenes. 1,4,7-Trien-3-ols can easily be modified to carry various substituents and yield the substituted benzene derivatives after the ruthenium-catalyzed ring-closing metathesis – applying Grubbs' first generation catalysts – followed by dehydration. [11]

Recent approaches in the synthesis of pyridines involve the application of oximes and enals in a synergistic copper/iminium catalysis [12] or the use of alkenes and α,β-unsaturated oxime

esters in a Rh(III)-catalyzed stereoselective reaction. [13] Yet a further option, valued due to its straightforward concept, easy availability of starting materials and synthetic flexibility, is the [2+2+2] cycloaddition reaction. It represents a possibility to generate pyridines as well as benzenes in a fast and atom-economic manner starting from alkynes and/or alkenes. Several of the total syntheses of natural substances involve cycloaddition reactions as one of the elementary steps to generate the backbone of the molecule (Scheme 1). Protoberberin alkaloide as well as the antitumor active anthracyclinaglycone were synthesized via a cyclization reaction of a 1,7-octadiyne moiety and another alkyne catalyzed by [$CpCo(CO)_2$] (**1**). [14] The (±)-strychnine synthesis for example involves the usage of **1** in an elementary synthetic step as well. [15]

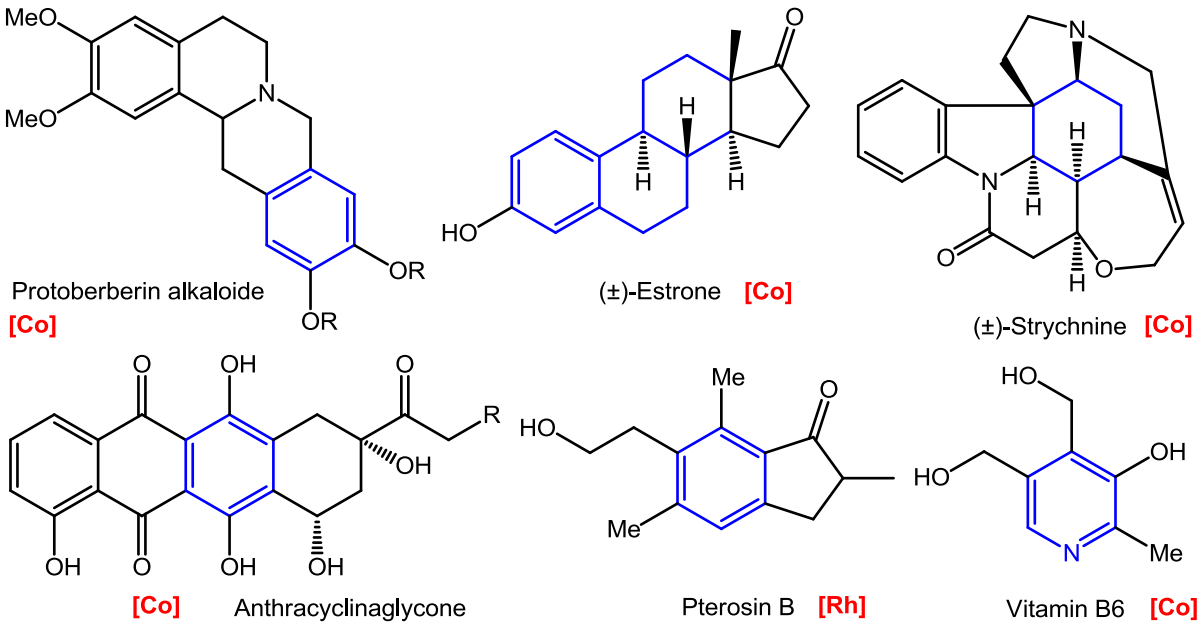

Scheme 1: Examples for [2+2+2] cycloaddition reactions as a key step for the synthesis of natural substances

Also the synthesis of (±)-estrone, explicitly the generation of the ABC-ring system in one step, was done by a simple [2+2+2] cycloaddition reaction catalyzed by **1**. [16] The formation of the benzene moiety of illudalane sesquiterpenoids like pterosin, calomelanolactone or alcyopterosin E was achieved by a cyclotrimerization reaction catalyzed by the Wilkinson catalyst [$RhCl(PPh_3)_3$] (**2**). [17] At slightly elevated temperatures this catalyst could also yield the core structure of the furanosteroidal antibiotic Viridin. [18] Last but not least precursors for the Vitamin B6 synthesis could easily be generated via a [2+2+2] cycloaddition reaction catalyzed by [CpCo(cod)] (**3**). [19]

1.2 [2+2+2] Cycloaddition

As demonstrated before the [2+2+2] cycloaddition reaction is a versatile tool to derive a huge number of different cyclic substances from simple molecules in an atom-efficient manner. Even though the thermal [2+2+2] cycloaddition is symmetry-allowed [20] only very few examples are known, which are often highly exothermic. [a,21] This sparsity might be attributed to entropic factors but especially to high activation barriers for the reaction. [22] Nevertheless, the vast majority of [2+2+2] cycloadditions are transition metal-catalyzed. [23] Many transition metals such as Ni, [24] Fe, [25] Co, [14, 26] Rh, [27] Ir, [28] Pd, [29] Ru [30] but also Nb [31] or combinations thereof like Ti-Mg [32] and Zr-Ni [33] are able to catalyze the cyclotrimerization of alkynes. However, group 9 transition metals – Co, Rh and Ir – represent the most important class of catalysts. [23e, 26a, 26b, 34]

Berthelot was the first to report the development of benzene from acetylene at high temperatures in 1866, [35] followed by Sir Ramsay, who described the formation of pyridine, when gaseous acetylene and hydrogen cyanide were led through a hot iron tube, in 1876. [36] But the first real transition metal-catalyzed cycloaddition reaction with a defined nickel catalyst was described by Reppe et al. He was able to vary the outcome of the cycloaddition reaction (with the major product being either cyclooctatetraene or benzene) by choosing different catalyst systems. [37]

Depending on the metal of the catalyst (Co, Rh, Ru, Ni and Fe) the reaction mechanism differs slightly. [25b, 38] Because merely Co- and Rh-complexes will be discussed in this thesis, only the Co(I)-catalyzed [2+2+2] cycloaddition reaction will be considered in more depth.

1.2.1 Mechanism

The broadly accepted mechanism for the Co(I)-catalyzed [2+2+2] cycloaddition reaction and the formation of pyridines is depicted in Scheme 2. The pre-catalyst has to be activated either by heat or irradiation with light to offer the alkyne substrates free coordination sites at the metal center. Two alkynes are coordinated side-on and through an oxidative coupling reaction the corresponding metallacyclopentadiene is formed. Coordination of the nitrile and either an insertion reaction or a formal [4+2] cycloaddition lead after reductive elimination to the pyridine derivative and the free metal core, which can re-enter the catalytic cycle anew. [39]

[a] The respective values can be calculated with the help of *Benson's* tables.

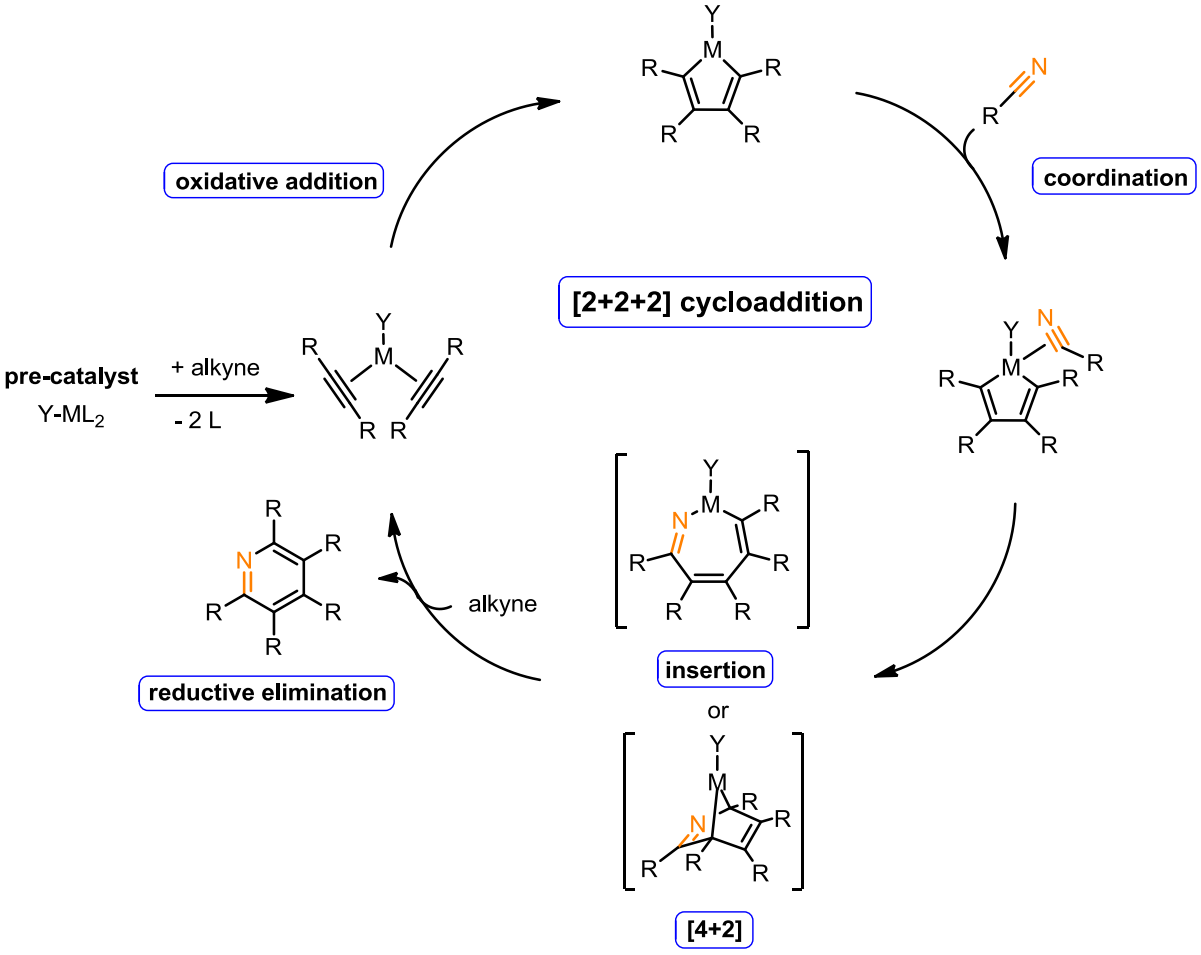

Scheme 2: Mechanism of the transition metal-catalyzed [2+2+2] cycloaddition (Y: steering ligand; M: metal; L: neutral ligand)

While the metallacyclopentadiene intermediate (sometimes with an additional neutral ligand such as PPh_3 or PMe_3 still coordinated to the metal center) has been isolated several times, [39c, 40] the second intermediate could not be isolated yet (at least in the case of Co), but extensive theoretical calculations have been done on determining which intermediate is the most likely.

1.2.2 DFT Calculations

The [2+2+2] cycloaddition mechanism for the CpCo(I)-fragments has been confirmed by several DFT calculations even though there are several slightly different proposed mechanisms.

The first difference concerns the coordination of one of the neutral ligands during the catalytic cycle. While one mechanism proposes that one ligand (exemplarily PPh_3) stays coordinated, leading to $18e^-$ species throughout all intermediates, [41] other plausible pathways involve the reaction of the $16e^-$ complex [$CpCo(\eta^2$-$HC{\equiv}CH)$] with another acetylene molecule forming the metallacyclopentadiene intermediate. [42] Wakatsuki et al. also discussed the retardation of the pyridine formation if a triphenylphosphine ligand is still present at the metal core. [43]

Regarding the coordination of the nitrile to the metal center, Koga et al. proved that if the nitrile coordinates to the metal center via the N atom – first end-on, then side-on – the reaction between the nitrile and the metallacyclopentadiene can be viewed as an intramolecular coupling and is a more favorable mechanism than an intermolecular [4+2] coupling between the metallacyclopentadiene and an uncoordinated nitrile. [39b]

Whether the formation of the pyridine proceeds via a [4+2] cycloaddition mechanism or an insertion mechanism is not well enough established yet. Various reaction pathways for the formation of 2-methylpyridine from acetylene and acetonitrile have been studied by Koga et al. They investigated the intra- and intermolecular [4+2] cycloaddition pathway as well as the one via the azacobaltacycloheptatriene for the singlet and triplet state of the complex. Their calculations showed that the most favorable process for a singlet state undergoes the [4+2] cycloaddition between the metallacyclopentadiene and the nitrile, while the one for the triplet state involves an azacobaltacycloheptatriene intermediate. [39b] But even slight changes in the electronic properties of the nitrile lead to different preferences, so that it could be tentatively summarized that electron-donating groups favor the [4+2] cycloaddition while electron-withdrawing groups favor the insertion of the C-N triple bond into the Co-C_α bond. [39a]

Harris et al. concluded – based on an ultra-fast IR study of the photochemistry of [$CpCo(CO)_2$] (**1**) in neat 1-hexyne or 1-hexene solutions – that in the case of **1**, the first ligand substitution takes place in the triplet state and undergoes a spin cross-over to the singlet state. Therefore both the singlet and triplet state play a role in the generation of the initially formed alkyne/alkene-coordinating species. [44]

After the formation of the metallacyclopentadiene a spontaneous relaxation into the triple ground state occurs. This species can be trapped – especially if σ-donors like phosphines, CO or THF are used – and the $18e^-$ compound (as previously discussed [41]) is generated. [45]

Danzinger et al. discussed the coordination sequence of the substrate molecules, whether two alkynes or one alkyne and a nitrile coordinate first. They investigated the synthesis of pyridine from acetylene and hydrogen cyanide exemplarily (Scheme 3). [38a]

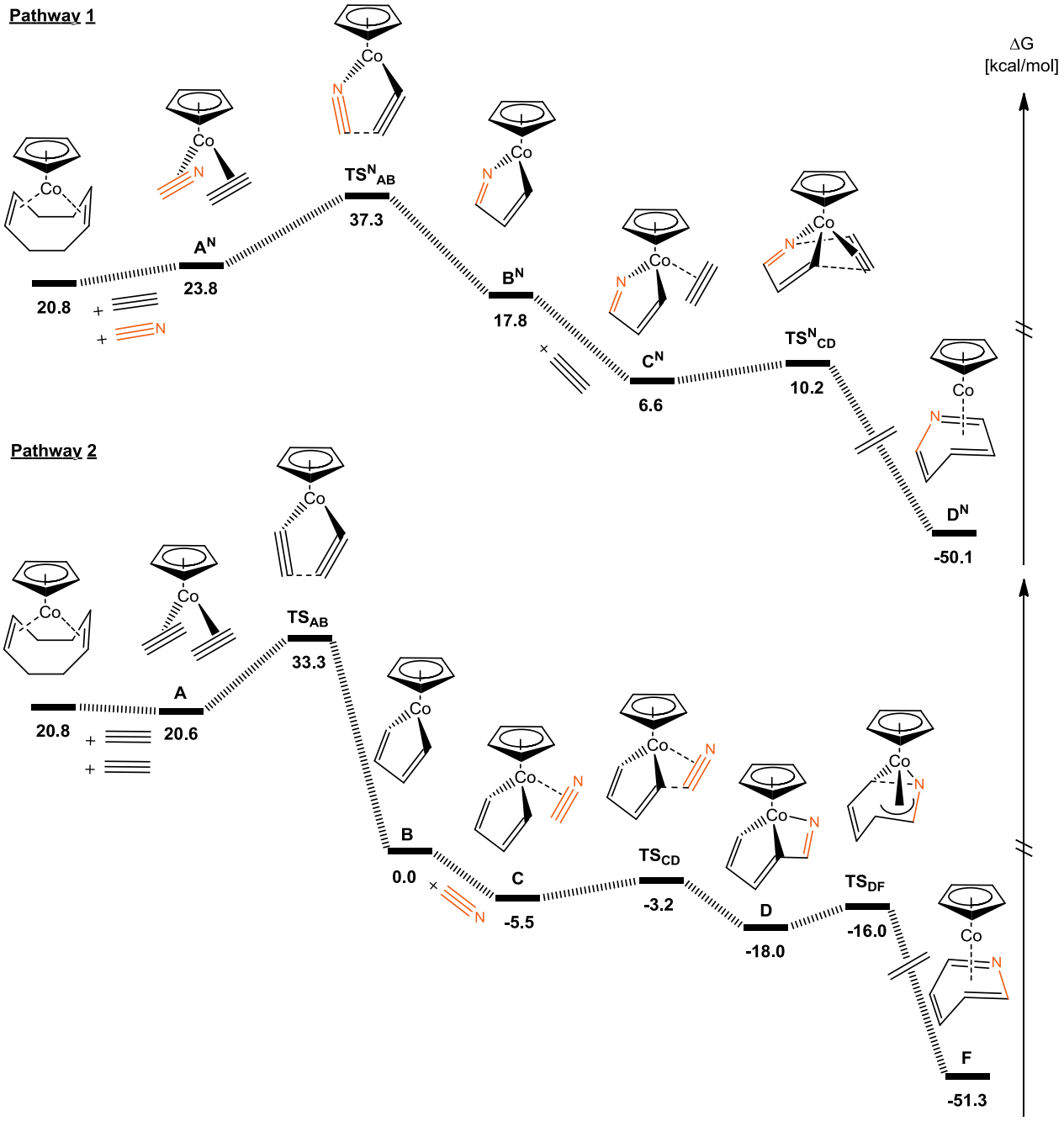

Scheme 3: Free energy profiles (in kcal mol^{-1}) for the different coordination sequences in the [2+2+2] cycloaddition reaction between acetylene and hydrogen cyanide

The replacement of the neutral ligands (here 1,5-cyclooctadiene) and the coordination of the two alkyne molecules to form **A** is essentially thermoneutral (even though activation energy is needed for many pre-catalysts), while the coordination of hydrogen cyanide and acetylene requires additional energy ($\mathbf{A}^{\mathbf{N}}$).

The oxidative coupling and formation of the metallacyclopentadiene and azametallacycle (**B** and $\mathbf{B^N}$) respectively is in both cases exergonic, but considering the small energetic difference between $\mathbf{A^N}$ and $\mathbf{B^N}$ this step of pathway 1 is essentially overall thermoneutral. Upon formation of the azametallacycle the coordination of the second acetylene molecule to yield $\mathbf{C^N}$ is more exergonic than the coordination of the hydrogen cyanide to **B**. The transition of $\mathbf{C^N}$ to $\mathbf{D^N}$ is highly exergonic. The same applies for the generation of the azacobaltacycloheptatriene **D** and subsequently **F**, which is the equivalent of $\mathbf{D^N}$. [38a]

1.2.3 Effect of the Ligands

In catalyst systems of the type $[YM(L)_2]$ all three variables – the steering ligand Y, the metal center M and the neutral ligands L – do have an effect on the reactivity of the respective complex. Focusing on the group 9 transition metals, our group has already demonstrated the effect of the metal center on the reactivity as well as selectivity of the catalyst. [34a, 46] We synthesized complexes of Co, Rh and Ir with an identical organic ligand sphere observing that the stability of the complexes $[CpM(H_2C{=}CHSiMe_3)_2]$ increased in the order M = Co < Rh < Ir while the reactivity towards the synthesis of pyridines follows the inverse order. If triynes were submitted to comparable conditions of the cycloaddition reaction as reported for the pyridine synthesis it was noticed that the Rh(I)-complex was the most active one.

The effect of the steering ligand has been studied by Bönnemann et al. and Jonas et al. respectively. Already in the early 1980's correlations between the neutral ligands [47] or substituents on the Cp-ring of the Co(I)-complexes [48] with the ^{13}C and ^{59}Co NMR shifts were reported. The ^{59}Co chemical shift can be correlated to the reaction temperature or activity of the Co(I)-complexes, essentially featuring a higher field shift of the ^{59}Co resonance the less active the complex. A dependency of the nature of a substituent attached to the Cp-ligand on the regioselectivity of $Cp^RCo(I)$-complexes can also be correlated to the ^{59}Co shift. Here electron-donating substituents lead to higher regioselectivity, but lower activity, hence show a more high field-shifted signal in the ^{59}Co NMR spectrum. [48] A similar observation can be made with regard to the neutral ligands. If one assumes that the ^{59}Co shift correlates to the energy gap between the frontier orbitals of the respective CpCo(I)-complex, which corresponds to the strength of metal-ligand interaction, the ^{59}Co shift could well function as an indicator for the complex's properties such as thermal stability or catalytic activity. [47]

One further example is the report of Heller et al., who noticed an effect of the steering ligand in the photocatalytic cyclotrimerization reaction between acetylene and a substituted nitrile. An acetyl-substituted cyclopentadienyl ligand led to a faster conversion than a "naked" Cp-ligand, while the indenyl-ligand proved to have the slowest conversion rate. [49] This is in accordance with the reports by Bönnemann et al. [48]

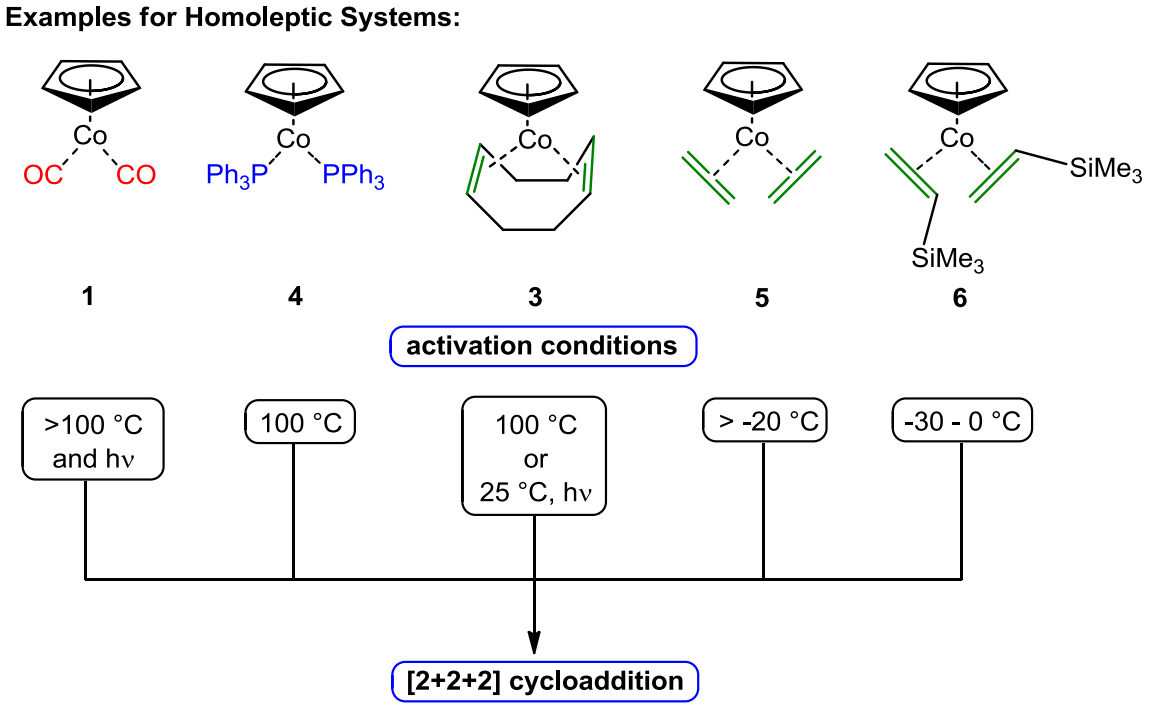

Scheme 4: Reaction conditions for several homoleptic CpCo(I)-complexes

Although the neutral ligands are thought to be immediately lost during the catalytic cycle they have a great effect on the stability of the pre-catalyst. Depending on the properties of the neutral ligands the activation barrier for their release and coordination of the substrate molecules can vary dramatically. Ligands such as triphenylphosphine, CO or the chelating olefin 1,5-cyclooctadiene (cod) coordinate very strongly to the cobalt center and therefore high activation energies (> 100 °C) are required to generate the active pre-catalyst (Scheme 4). Using the aid of irradiation Heller et al. reported on the reaction of benzonitrile and acetylene at various temperatures (-40 - 60 °C) with [CpCo(cod)] (**3**) yielding 2-phenylpyridine in high yields. [49]

Complexes with non-chelating olefin ligands like the Jonas reagent **5** [50] or complex **6** from our group are less stable and need lower activation energy to act as catalysts in the [2+2+2] cycloaddition reaction. This has been demonstrated by our group who calculated the relative

energy values for the CpCo(I)-system upon the ligand substitution reaction of **6** with several chelating and non-chelating olefin ligands (Scheme 5). [51]

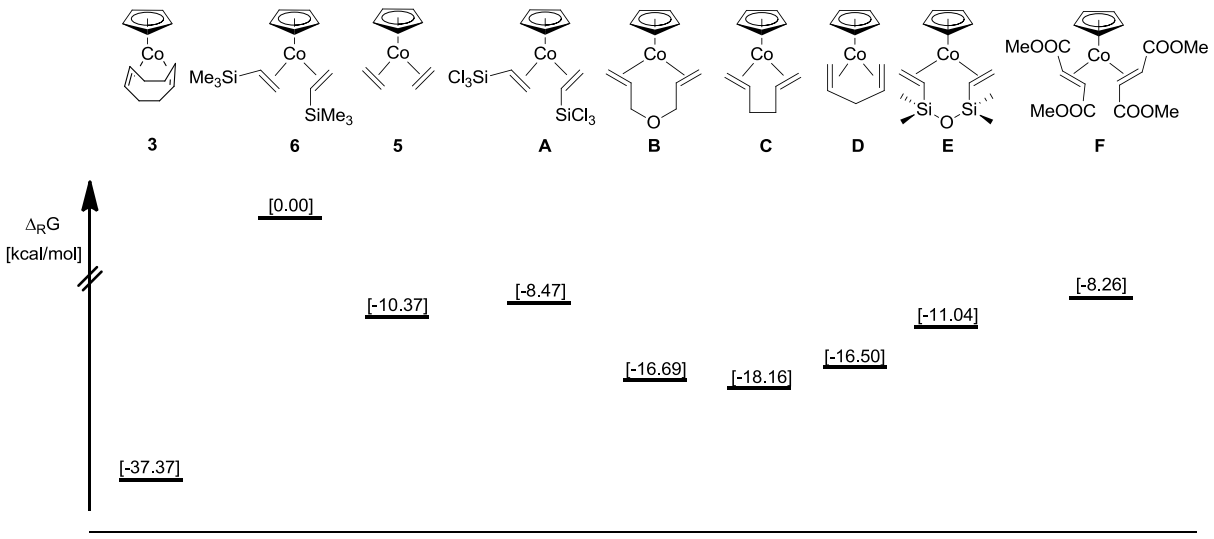

Scheme 5: Relative energies for various CpCo(I)-complexes with chelating and non-chelating olefin ligands [51]

The calculations corroborated the expected results that chelating olefins are always more stable than complexes with two single olefin ligands (Scheme 5, compare **B**-**E** and **3** with **6**, **5**, **A** and **F**). Depending on the type and, for example, electronic properties of the olefin ligand, the calculated relative energies vary, confirming that electron-deficient olefins do not stabilize the CpCo(I)-fragment as sufficient as electron-rich olefins and therefore lead to more labile complexes.

Cobalt complexes with two different ligands – no matter if both ligands are from the same ligand class or entirely different classes – have been explored as well. Numerous examples showed that these heteroleptic compounds exhibit different stabilities from their respective homoleptic analogs.

The substitution of one olefin ligand for a CO or a Cp-tethered phosphine ligand has a great stabilizing effect on the complex. While the Jonas complex (**5**) and **6** are active at low temperatures and **F** is also supposed to be as active as the Jonas complex (Scheme 5), the heteroleptic complex **7** requires reaction temperatures as high as 110 °C or irradiation with light. [52] Likewise, **8** needs temperatures higher than 25 °C and **9** – containing a Cp*-tethered olefin ligand – even turns out to be completely inactive towards [2+2+2] cycloaddition reactions (Scheme 6). [53] This proves what kind of impact the neutral ligands have on the stability as well as activity of the respective CpCo(I)-complexes.

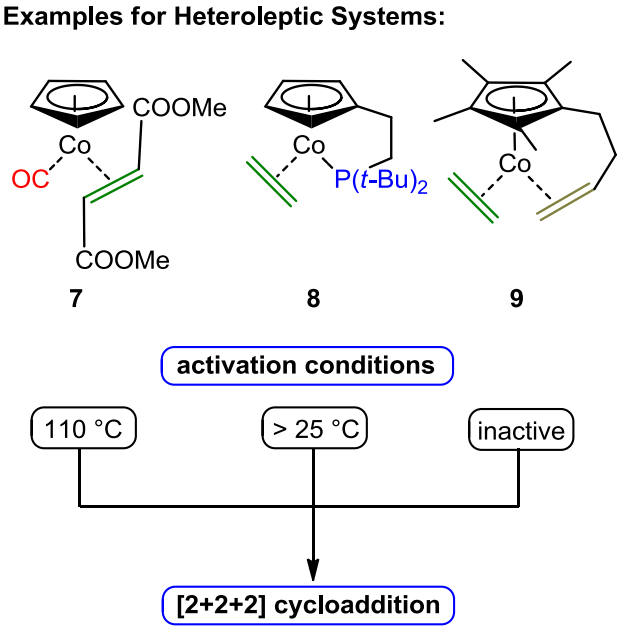

Scheme 6: Reaction conditions for several heteroleptic CpCo(I)-complexes

Only few heteroleptic CpCo(I)-complexes have actually been applied in the [2+2+2] cycloaddition reaction. Most often they have been synthesized out of pure proof of principle and only their reaction towards modifications has been investigated in more detail. Cobalt complexes with a Cp-tethered unsaturated amine ligand and an additional CO or triphenylphosphine ligand have been described by Collum et al., [54] (bicyclo[3.2.0]hepta-1,3-dienyl)cobalt(I)-complexes with one dimethylfumarate ligand and three different phosphine ligands were synthesized by Butenschön et al. [55] and a cobalt complex with a Cp-tethered phosphine and an alkyne ligand, namely tolan, has been reported by the latter as well, [53c] just to name a few examples.

Werner et al. studied the substitution of several CpCo(I)-precursors extensively yielding phosphine-CO, [56] phosphite-phosphine, olefin-phosphine, olefin-phosphite and olefin-CO complexes. [57] They also described the great potential of [CpCo(PMe_3)(CO)] as a precursor to gain access to numerous types of complexes. While ligands such as carbon disulfide or the electron-poor olefin $C_2(CN)_4$ can substitute the CO ligand, phosphites only substitute the phosphine ligand. [58] A similar study was done by Hong et al. who prepared a number of complexes of the type [CpCo(olefin)(L)] with L being triphenylphosphine, CO or an isocyanide by reacting the respective [CpCo$(L)_2$] complex with olefins containing electron-withdrawing groups. [59]

There have also been several reports on heteroleptic CpCo(I)-complexes bearing NHC-ligands (*N*-heterocyclic carbene), which are very strong σ-donors. If **1** is stirred with bis(1,3-dimethyl-imidazolindin-2-ylidene) in methylcyclohexane at 100 °C, one CO ligand is replaced by a NHC-ligand. [60] Further examples for CpCo(I)-complexes with one NHC-ligand and one CO, ethene or PPh_3 ligand have been reported by Markwick and O'Connor et al. as well as Tilset et al. [61]

Investigations towards the kinetics of these ligand substitution reaction of $Cp^*Co(CO)_2$ with various ligands such as *t*-BuNC, phosphines or phosphites were performed by Rerek and Basolo taking in account the basicity and cone angle of the tested ligands. [62]

With regard to the application of these heteroleptic compounds in [2+2+2] cycloaddition reactions a lot of possibilities are still unexplored. The modification of long known complexes and therefore alteration of their characteristics (e.g. stability and activity) should prove a fruitful venture.

1.3 Further Modifications of Cobalt(I)-Complexes

There are several possibilities to further modify cobalt(I)-complexes, of which only two will be discussed here in more detail.

While high substrate conversions are essential for the application of catalysts, easy handling and especially (high) recyclability of any catalyst is equally viewed as an attractive property. For the stabilization of CpCo(I)-complexes the neutral ligands play a large role particularly if heteroleptic complexes are synthesized, which might be the solution to a potential stability problem. The recyclability of CpCo(I)-complexes is a different matter. There are various possibilities to enhance or rather simplify the recycling of a catalyst. Linking the respective complex via a neutral ligand or the Cp-ligand to a solid phase allows the easy separation of reactant solution and catalyst.

Solid phase synthesis has been predominantly used for the sequential synthesis of polypeptides, polynucleotides or even polysaccharides. In the 1970's various insoluble polymers were discovered to solve the problem of necessary but not easily removable additives. Covalently linking these additives to a polymer provided a smooth way to remove these after the organic reaction. [63] In certain cases the polymer can be seen as an organocatalyst, but polymers with an actual metal catalyst covalently bound to them were represented only with loose examples.

In respect to recoverability of the catalyst and minimization of work-up of the reaction the attachment of homogeneous organo- or metal-catalysts to supporting materials has become more favorable over the years. A number of different supporting materials – organic and inorganic – [64] such as nanoparticles, [65] dendrimers, [66] inorganic oxides like silica, [67] sol-gel matrices, [68] polystyrol / Merrifield resin [69] or other resins [70] have been used to covalently bind one of the catalyst's coordinating ligands to the solid support.

However, there have not been many examples for the reuse and recyclability of catalytic systems applied in [2+2+2] cycloaddition reactions. Those that have been reported, follow various strategies. A recent example would be the usage of dendritic phosphoramidite ligands loaded with Rh(I) to enhance the enantioselectivity of [2+2+2] cycloadditions between diynes and alkynes as Pla-Quintana and Caminade et al. describe. They were able to recycle the catalyst at least three times without loss of enantioselectivity. [66b]

Conte and Tagliatesta et al. reported on a ruthenium porphyrin catalyst, which could be easily recycled and frequently applied in cyclooligomerization reactions of arylethynes in ionic liquids. [71] Lin et al. also worked with ionic liquids as solvent using a cyclotrimerization catalyst based on a Pd(II)-complex supported on gold nanoparticles. This compound was easily recycled and quantitatively recovered by a simple filtration. [65] The cyclization of triynes in molten [*n*-Bu_4N]Br using either [$RhCl(PPh_3)_3$] (**2**) or $PdCl_2$ and the precipitation of the product by the addition of water is an alternative method. [72]

Yet another approach was executed by Tsai et al., who developed a cationic rhodium(I)/2,2'-bipyridyl-catalyzed [2+2+2] cycloaddition of α,ω-diynes with alkynes. Since the reaction took place in water a simple extraction with organic solvents was sufficient to remove the reaction products and leave the residual catalyst system ready for the next cycle. [73]

The only supported Co(I)-catalyst tested for its activity in cycloaddition reactions was [$CpCo(CO)_2$] (**1**) covalently bound to divinylbenzene cross-linked polystyrene. To the disappointment of Vollhardt et al. this supported catalyst rapidly deactivated and afforded the cyclization product only in mediocre yields. [74] Therefore a modification of the Cp-ligand with a group that could be used to covalently bind the respective complex to a solid phase and the employment of heteroleptic cobalt(I)-complexes seems to be the simplest as well as most promising path to gain access to more stable as well as reusable complexes.

A totally different but nevertheless important area is the highly selective synthesis of products. The selective [2+2+2] cycloaddition reaction to generate exclusively one

stereoisomer, diastereomer or enantiomer is still a most challenging discipline. If symmetrically substituted alkynes were used, penta-substituted pyridines or hexa-substituted benzenes can be obtained. In the case of terminal alkynes stereoisomers are formed usually in a more or less 1:1 ratio of the 1,3,5- and 1,2,4-trisubstituted products with almost no 1,3,4-trisubstituted product. The observed regioselectivity can be attributed to steric and electronic effects. [75] There have been several reports on regioselective cycloaddition reactions by tuning the properties of the substrates to selectively form a certain regioisomer. [23e, 23f, 76] One special example is the highly regioselective cyclization reaction of a resin-supported diyne and a nitrile catalyzed by [$CpCo(CO)_2$] (**1**) in the microwave. [77]

Shibata et al. have been the first to explore the iridium-catalyzed enantioselective [2+2+2] cycloaddition reaction in more detail. They reported on various intramolecular cyclization reactions such as the synthesis of chiral cyclohexa-1,3-dienes from enediynes, [78] atropisomeric chiral ortho-diarylbenzenes from triynes [79] or axially chiral biaryl systems from tetraynes and hexaynes, [28e, 80] as well as intermolecular cyclization reactions including the construction of axially chiral teraryl compounds from diynes and alkynes. [28c, 28d] They always used a simple Ir(I)-precursor such as $[IrCl(cod)]_2$ and a chiral phosphine ligand, for example MeDUPHOS (1,2-bis(2,5-dimethylphospholano)benzene), achieving good yields and high enantioselectivities. However, most of their systems require high temperatures and consequently certain substrate combinations to assure racemization-stable products.

The Rh(I)-catalyzed enantioselective [2+2+2] cycloaddition reaction has been explored in depth by Tanaka et al. [76] They usually applied a catalytic system containing a Rh(I)-precursor such as $[Rh(cod)_2]BF_4$ or $[Rh(cod)Cl]_2$ and chiral BINAP or Segphos (4,4'-bis-1,3-benzodioxole-5,5'-diylbis(diphenylphosphine)) ligand. With these systems they were able to generate axially chiral phthalides [81] and biaryls [82] in high yields and enantiomeric excess, covering intra- as well as intermolecular [2+2+2] cycloaddition reactions. While the application of tetraynes for the synthesis of axially chiral biaryls, bipyridines and bipyridones resulted in moderate *ee* values and yields (Scheme 7), [83] the enantioselective cycloaddition between diynes and isocyanates yielding 2-pyridones was accomplished in high enantiomeric excess. [84] Recently Tanaka et al. described the enantioselective synthesis of planar-chiral carba-paracyclophanes using $[Rh(cod)_2]BF_4$ and a chiral bisphosphine ligand in good yields. [85] Applying the same catalyst combination Gandon and Aubert et al. reported on the

enantioselective [2+2+2] cycloaddition of diynes and sulfonimines yielding the respective 1,2-dihydropyridines. [86]

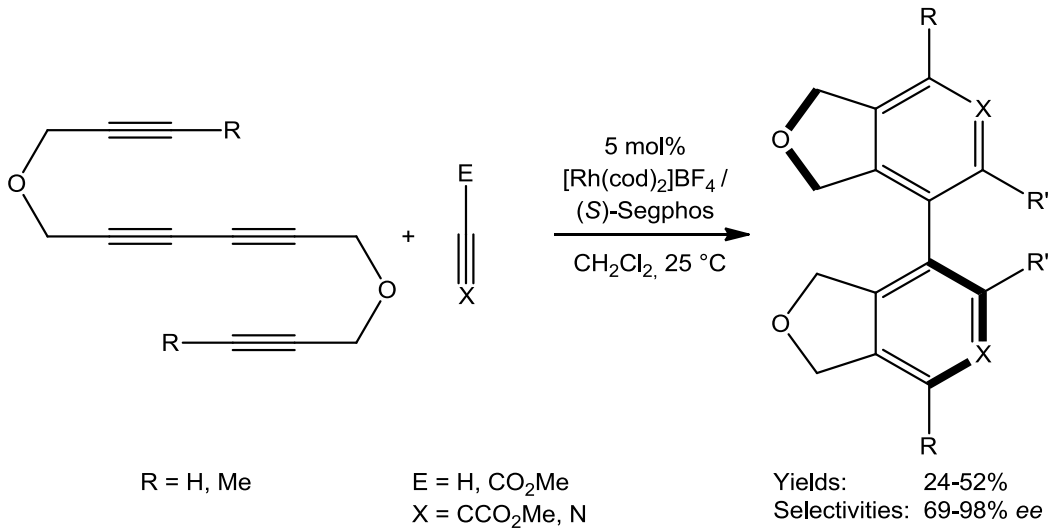

Scheme 7: Synthesis of axially chiral biaryls and bipyridines

Enantioselective cobalt-catalyzed [2+2+2] cycloaddition reactions have been reported by Gutnov and Heller et al. A chiral menthyl-derived indenyl-based Co(I)-complex (**10**) [87] was shown to yield enantiomerically enriched atropisomers of 2-arylpyridines. [88] Later on our group showed that the same complex led to the asymmetric synthesis of axially chiral 1-aryl-5,6,7,8-tetrahydroisoquinolines in good yields with great enantioselectivities (Scheme 8). [89]

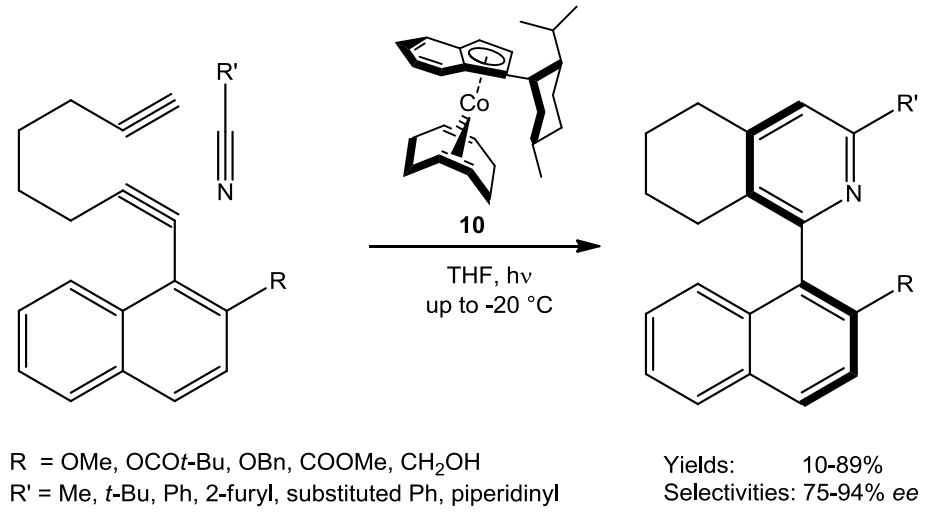

Scheme 8: Application of a chiral Co(I)-catalyst in the synthesis of biaryls

The reaction of chiral proline-based naphthyl diynes with different nitriles via a cobalt-catalyzed [2+2+2] cycloaddition reaction provided diastereomeric atropisomers in good yields and nearly 1:1 ratios under thermal as well as photochemical conditions, which could be seperated by column chromatography. [90]

These chiral Co(I)-based complexes from Heller et al. require light for activation and up to date there is no example of a thermally activated chiral Co(I)-catalyst for [2+2+2] cycloaddition reactions and the synthesis of pyridines. Consequently the synthesis of thermally activatable chiral Co(I)-complexes is another research focus prone to yield promising results.

2. INTENTION OF THIS THESIS

The cobalt-catalyzed [2+2+2] cycloaddition reaction has been known for decades. However, no systematic study of the effects of a methodical variation of the neutral ligands of CpCo(I)-complexes especially in heteroleptic complexes has been done. The investigation of the influence of the neutral ligands on the ability to activate and/or stabilize the respective CpCo(I)-complexes – with a focus on heteroleptic systems – as well as the application of so derived CpCo(I)-catalyst in [2+2+2] cycloadditions is therefore a main goal of this thesis.
Since small variations on the neutral ligands can lead to drastic variations in the stability of the compound as already discussed before, the idea of moving from phosphine ligands towards phosphite ligands seemed to be promising. Phosphites should coordinate less strongly since they are more electron-deficient σ-donors, therefore they should also allow weaker π-backbonding compared to the corresponding phosphine analogues. [91] On the other hand they should bind tighter to the metal than olefins. In addition CpCo(I)-complexes with phosphite ligands have not been reported very often [92] and never systematically tested in the [2+2+2] cycloaddition reaction.

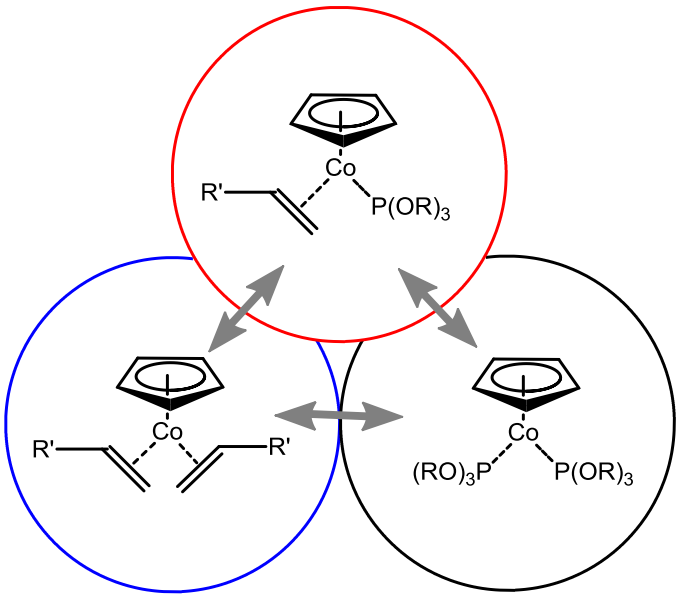

Scheme 9: Systematic neutral ligand variation of CpCo(I)-complexes, focusing on olefin and phosphite ligands

To combine the expertise from previous results with CpCo(I)-olefin complexes the synthesis of the novel class of heteroleptic CpCo(I)-complexes with one olefin and one phosphite ligand is envisioned to be the main target.

Fine-tuning of the neutral ligands or the combination of different ligands might result in a novel catalytic system that exhibits a high catalytic performance by being easily activated, but that is still stable enough to be handled at room temperature and maybe even under not inert conditions.
All synthesized complexes will be applied in [2+2+2] cycloaddition reactions and investigated regarding their substrate scope for the formation of pyridines, benzenes and other aromatic (hetero)cycles.

Based on the results of these investigations, synthetic modifications of the best CpCo(I)-catalysts to gain access to complexes with better recyclability and/or enantioselectivity are a natural enhancement of the once newly developed catalysts as long as they are easily prepared and display a reasonable activity towards the [2+2+2] cycloaddition.

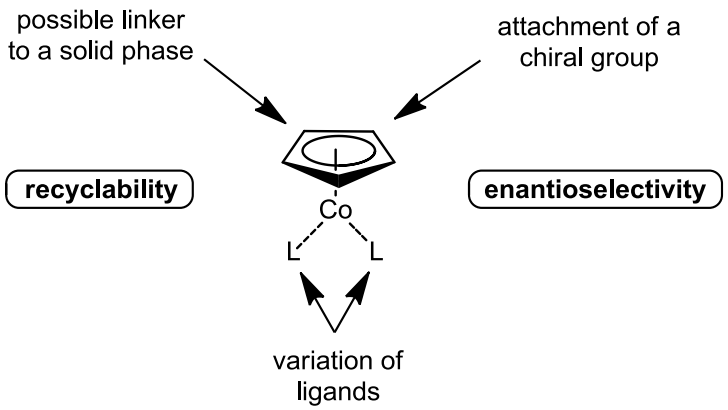

Scheme 10: Possible modifications of CpCo(I)-complexes with regard to recyclability and enantioselectivity

In addition *in situ* generated Co(I)-based systems for enantioselective [2+2+2] cycloaddition reactions analog to those known for rhodium(I) and iridium(I) will be in the focus. Here not only the traditional source of chiral induction – chiral ligands – will be applied but also the influence of chiral anions will be investigated.

3. RESULTS AND DISCUSSION

3.1 Synthesis of Novel CpCo(I)-Complexes for [2+2+2] Cycloaddition Reactions

3.1.1 Synthesis of [CpCo(H_2C=CHSiMe_3)(phosphite)]-Complexes – Variation of Phosphites

As our group previously reported, **6** is a great precursor for the synthesis of a broad variety of different CpCo(I)-bisolefin complexes. [51] Ligand replacement of the trimethylvinylsilane ligands is easily accomplished by simply stirring **6** with an excess of the respective olefin ligands. Therefore a straight forward substitution reaction for **6** with phosphite ligands was anticipated. As Scheme 11 shows, a broad spectrum of monosubstituted mixed [CpCo(H_2C=CHSiMe_3)(phosphite)] complexes (**11**-**16**) were obtained in very good yields if one equivalent of phosphite was added to a solution of **6** in diethyl ether at -78 °C and slowly warmed to room temperature. The obtained mixed olefin-phosphite complexes **11**-**16** are red oils which are stable at room temperature.

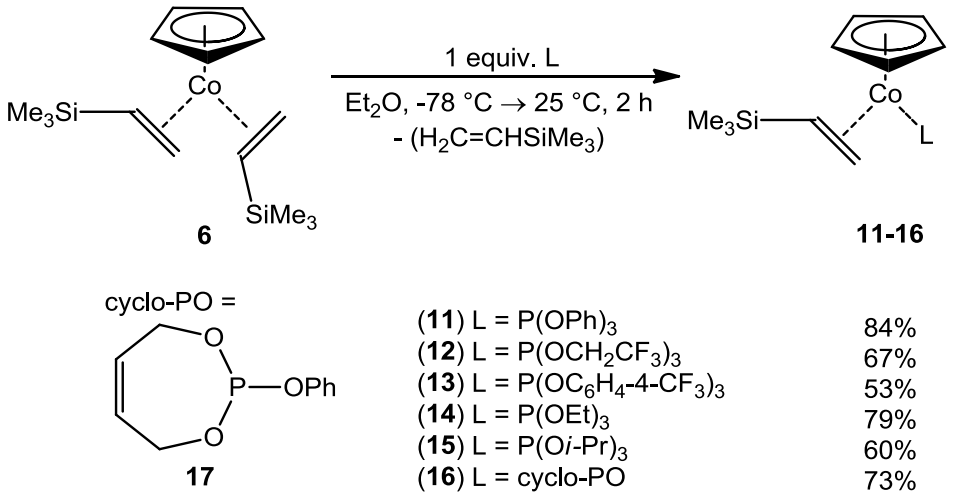

Scheme 11: Synthesis of mixed CpCo(I)-olefin-phosphite complexes

Interestingly no substitution of the second trimethylvinylsilane could be accomplished even when an excess of the respective phosphite ligand was used at elevated temperatures (50 °C). A similar observation was described by Brookhart et al., who were trying to substitute the trimethylvinylsilane ligands of [(Me_5C_5)Co(H_2C=CHSiMe_3)$_2$] with trimethylphosphite. [93] They remarked that a large excess (10-fold) of trimethylphosphite (and higher temperatures)

were necessary to remove the second trimethylvinylsilane ligand of $[(Me_5C_5)Co(H_2C{=}CHSiMe_3)\{P(OMe)_3\}]$ to yield $[(Me_5C_5)Co\{P(OMe)_3\}_2]$. Substitution reactions with N-donor ligands like pyridine and 2,2'-bipyridine were also reported. [94]

3.1.2 Synthesis of $[CpCo(phosphite)_2]$-Complexes

Since the synthesis of $[CpCo\{P(OPh)_3\}_2]$ (**18**) could not be accomplished through a second substitution of the trimethylvinylsilane ligand in **6**, a different route had to be found (Scheme 12). The first synthesis for **18** was published by Werner et al. in 1971. [92b] Refluxing cobaltocene and an excess of triphenylphosphite in toluene for a week led to the desired complex in 46% yield. This procedure was optimized by McKinney by the addition of 2-butyne, which is proposed to react with the Cp-ligands of two different cobaltocenes forming an instable, bridged intermediate, which was postulated to lower the activation barrier and leading to **18** after refluxing the reaction mixture in *n*-hexane for 3-6 h at 70 °C. [75, 92c] But these reaction conditions did not allow the use of a broad variety of phosphite ligands, leading to either decomposed phosphites or no reaction at all.

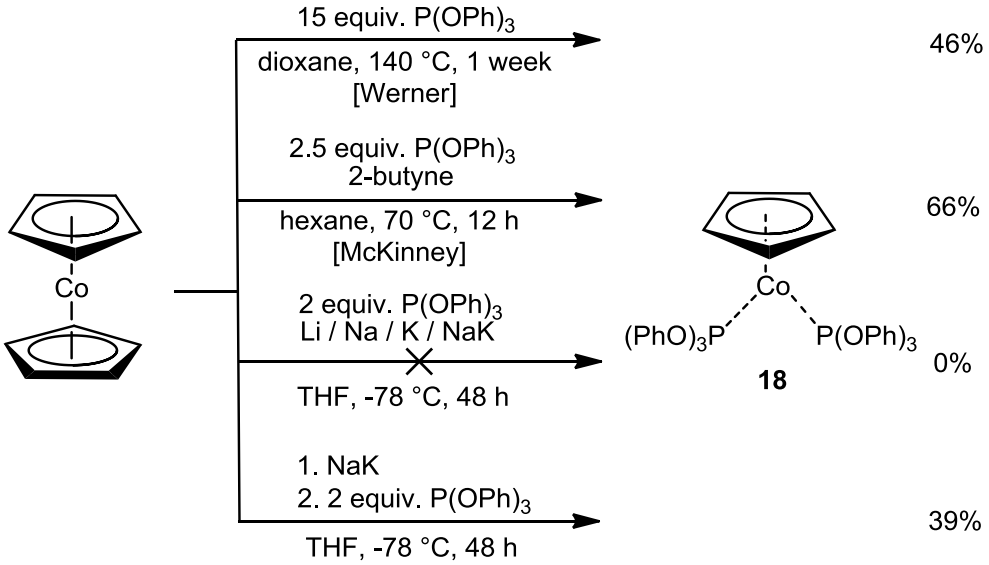

Scheme 12: Different routes for the synthesis of **18**

The reduction of cobaltocene with an alkali metal such as lithium, sodium or potassium in the presence of the triphenylphosphite ligand was unsuccessful and the starting material could be recovered. This is very surprising since the synthesis of $[CpCo(PPh_3)_2]$ (**4**) can be easily accomplished by stirring cobaltocene with elemental lithium and two equivalents of

triphenylphosphine in THF. [95] Only the use of NaK resulted in 39% of **18** after stirring at -78 °C for 48 h.

After these disillusioning results a different approach had to be developed. Taking advantage from our experience with photocatalytic reactions [CpCo(cod)] (**3**) seemed to be a promising precursor. The cod ligand can be easily removed through irradiation with light, leaving both coordination sites free for the coordination of the phosphite ligands. This simple substitution reaction generates the respective bis(phosphite) complexes **18**-**22** in excellent yields and is applicable to all kinds of different types of phosphites (Scheme 13). Only in the case of phosphites incorporating sterically bulky groups such as tris(2,4-di-*t*-butylphenyl)phosphite the reaction did not take place and only starting material could be recovered. Therefore, in contrast to **6**, [CpCo(cod)] (**3**) proved to be an excellent precursor for the synthesis of CpCo(I)-bis(phosphite) complexes.

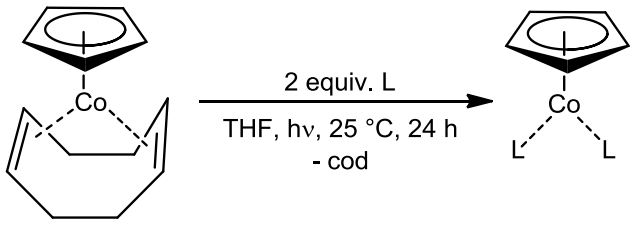

3 **18-22**

(**18**) L = $P(OPh)_3$ 90%
(**19**) L = $P(OEt)_3$ 99%
(**20**) L = $P(O\textit{i}\text{-}Pr)_3$ 79%
(**21**) L = $P(OCH_2CF_3)_3$ 84%
(**22**) L = $P(OC_6H_4\text{-}4\text{-}CF_3)_3$ 50%

Scheme 13: Synthesis of CpCo(I)-bis(phosphite) complexes

In an additional experiment the synthesis of [CpCo(H_2C=CH$SiMe_3$){$P(OPh)_3$}] (**11**) via photoactivation of **3** was investigated. Here a solution of triphenylphosphite (1 equiv.), trimethylvinylsilane (10 equiv.) and **3** in THF was irradiated with light for 24 h. After work up a 2:2:1 mixture of **3**, **18** and **11** could be detected. This is in accordance to observations by Butenschön et al. who described low to mediocre yields if [(bicyclo[3.2.0]hepta-1,3-dienyl)Co(cod)] was reacted with a fivefold molar excess of phosphine and a fivefold molar excess of dimethylfumarate in boiling *o*-xylene. [55]

3.1.3 Synthesis of [CpCo(olefin)(phosphite)]-Complexes – Variation of Olefins

To expand the library of the [CpCo(olefin)(phosphite)] compounds and to investigate the influence of the olefin ligand the synthesis of complexes with different olefin/phosphite combinations was approached. Starting from [CpCo(H_2C=$CHSiMe_3$)$_2$] (**6**) [51] and first replacing one trimethylvinylsilane ligand for a phosphite followed by the substitution of the second one for another olefin at elevated temperatures resulted only in the case of triphenylphosphite and dimethylfumarate in an excellent yield of [CpCo(dimethylfumarate){$P(OPh)_3$}] (**26**) (98%). Hence, we set forth to pursue a different approach starting from the commercially available [CpCo$(CO)_2$] (**1**) and two successive ligand replacements. The first CO ligand is easily exchanged for a phosphite ligand, by simply stirring the two liquids at room temperature for 24 h. [56, 62, 96] This exchange has also been accomplished for NHC-ligands.[60, 97] Removal of the second CO ligand also takes place at room temperature but requires radiation with light.[58] Both steps are achieved in excellent yields (Scheme 14). While complexes **23** and **24** are air-sensitive as most CpCo(I)-complexes, **25** and **26** are air-stable solids and can be stored on the bench for months.

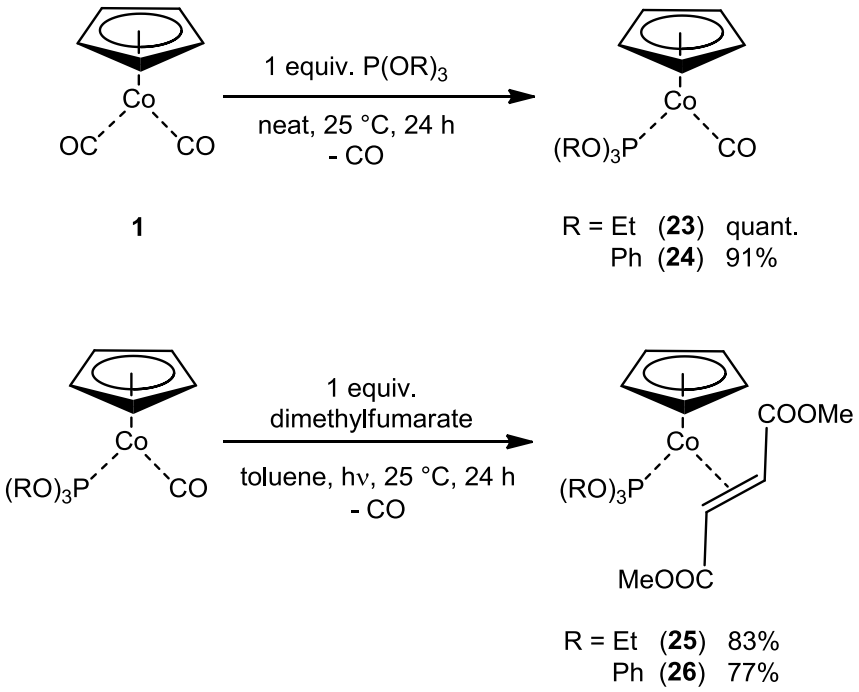

Scheme 14: Synthesis of air-stable CpCo(I)-olefin-phosphite complexes

Interestingly the sequential substitution has to be in the order phosphite - olefin to yield the clean compounds **25** and **26** in excellent yields (Scheme 15). If dimethylfumarate is reacted with **1** the mixed [CpCo(CO)(dimethylfumarate)] complex **7** is formed in very good yields. [52] Addition of one equivalent of triethylphosphite and irradiation of the reaction mixture with light only yields 40% of **25**. The reaction mixture contains additional **23** (32%), **19** (20%) and free dimethylfumarate (8%). This suggests that the phosphite can substitute the CO as well as the olefin ligand in **7**, leading to both mono(phosphite) complexes as well as the bis(phosphite) complex through a second substitution reaction. It can therefore be assumed that under these conditions the phosphite ligand coordinates more strongly to the cobalt center than the dimethylfumarate.

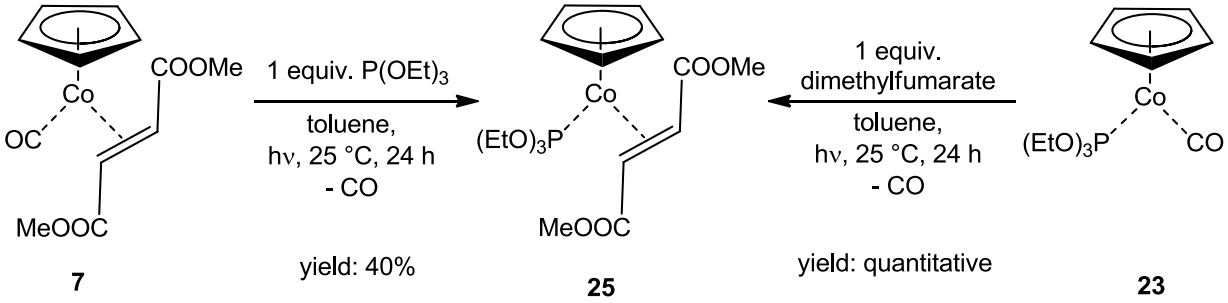

Scheme 15: Different synthetic pathways to **25**

Crystals of **25** as well as **26** suitable for X-ray analysis were obtained from *n*-pentane solutions at 4 °C (Figure 1). The characteristic data for **25** and **26** like the double bond length of the coordinated olefin are in agreement with those described for Gandon's complex [CpCo(CO)(dimethylfumarate)] (**7**). The length of the coordinated double bond of the dimethylfumarate ligand is 1.422(4) Å, 1.43(2) Å and 1.44(2) Å [52] for **25**, **26** and **7** respectively and does not vary to such an extend as to propose an effect of the second coordinating ligand (phosphite/CO) on the character of the double bond. The structural features of **25** and **26** with respect to the phosphites are very similar, which can be seen for example in the Co-P distances (**25**: 2.1200(8) Å; **26**: 2.1092(3) Å) and the P1-Co-C1 and P1-Co-C2 angles (**25**: 95.67(9)° and 102.14(8)°; **26**: 94.45(4)° and 101.10(4)°).

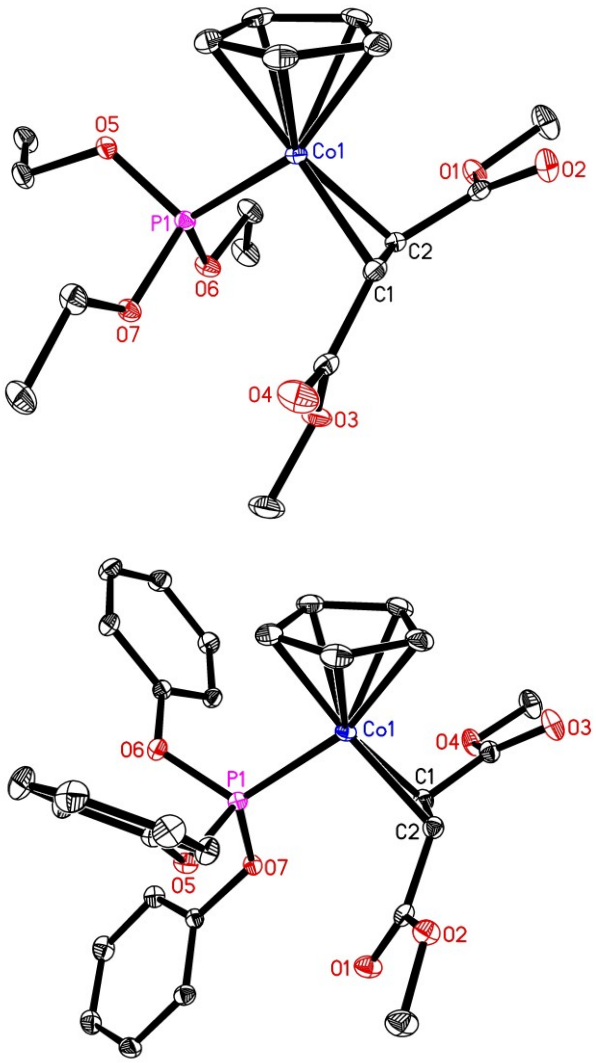

Figure 1: ORTEP drawings of the molecular structure of **25** (left) and **26** (right). Ellipsoids are set at 30% probability. Hydrogen atoms are omitted for clarity (comparison of interatomic distances: **25** C1-C2, 1.422(4) Å; **26** C1-C2, 1.43(2) Å)

Having found these new air-stable compounds we set out to synthesize analogues with other olefin ligands. In the case of *cis*-cyclooctene (coe) the exchange reaction proceeded only smoothly when reacted with **23** to yield [CpCo(coe){$P(OEt)_3$}] (**27**). If **24** was used instead, only 41% yield of the desired complex [CpCo(coe){$P(OPh)_3$}] (**28**) could be obtained, the major product being [CpCo{$P(OPh)_3$}$_2$] (**18**) (yield: 45%).

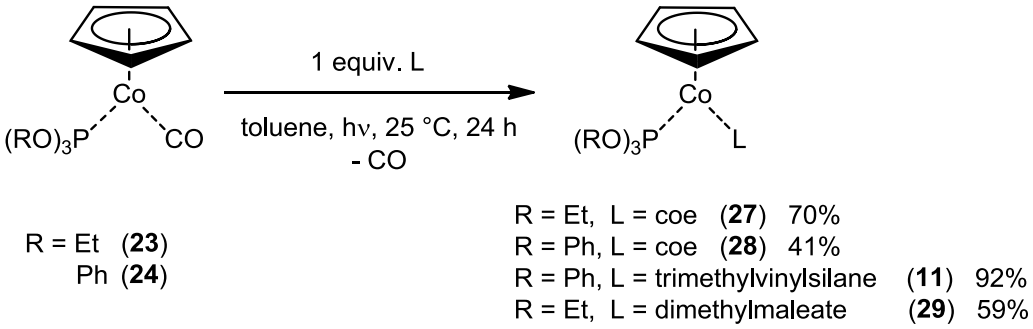

Scheme 16: Synthesis of CpCo(I)-olefin-phosphite complexes with varying olefins

Using an excess of trimethylvinylsilane and irradiation of the solution of **24** for only 4 h led to **11** in 92% yield. An experiment with dimethylmaleate resulted in a mixture of 59% [CpCo(*cis*-$MeO_2CCH{=}CHCO_2Me$){$P(OEt)_3$}] (**29**), 17% [CpCo{$P(OEt)_3$}$_2$], 6% **25** and 17% dimethylmaleate. The use of olefins such as norbornene or fluorinated olefins such as (*E*)-5H,6H-perfluorodec-5-ene did not lead to any product at all and the starting compound was reisolated. Interestingly in case of **24** mostly [CpCo{$P(OPh)_3$}$_2$] (**18**) could be recovered, while **23** did not yield any disubstituted complex.

Surprisingly all new complexes (except **29**) with olefin ligands other than dimethylfumarate proved to be air-sensitive. This is in accordance with reported results on the stabilizing effect of electron-poor olefins on the metal catalyst. [98] Therefore one might assume that the more electron-deficient the olefin ligand the more (air-) stable the final complex. Nevertheless steric properties of the olefin ligand as well as the principle of optimizing π-donation to vacant d-orbitals [98a] play a large role and account for unusual stabilities as seen with the much preferred sterically more demanding dimethylfumarate compared to dimethylmaleate.

3.1.4 Synthesis of CpCo-Complexes with Chelating Phosphite-Olefin Ligands

To investigate the influence of the ligands a bit further the application of chelating phosphite-olefin ligands seemed to be promising. Therefore two different phosphite ligands, namely the cyclic phosphite **17** and the linear phosphite **30**, were synthesized (for details see experimental section). [99] The respective complexes with one CO ligand could be prepared in very good yields as described above (Scheme 17).

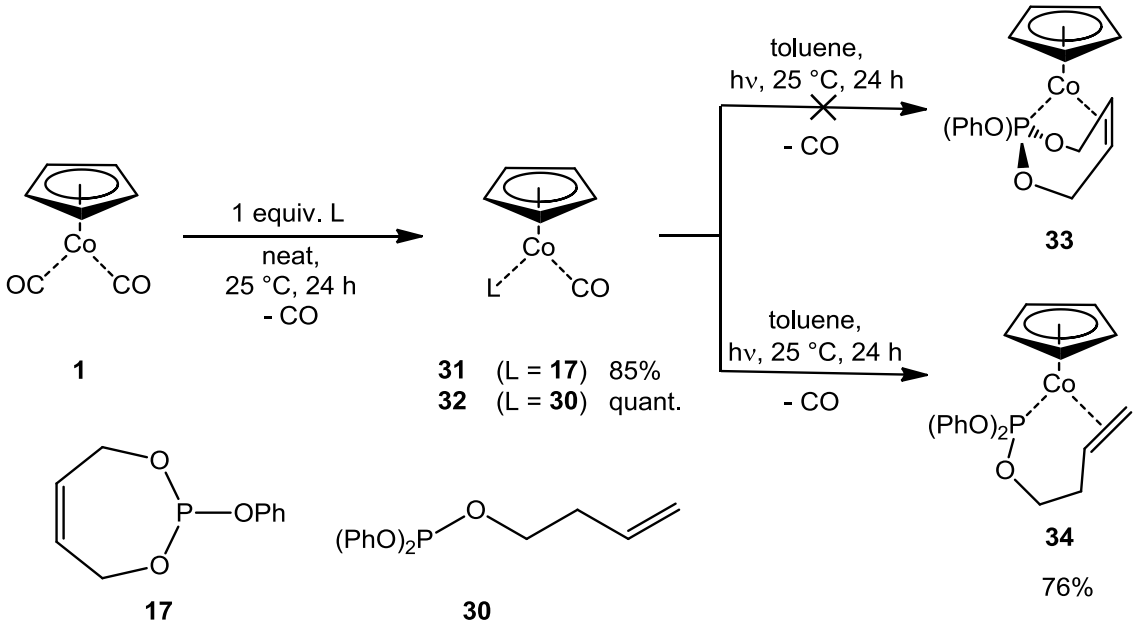

Scheme 17: Synthesis of chelating CpCo-olefin-phosphite complexes

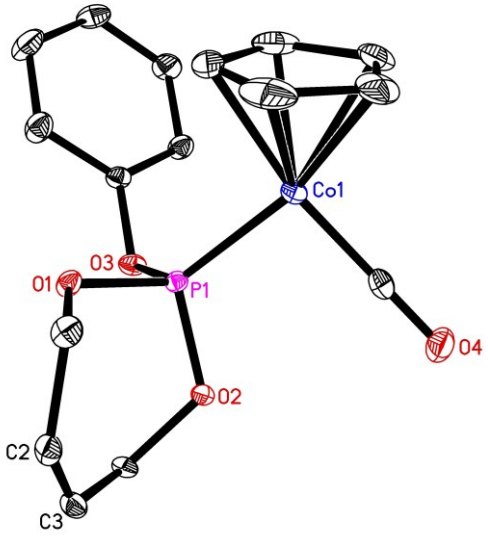

Figure 2: ORTEP drawings of the molecular structure of **31**. Ellipsoids are set at 30% probability. Hydrogen atoms are omitted for clarity.

Crystals of **31** suitable for X-ray analysis were obtained from a *n*-pentane solution at 4 °C. Figure 2 proves unambiguously that the phosphite-olefin ligand is definitely only coordinated via the phosphorus atom and one CO ligand is still attached to the cobalt center.

In the case of **32** three sets of signals were detected in the ^{1}H and ^{31}P NMR spectra presumably corresponding to conformers of **32** due to different arrangements of the two phosphite phenyl groups. Since these conformers could not be separated, the mixture was

applied in the next reaction step. The irradiation with light and the release of the second CO ligand only led to a successful chelation in the case of ligand **30**.

If **31** is irradiated with light at 25 °C or even at temperatures as low as -20 °C a black solid precipitates and no ^{31}P NMR signal can be detected in the red solution.[b] Filtration of the solution over neutral aluminum oxide and removal of the solvent affords a red, highly volatile solid in 41% yield. The ^{1}H NMR spectrum of this red complex is depicted in Figure 3 showing the characteristic signal for a Cp-ligand as well as for a coordinated double bond. A ^{1}H-^{1}H COSY NMR-spectrum proved that the three signals H_a, H_b and H_c are all coupling with each other.

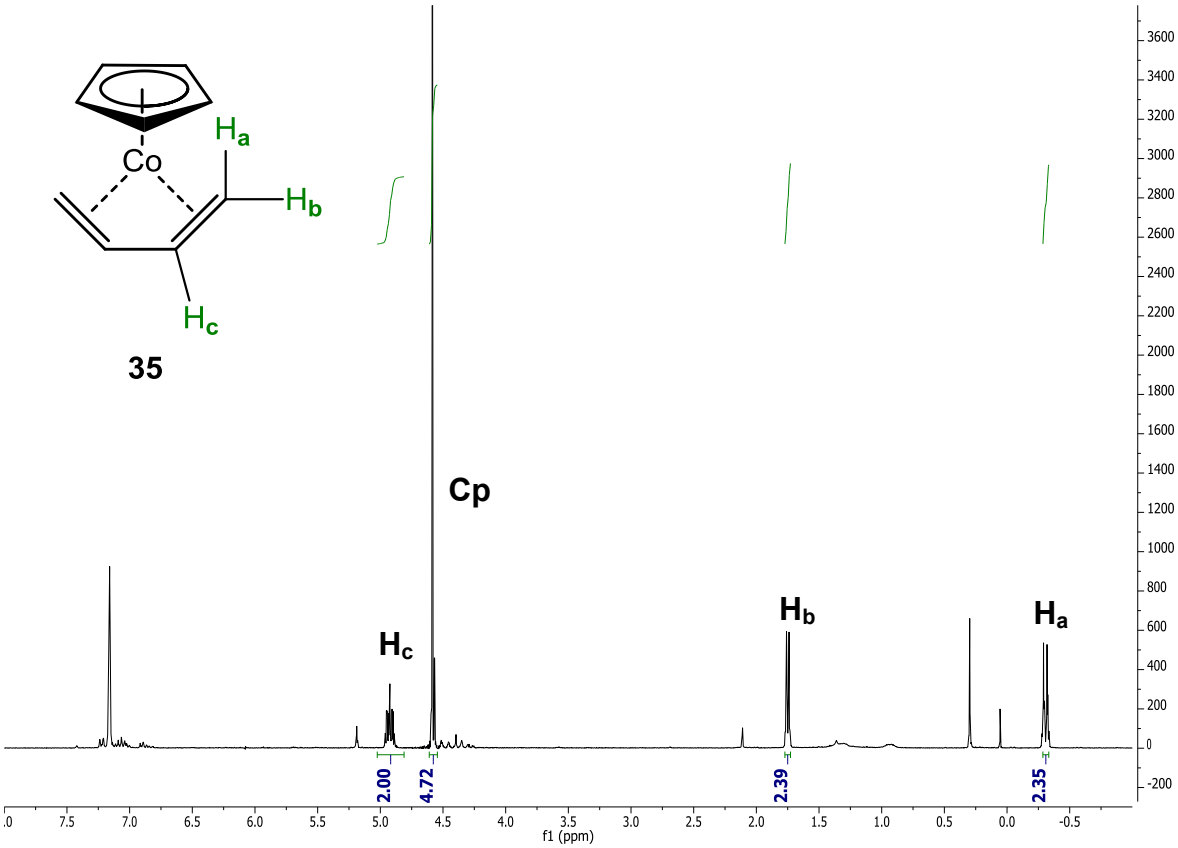

Figure 3: ^{1}H NMR spectrum of the photolysis product of **31**

The results of the mass spectroscopic analysis, which showed a signal at m/z 178, corresponded with the formation of [CpCo(η^4-1,3-butadiene)] (**35**). Pruett and Myers already described **35** as a volatile red solid prepared from **1** and excess 1,3-butadiene at elevated temperatures, [100] but only Bergman et al. published a full characterisation of **35**, the NMR

[b] Irradiation of the ligand **17** or the bis(phosphite) complex [CpCo(**17**)$_2$] did not lead to decomposition of the phosphite ligand.

data being in accordance with our findings. [101] The shifts of the signals in the ^{1}H NMR spectrum were also in good agreement with data reported by Vollhardt, who investigated the isomerization reaction of late transition metal-1,3-butadiene-derived complexes. [102], [103]

The degradation mechanism of **31** is not yet fully understood (Scheme 18). It seems that the cleavage of the C–O bond is preferred over the P–O bond although both bond energies are very similar (C–O: 85.5 kcal/mol; P–O: 80 kcal/mol). [104] However, it has been observed that a CO_2-laser has the same effect on phosphite compounds. McDonald et al. described the decomposition of various alkyl phosphites when subjected to a CO_2-laser for 20 seconds. [105] They never found alcohols, which are the decomposition products from normal, thermal pyrolysis, therefore hinting at a C–O bond cleavage leaving the P–O bond intact.
GC-MS analysis of the reaction mixture showed several signals at very early retention times (1-2 min). Only some of these signals could be assigned to for example 1,3-butadiene, cyclopentadiene and fragments of aromatic ring systems.

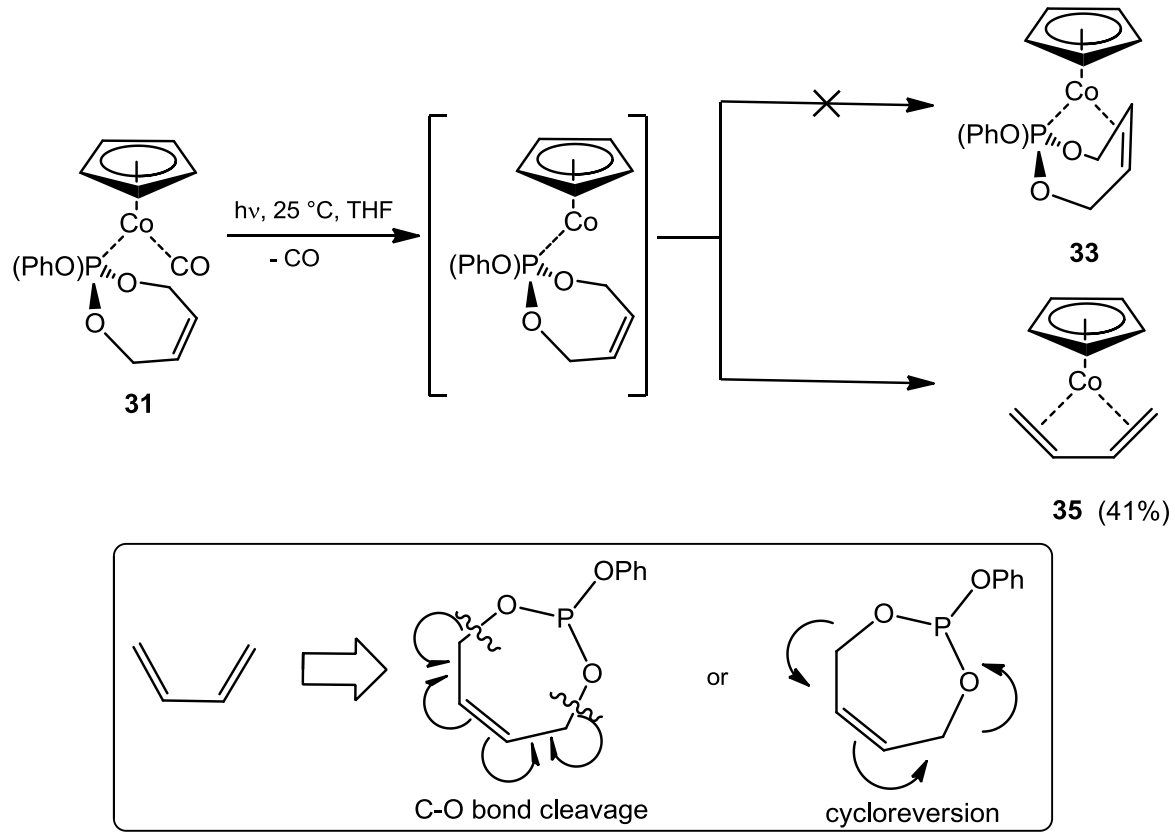

Scheme 18: Possible cleavage mechanism of the phosphite ligand in **31** to form **35**

Elemental analysis of the precipitated green-black solid showed a cobalt content of around 26% and a phosphorus content of roughly 10%, which strongly suggests a cobalt-phosphorus cluster. This would explain the absence of phosphorus in the final complex. The reactivity of **1** with free phosphines yielding phosphorus-bridged clusters has previously been reported by Lal De and Maiti. [106]

3.2 Catalytic Screening

3.2.1 Catalytic Screening of the Synthesized CpCo(I)-Complexes

Having prepared a large array of new potential pre-catalysts with different olefin and phosphite ligands, the catalytic activity still needed to be tested. All synthesized catalysts were tested in the [2+2+2] cycloaddition reaction between 1,6-heptadiyne (**36**) and benzonitrile (**40**) giving pyridine **43**.

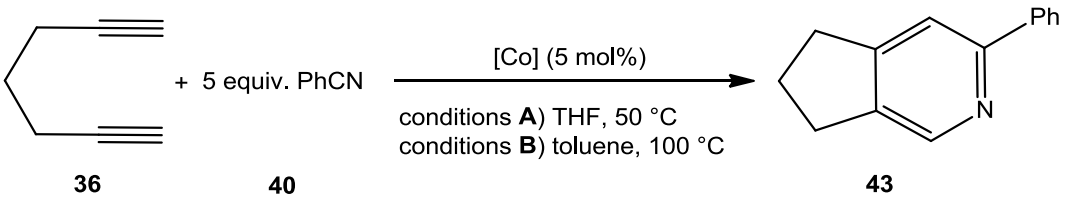

Scheme 19: Catalytic test reaction between 1,6-heptadiyne (**36**) and benzonitrile (**40**)

3.2.1.1 Catalytic Screening of Complexes **11-16**

The catalytic activity of the complexes **11-16** were evaluated at 50 °C in THF (Scheme 19, condition **A**). As Figure 4 shows, almost all of the synthesized complexes of the type [$CpCo(H_2C{=}CHSiMe_3)\{P(OR)_3\}$] resulted in very high conversions and yields of pyridine **43** after short reaction times (just 1 h).

The only exception is **16**, which reaches a conversion around 65% only after reaction times longer than 20 h.

It can therefore be concluded that the nature of the phosphite ligand does not play a large role in providing high reactivity, but rather in stabilizing the complex by coordinating more strongly to the cobalt center than the two olefin ligands in **6**.

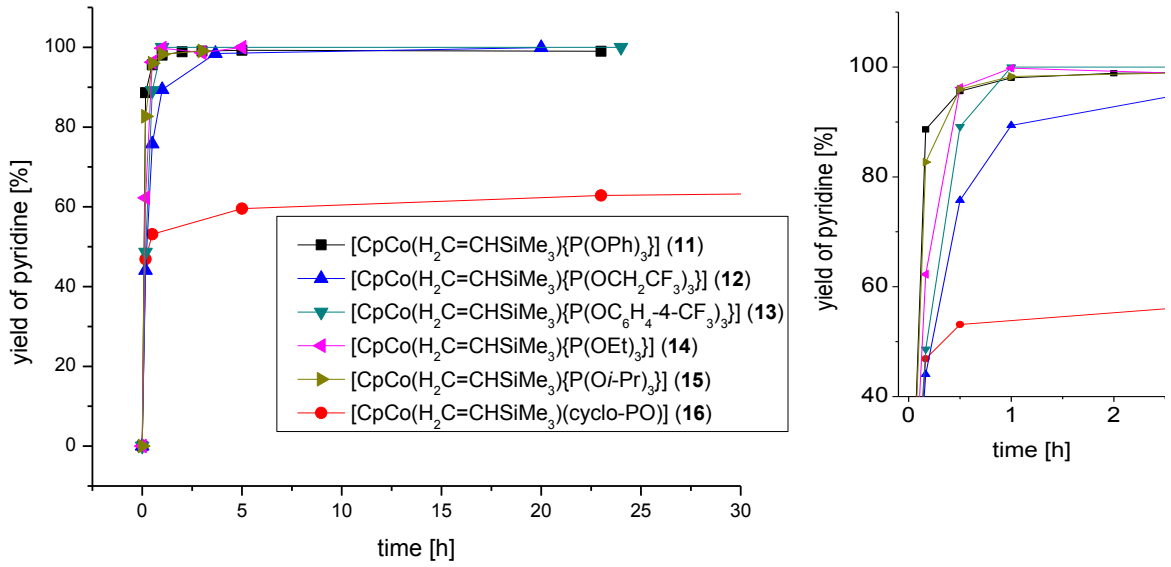

Figure 4: Catalytic activity of **11-16** (condition **A**, Scheme 19) (right: excerpt of the initial phase)

3.2.1.2 Catalytic Screening of Complexes **18-22**

The catalytic performance of **18-22** was investigated in the same catalytic screening setting. The outcome showed that the second phosphite ligand improves the stability of the catalyst even more, because all these complexes show lower reactivities than the monosubstituted complexes. However, the most active complex **20** exhibits almost full conversion of the substrate already after 3 h (Figure 5).

Now, the role of the respective phosphite ligands also becomes apparent. It seems that the electronic properties of the phosphite play a large role with regard to the catalytic activity of the pre-catalysts. While electron-rich phosphites such as P(O*i*-Pr)$_3$ and P(OEt)$_3$ (**20**, **19**) lead to easily activated complexes, which reach quantitative conversions to the pyridine derivative, more electron-deficient phosphites such as P(OPh)$_3$ (**18**) only reach conversions up to 20% after 24 h. The introduction of electron-withdrawing groups as in the case of P(OC$_6$H$_4$-4-CF$_3$)$_3$ even induces a complete loss of activity of the respective complex **22**. P(OCH$_2$CF$_3$)$_3$ is an exception being rather electron-deficient but reaching conversions up to 33% in 24 h under these conditions (**21**). This demonstrates that electron-withdrawing groups lead to a stronger coordination of the respective phosphite to the cobalt center owing to a stronger π-backbonding.

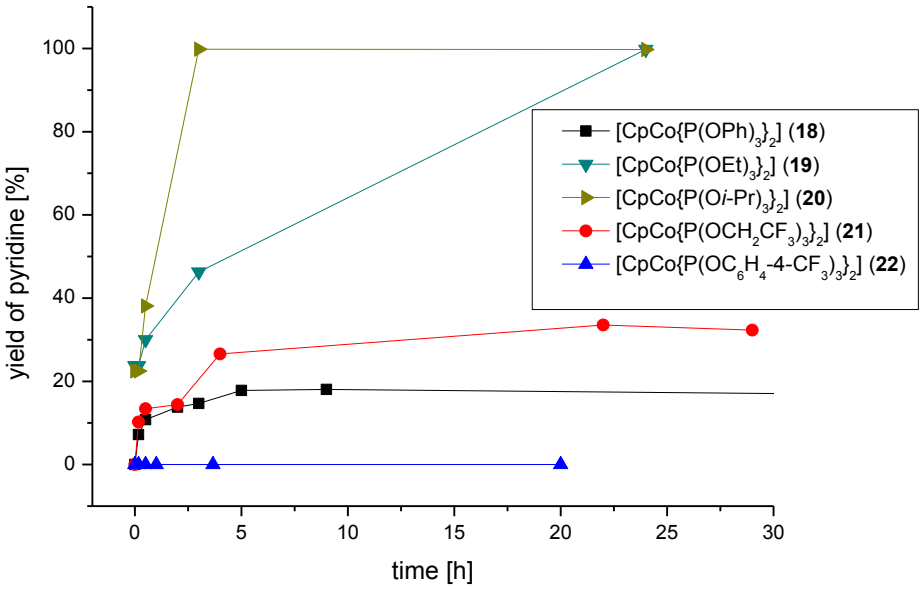

Figure 5: Catalytic activity of **18-22** complexes (condition **A**, Scheme 19)

3.2.1.3 Catalytic Screening of Complexes **23- 27**

The catalytic activity of the other mixed CpCo(I)-olefin-phosphite-complexes, which have been obtained through sequential substitution of the CO ligands of **1**, has been assessed as well.

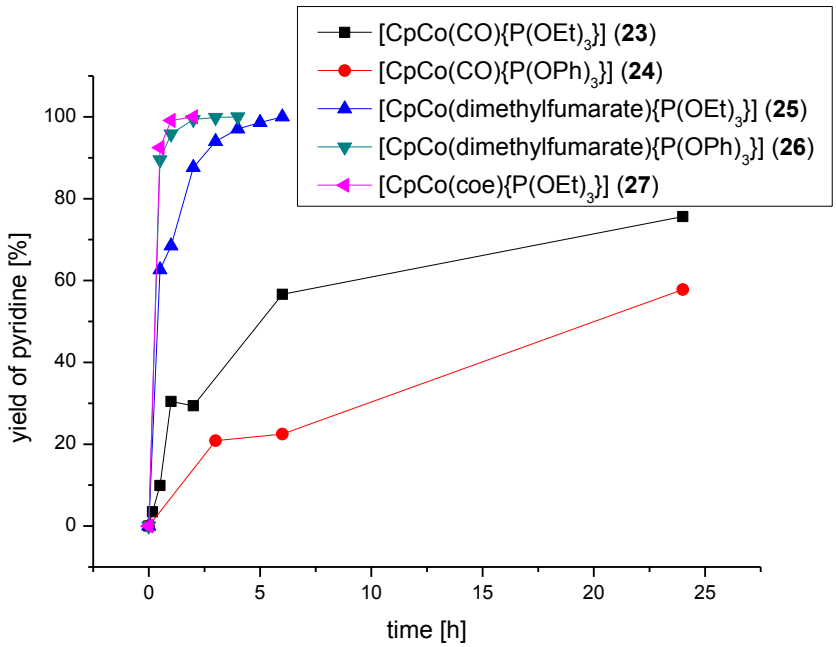

Figure 6: Catalytic activity of **23-27** (condition **B**, Scheme 19)

Figure 6 shows clearly that a ligand combination of olefin and phosphite is once again superior to a combination of CO and phosphite with regard to the catalyst's activity. While complexes **23** and **24** need reaction times as long as 24 h to reach yields between 50 and 70%, **25**, **26** and **27** reach full conversions after 3-5 h at 100 °C.

2.2.1.4 Catalytic Screening of Complexes **31**, **32** and **34**

To obtain a better idea of the effect of the chelating ligand the catalytic activity of the three complexes **31**, **32** and **34** was investigated in the same [2+2+2] cycloaddition test reaction as before (Scheme 19). Figure 7 clearly indicates that again the ligand combination of phosphite-olefin (**34**) is more efficient than the phosphite-CO combination (**31** and **32**), providing complete conversion after short reaction times.

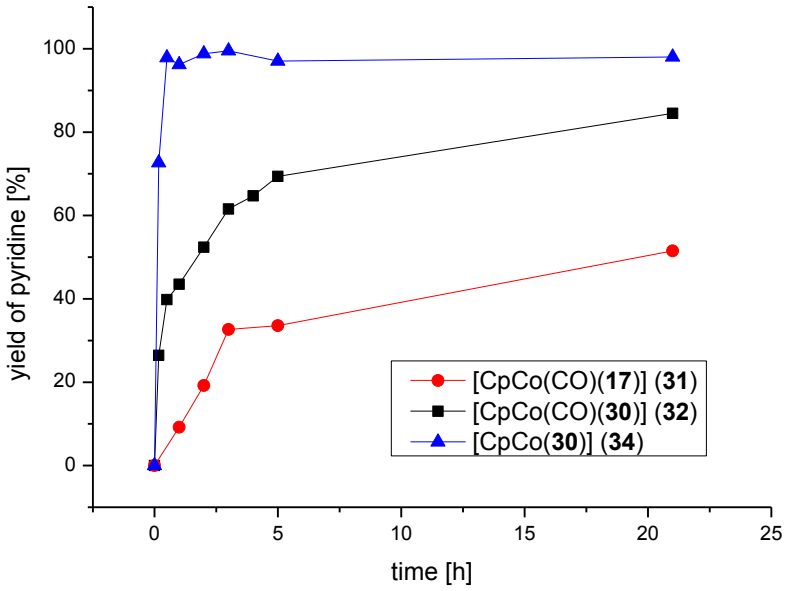

Figure 7: Catalytic activity of **31**, **32** and **34** (condition **B**)

If one compares the catalytic activity of **34** with those of complexes containing non-chelating phosphite-olefin ligand variations such as **25** and **26** (compare Figure 6), no visible stabilizing effect due to the chelatisation can be detected. Therefore, the effect of the chelating ligand on the catalytic performance is significantly less than that of a strongly coordinating monodentate ligand like CO.

3.2.2 Performance of **18** and **25** under Various Conditions

To further test the stability and manageability of the two complexes **18** and **25** exemplarily, their catalytic activity was tested under several conditions. Consequently it was also possible to perform the cycloaddition reaction with **18** in undried and non-degassed toluene without loss of product yield (Figure 8, left).

In the case of the air-stable complex **25** the reaction could also be run in undried and not degassed solvent taken straight from the bottle and air with only a slight loss in yield (Figure 8, right). The only disadvantage of running the reaction in air is the decomposition of the complex during the reaction compared to the recyclability of **25** when the reaction is run under an inert atmosphere (see chapter 3.3).

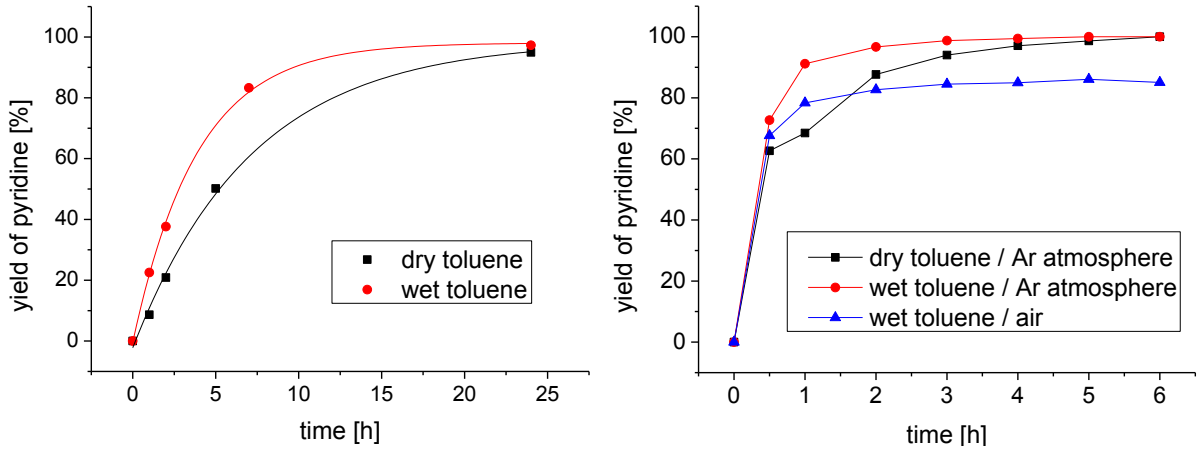

Figure 8: Performance of **18** (left) and **25** (right) respectively under various conditions

3.2.3 Performance of **19**, **23**, **25** and **7** under Conventional Heating Conditions and Irradiation with Light

Up to now all novel synthesized complexes have been screened as catalysts for the [2+2+2] cycloaddition reaction under conditions that involve conventional heating. Since in the case of **18-22** and **25-29** the complex synthesis involved the irradiation with light, it seemed likely that some of these complexes might also be activated by light for catalysis. The same test reaction between **36** and **40** was investigated at 25 °C, while the reaction mixture was irradiated with light. Figure 9 clearly proves that all tested complexes (**19**, **23**, **25** and **7**) show

improved yields of the product **43** if they are subjected to the irradiation with light. In all cases a conversion of >90% can be achieved in only two hours. Interestingly the positive effect of the irradiation with light is the greatest for **23** followed by **19**. In the case of **25** and **7** the increase in reactivity and yield is much smaller.

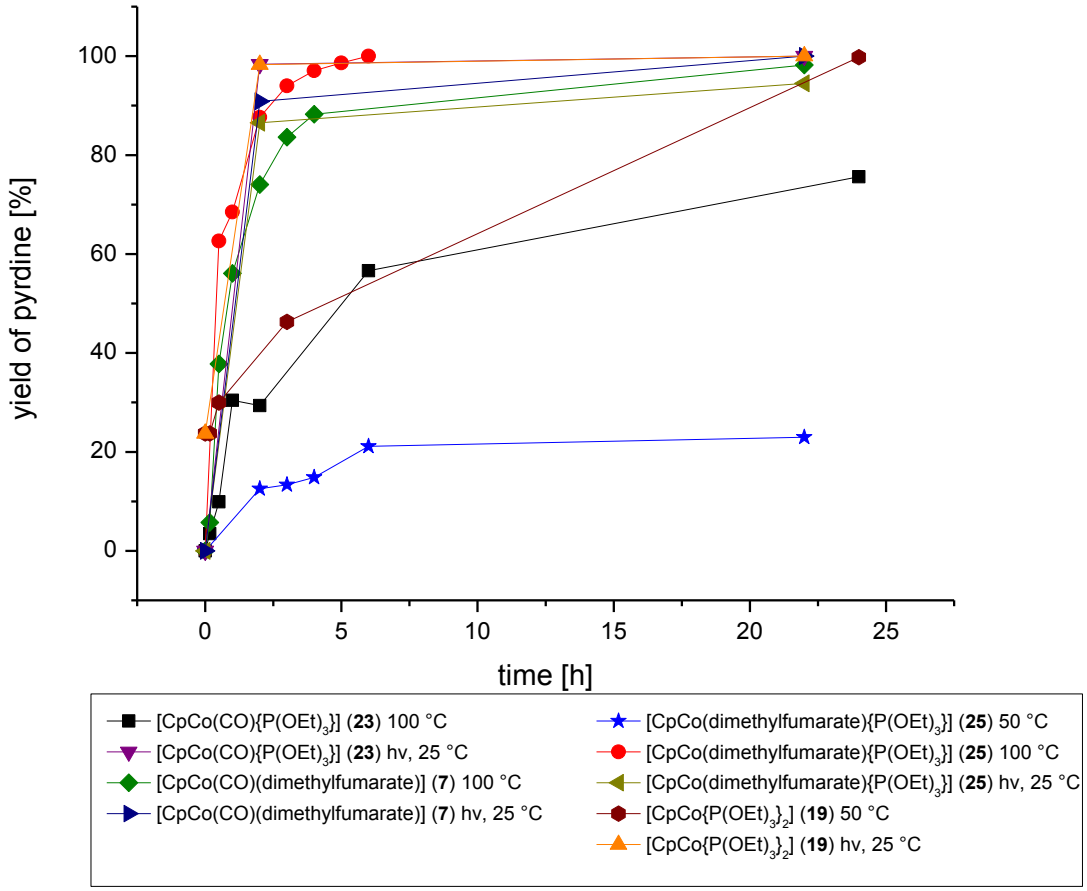

Figure 9: Performance of **19**, **23**, **25** and **7** under conventional heating conditions and irradiation with light

To explore and understand these observations a bit more, the UV-VIS spectra of several CpCo(I)-complexes were recorded. As Figure 10 shows, most of the spectra are very similar. The absorption maxima are between 265 nm and 320 nm. Nevertheless it is obvious that the UV-VIS absorption is largely dependent on the respective ligands.

Complexes bearing at least one phenyl ring show a maximum at 300 nm, while complexes **1**, **7**, **19** and **3**, which have no aromatic ligand, do not absorb at that wave length. All complexes with a dimethylfumarate ligand show a second absorption maxima around 330-380 nm. This can explicitly be seen in the case of **25**, **26** and **7**. A second or third maximum for some of the complexes lies between 330-380 nm and 400-450 nm respectively.

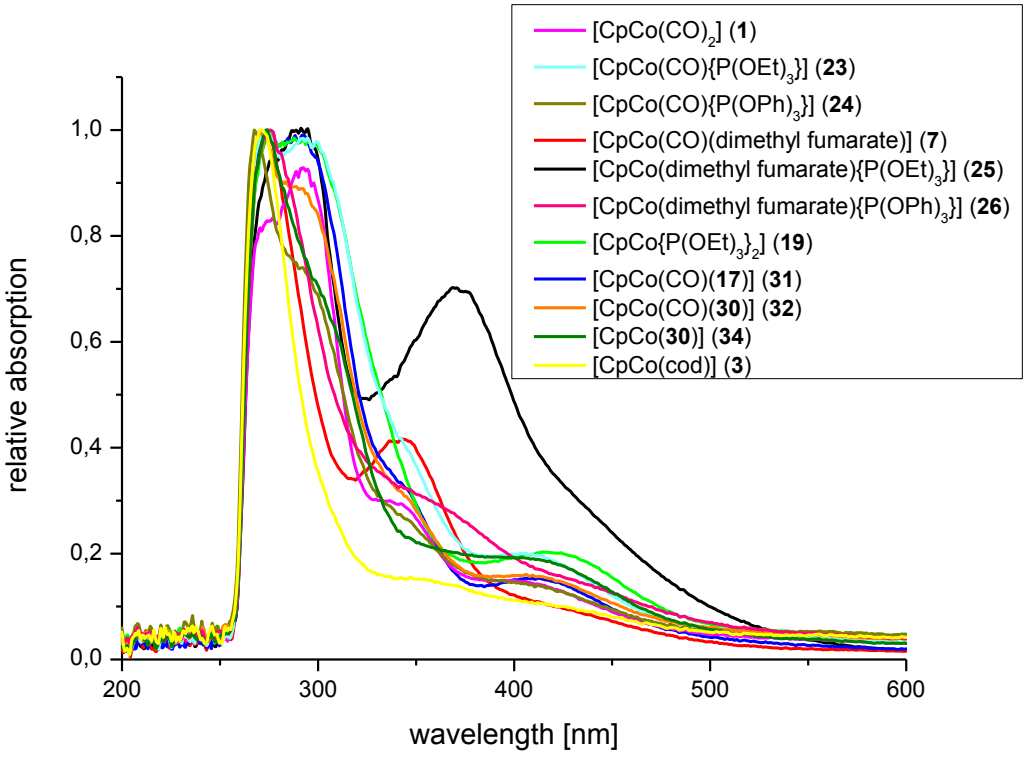

Figure 10: Relative UV-VIS absorption spectra of CpCo(I)-complexes **1**, **3**, **7**, **19**, **23**-**26**, **31**-**32** and **34**

To further investigate the influence of the light, the reaction between **36** and **40** was examined using different wavelengths. These screenings were carried out exemplarily for **23** and **25**. Figure 11 clearly shows that the reaction proceeds at any of the used wavelengths and always leads to a full conversion to **43** after 2 h.

The activation of the complexes does not seem to be greatly influenced by the nature of light used even though light as an activator is necessary since control reactions carried out in the dark at 25 °C did not show any progress of the reaction. The greatest difference in yield can be seen after a reaction time of 10 min (Figure 12). At least for **23** (Figure 12, left) one might deduce an effect in the activation of the catalyst moving from shorter to longer wavelengths.

The internal standard DHT does not have any effect on the catalysis and does not act as a photosensitizer since reactions carried out without the addition of DHT proceeded at the same rate, when irradiated under identical conditions.

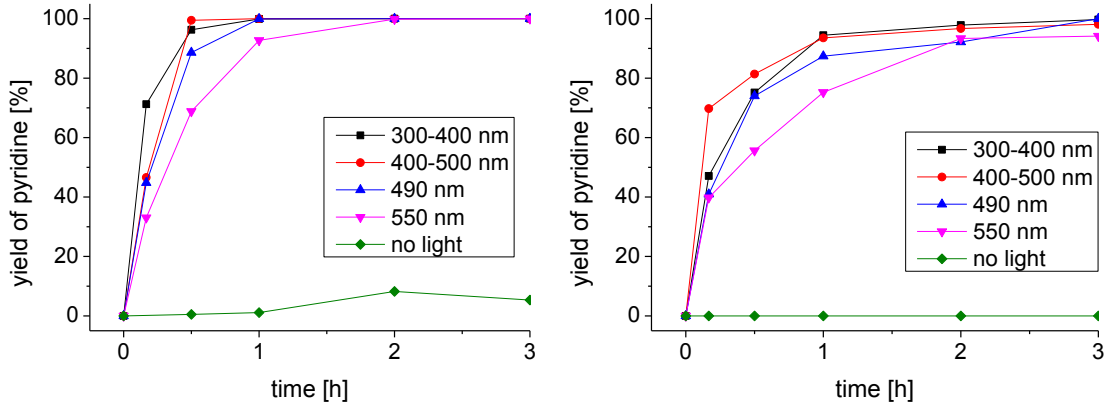

Figure 11: Performance of **23** (left) and **25** (right) during irradiation with different wavelength ranges

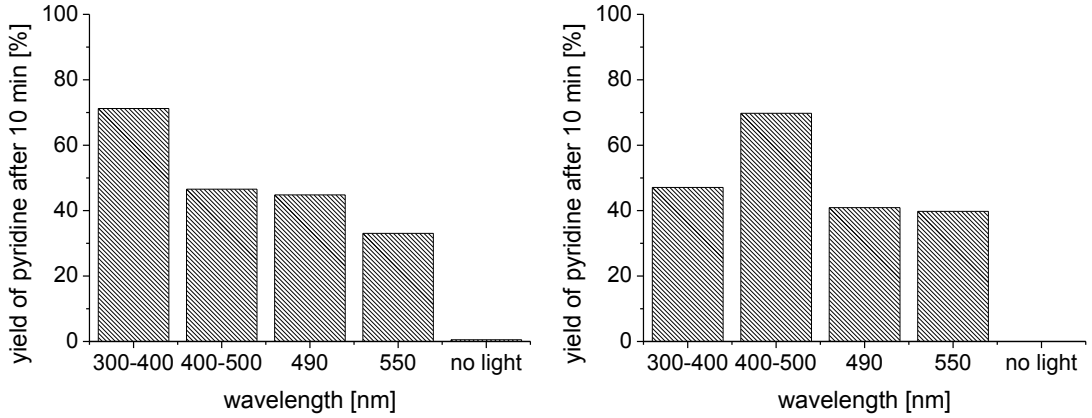

Figure 12: Performance of **23** (left) and **25** (right) after irradiation with different wavelength ranges

While there is a profound activation hierarchy depending on the neutral ligands for thermal activation, the use of light as source of activation energy proved to be always efficient irrespective of the neutral ligands (see Figure 9). This effect of light, heedless of the used wavelength (Figure 11), on the activation of CpCo(I)-complexes has not yet been fully understood. It might be possible that a similar effect as described by the Woodward-Hoffmann rules, which concern the difference in stereoselectivity of organic cyclization reactions whether heat or light is applied, might be responsible. Electrons of the ligands or the metal center might be raised into elevated orbitals reducing the orbital overlap and in the process weakening the bond between metal and ligand leading to complexes activatable at room temperature.

3.2.4 Comparison of the Reactivity of **6**, **11** and **18**

In order to obtain a better impression of the reactivities of the three types of CpCo(I)-complexes namely [CpCo(olefin)$_2$], [CpCo(olefin)(phosphite)] and [CpCo(phosphite)$_2$], a series of catalytic experiments at different temperatures and within different time frames was performed. This comparative reactivity profile for the [2+2+2] cycloaddition between **6**, **11** and **18** is shown in Figure 13.

It is a rare opportunity to compare different CpCo(I)-complexes with homoleptic ligands and the combination of both ligands in one complex to demonstrate the influence of the neutral ligands.

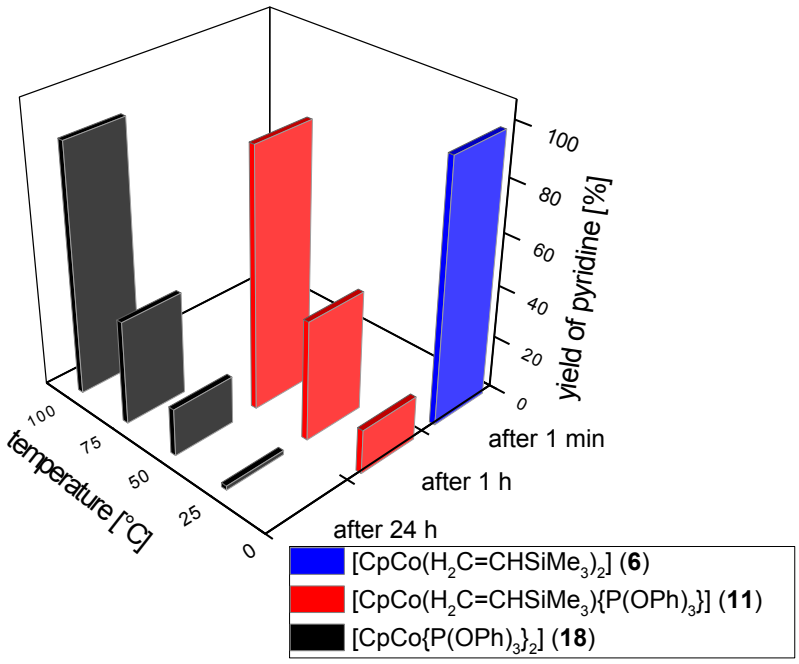

Figure 13: Temperature-dependent yields of pyridine (**43**) determined for [CpCo(H_2C=$CHSiMe_3$)$_2$] (**6**, blue), [CpCo(H_2C=$CHSiMe_3$){$P(OPh)_3$}] (**11**, red) and [CpCo{$P(OPh)_3$}$_2$] (**18**, black), respectively

While complex **6** is most active, accomplishing the reaction at 0 °C in a very short periode of time (within minutes), the chart shows very clearly that the stable complex **11** still maintains a significantly high reactivity as pre-catalyst, leading to completion of the pyridine formation already at 50 °C within an hour and also showing some reactivity at temperatures as low as 0 °C. Complex **18** requires 100 °C for completion of the cycloaddition reaction and a much longer reaction time (24 h). However, the reaction temperature is still lower or at least in the same range than for many other CpCo(I)-complexes used as catalysts. This comparison therefore explicitly shows the stabilizing influence of the phosphite ligands.

3.2.5 Substrate Screening

3.2.5.1 Partially Intermolecular Reaction

A number of diynes and nitriles have been tested exemplarily for [CpCo(H_2C=$CHSiMe_3$){$P(OPh)_3$}] (**11**) and [CpCo(dimethylfumarate){$P(OEt)_3$}] (**25**) in the [2+2+2] cycloaddition reaction (Scheme 20). As one can see from Table 1 and Table 2 both catalysts achieve similar yields of the respective pyridine derivatives.

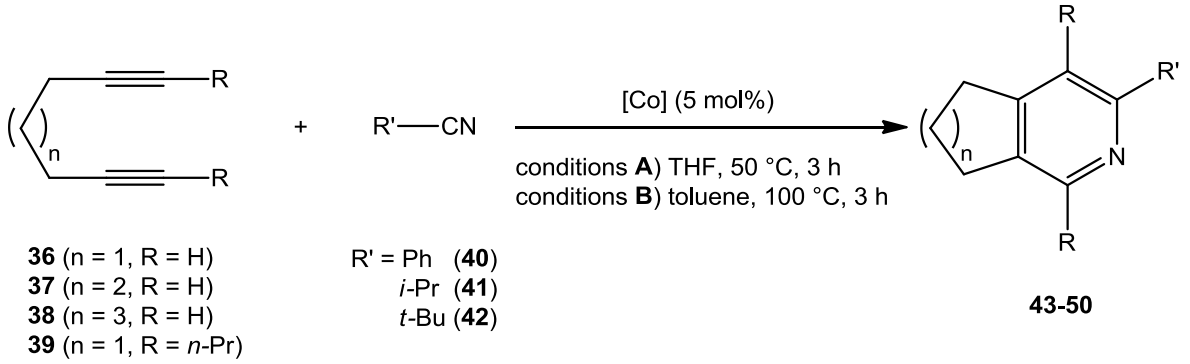

Scheme 20: Substrate screening conditions **A** were used for **11**, conditions **B** for **25**

As noticed before, [2+2+2] cyclization reactions leading to an annulated five-membered ring in the backbone proceed in better yields than those yielding the respective annulated six- or seven-membered rings. [51] The decrease in yield moving from **40** over **41** to **42** can be attributed to the steric hindrance of the nitrile's R'-group. The same principle applies to the low yields of **50** and **52** (Scheme 21). Here the *n*-propyl or naphthyl group respectively contribute enough steric bulk to slow down the reaction.

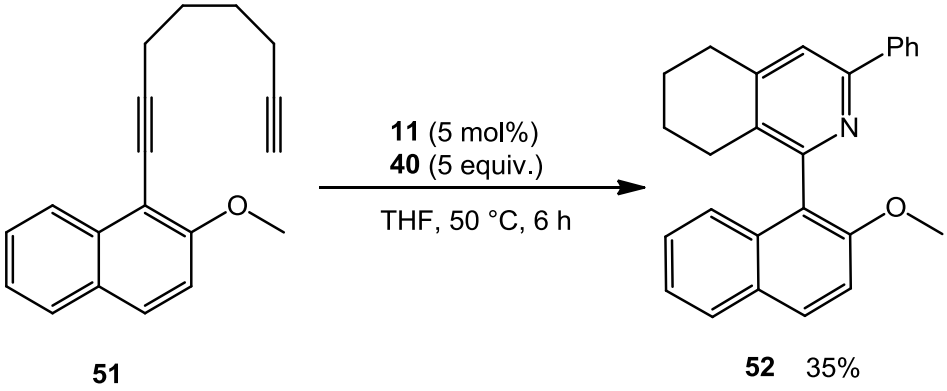

Scheme 21: Synthesis of biaryl **52** with **11**

Table 1: Substrate screening for **11** (conditions **A**, Scheme 20)

Entry	Diyne	Nitrile	Product		Yield [%] [a]
1	**36**	**40**	**43**		98 [b], 97 [c]
2	**36**	**41**	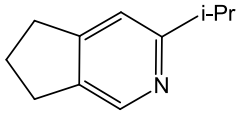	**44**	96
3	**36**	**42**	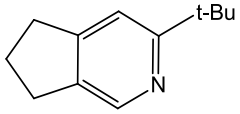	**45**	49
4	**37**	**40**	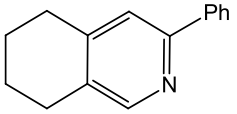	**46**	67
5	**37**	**41**	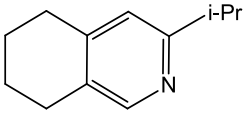	**47**	46
6	**37**	**42**	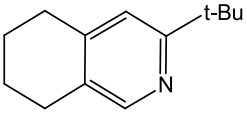	**48**	35
7	**38**	**40**	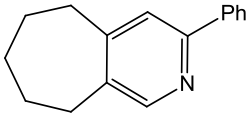	**49**	0
8	**39**	**40**	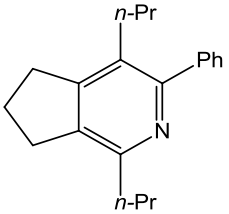	**50**	42 [d]

Table 2: Substrate screening with **25** (conditions **B**, Scheme 20)

Entry	Diyne	Nitrile	Product	Yield [%] [a]
1	**36**	**40**	**43**	94 [b]
2	**36**	**41**	**44**	57
3	**36**	**42**	**45**	71
4	**37**	**40**	**46**	63
5	**37**	**41**	**47**	40
6	**37**	**42**	**48**	38

[a] isolated yields; [b] GC yield; [c] 1 mol% **11**; [d] after 6 h

3.2.5.2 Intramolecular Reaction

The intramolecular reaction of two triynes (**53** and **54**) has been examined as well (Scheme 22). Again both complexes **11** and **25** have been used as catalysts. While **11** only leads to mediocre yields for the benzene derivatives **55** and **56** (Table 3), **25** produces higher yields especially if subjected to microwave irradiation (Table 3, entry 5+6). Interestingly applying microwave conditions leads to an increased yield for benzene **55** while the yield of **56** decreases. Nevertheless these results are in the range of yields achieved with Gandon's complex **7**. [52]

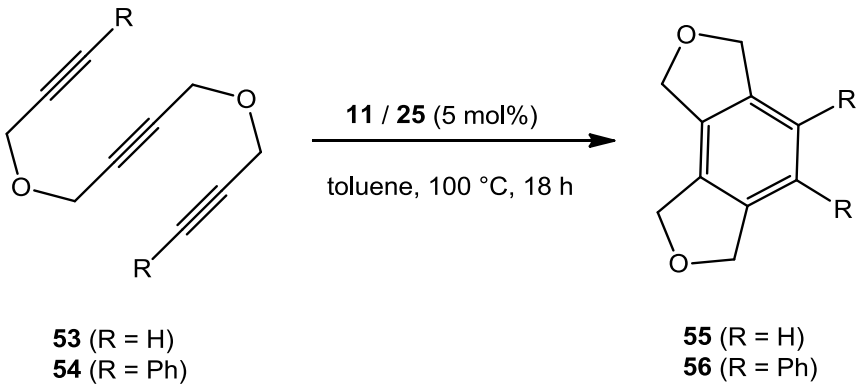

Scheme 22: Substrate screening conditions for **11** and **25**

Table 3: Substrate screening for **11** and **25**

Entry	Catalyst	Triyne	Product	Yield [%]
1	**11**	**53**	**55**	41
2	**11**	**54**	**56**	39
3	**25**	**53**	**55**	36
4	**25**	**54**	**56**	87
5	**25**	**53**	**55**	74 [a]
6	**25**	**54**	**56**	52 [a]

[a] triyne (1mmol), **25** (5 mol%), DMF (3 mL), microwave, 200 °C, 10 min

3.2.5.3 Intermolecular Reaction

The intermolecular [2+2+2] cycloaddition between two alkynes (**57** and **58**) and a nitrile (**40**) was investigated next (Scheme 23). 3-Hexyne (**57**) as an internal alkyne and phenylacetylene (**58**) as a terminal alkyne were chosen as model substrates. It is obvious that **11** is the superior catalyst reaching yields up to 80% for **59**, while **25** only yields 21% of the desired product. The cyclization of **58** with **11** results in 4 regioisomers (GC-MS analysis: 1:6:16:26), which could not be separated by column chromatography. The combined yield of the isomers is as high as 92%.

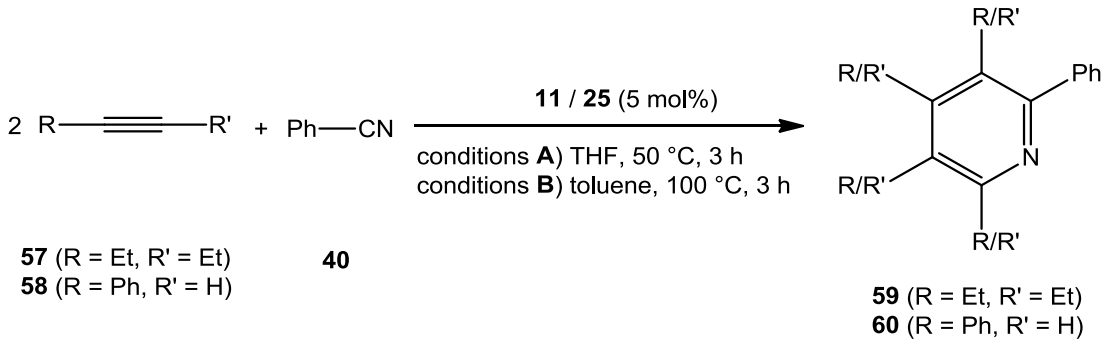

Scheme 23: Substrate screening conditions **A** were used for **11**, conditions **B** for **25**

Table 4: Substrate screening for **11** and **25**

Entry	Catalyst	Alkyne	Nitrile	Product	Yield [%]
1	**11**	**57**	**40**	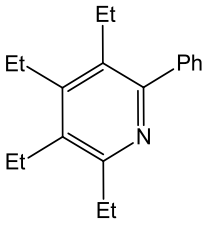 **59**	80
2	**11**	**58**	**40**	**60** (4 isomers)	92
3	**25**	**57**	**40**	**59**	21

3.2.5.4 Other Substrates

The reaction between **36** and phenylisocyanate **61** applying **11** as catalyst did not lead to the respective pyridone, but afforded isocyanurate **62** in 75% yield, which precipitated from the reaction mixture (Scheme 24).
Control experiments with 2 mol% triphenylphosphite or no additive at all resulted both times in no yield of **62**. Therefore **11** does act as a catalyst for this unusual trimerization reaction. Interestingly **61** was the only isocyanate that would undergo this reaction in the presence of **11**.

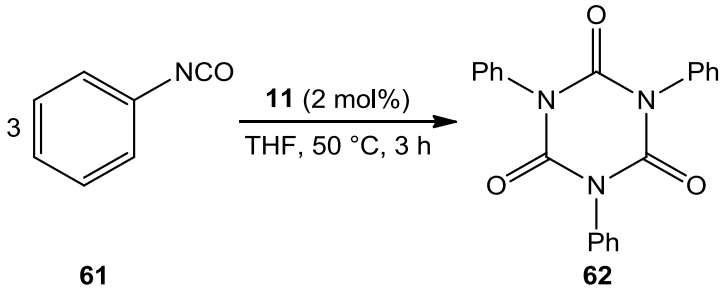

61 **62**

Scheme 24: Generation of isocyanurate **62**

n-Butyl-, *n*-propyl-, cyclohexyl-, tolyl-, 3-acetylphenyl- and 4-nitrophenylisocyanate could be quantitatively recovered after the reaction. This is in accordance with a report by Taguchi et al., who reported that isocyanates which have bulky alkyl groups such as *t*-butyl and cyclohexyl did not trimerize even under a pressure of 800 MPa. [107]

The reaction between 2-butyne and 5-hexynenitrile did not yield any product. A similar report was made by Yamamoto et al. who described the failed cycloaddition of 1-hexyne and 2-(prop-2-yn-1-yloxy)acetonitrile proposing the inhibition of the catalytically active Cp*RuCl-fragment due to the formation of a stable metallacycle. [108]

3.3 Recycling Experiments

Recycling experiments have been conducted exemplarily for **25** in the reaction between **36** and **40** to yield pyridine **43**. The complex could be reisolated quantitatively in three successive cycles through column chromatography, with no decrease in the yield of the cyclotrimerization product. The decrease in the yield of recovered catalyst in the third cycle is due to partial decomposition of the complex in the NMR tube prior the third catalytic cycle (Table 5).

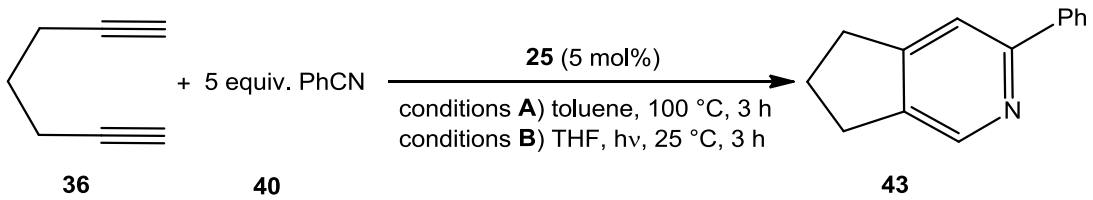

Scheme 25: Reaction conditions for recycling experiments with **25**

Table 5: Recycling experiments of **25** (conditions **A**, Scheme 25)

Cycle	Yield of recovered catalyst [%]	Yield of pyridine [%]
1	quant.	99
2	quant.	99
3	59	79

This "boomerang effect" observed with the ligands of **25** seemed interesting and was investigated in more detail (Scheme 26). Dimethylfumarate with deuterated methyl groups was synthesized and 2 equivalents with regard to **25** added to the catalytic reaction between **36** and **40**. ^{1}H NMR analysis of the recovered catalyst showed that 40% of the original dimethylfumarate were substituted by the deuterated analog. This suggests that the olefin does not stay bound to the cobalt center during the cycloaddition reaction. A control reaction, where only **25** and 2 equivalents of the deuterated dimethylfumarate were stirred at 100 °C for 3 h, proved that the olefin could be substituted at elevated temperatures since ^{1}H NMR analysis showed that 53% of the original dimethylfumarate had been substituted by the deuterated analog. These are strong indications that both ligands do dissociate (the phosphite even before the olefin, see chapter 3.4.2) during the catalytic cycle and in fact recoordinate after the reaction is finished, again furnishing the starting complex **25**.

Conditions:
Cycloaddition (see Scheme 19, conditions B + 2 equiv. d_6-dimethylfumarate): **25** (60%) + d_6-**25** (40%)
Substitution (toluene, 3 h, 100 °C + 2 equiv. d_6-dimethylfumarate): **25** (47%) + d_6-**25** (53%)

Scheme 26: Ligand exchange of the dimethylfumarate ligand for the deuterated analogue during cycloaddition and substitution reaction as control experiments

Interestingly **25** can not be recycled as often if used in catalytic reactions irradiated with light. Table 6 clearly shows that while the product can be obtained in both cycles in very high yields the catalyst can only be reisolated once. After the second cycle no red band on the column containing the catalyst can be observed during chromatographic purification of the product.

Table 6: Recycling experiments of **25** (conditions **B**, Scheme 25)

Cycle	Yield of recovered catalyst [%]	Yield of pyridine [%]
1	86 / 59	97 / 98
2	0 / 0	91 / 57

Thus it seems that light has a greater influence on the stability of complex **25** than temperature. A sufficient explanation could be that the olefin ligand dimethylfumarate isomerizes into its *trans*-form dimethylmaleate under irradiation with light, which does not coordinate as good to the cobalt center as dimethylfumarate and allows to some extent the generation of the respective air-sensitive bis(phosphite) complex **19** (see chapter 3.1.3). Gandon et al. made a similar observation, even when starting from **1** and pure dimethylmaleate as a ligand, they could isolate the respective dimethylfumarate complex **7** in 73% yield. [52] Therefore the amount of air-stable complex **25** is decreased with every cycle of the recycling experiments in favor of the air-sensitive complexes **19** and **29**, which are not recoverable.

3.4 DFT Calculations

To strengthen the experimental results discussed above, DFT calculations were performed on the formation of the complexes as well as the ligand dissociation, as the initial step in the catalytic cycle. In all calculations only real-sized complexes and ligands were used (computational details can be found in the appendix).

3.4.1 DFT Calculations for the Synthesis of Complexes Starting from **6**

Initially the stepwise exchange reaction of one trimethylvinylsilane ligand of **6** by a phosphite ligand to form first **11** and then **18** was studied. The phosphite ligand $P(OPh)_3$ has three isomers, of which the isomer with C_1 symmetry is more stable than the C_3 as well as the C_s isomer by 1.34 and 0.94 kcal/mol, respectively. Therefore the C_1 isomer was used for the energetic comparisons. It has been found that the formation of **11** is highly favorable as indicated by the computed negative free energy (-6.01 kcal/mol) (Scheme 27). However, for the formation of **18** the negative free energy (-2.54 kcal/mol) still indicates a favorable process, but in much less extent compared to the formation of **11**.

The stability of complexes **6**, **11** and **18** towards ligand dissociation has also been computed. It is found that the $16e^-$ complex $[CpCo(H_2C{=}CHSiMe_3)]$ (**A**) has a triplet ground state, which is more stable than the corresponding singlet state by 11.84 kcal/mol. The computed dissociation free energy is -2.20 kcal/mol, revealing the instability of complex **6** at ambient conditions. This reflects the experimentally discovered instability of complex **6** above –30 °C. For complex **18**, the mono(phosphite) complex $[CpCo\{P(OPh)_3\}]$ (**B**) has a triplet ground state as well, which is 16.4 kcal/mol more stable than the singlet state. The computed dissociation free energy of complex **18** is 10.41 kcal/mol, indicating its high stability towards dissociation, which is in agreement with the experimental findings.

In the case of complex **11**, both the olefin and phosphite ligand can dissociate. Here the selectivity depends solely on the dissociation free energies of each ligand. It is found that the dissociation of the phosphite leading to the formation of complex **A** needs lower free energy than the olefin dissociation with the formation of complex **B** (3.81 vs. 7.88 kcal/mol). This indicates that complex **11** dissociates selectively into complex **A**, subsequently leading to the active catalyst. This also explains why the reactivity of the mixed complexes did not largely

depend on the type of phosphite ligand, as Figure 4 showed, since in each case the phosphite is dissociating first, leading to the same intermediate **A**.

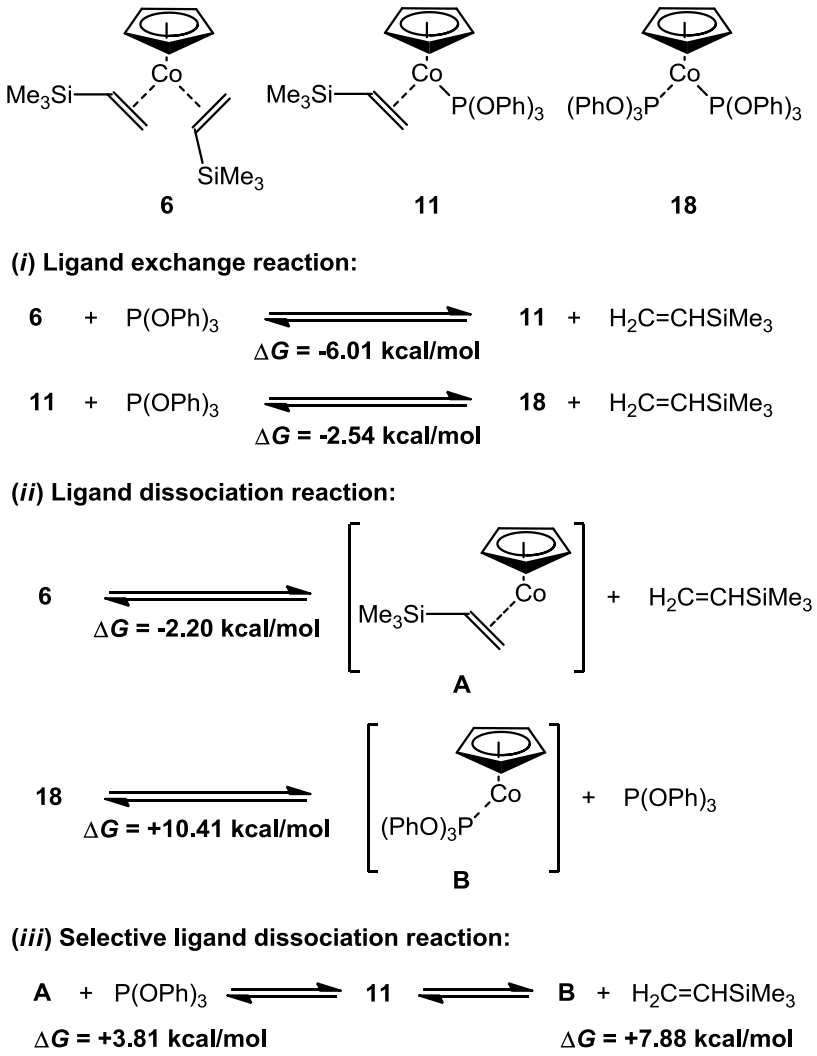

Scheme 27: Calculations on the formation of the new complexes **11** and **18** and free energies of ligand dissociation from **6**, **11** and **18** at BP86/TZVP level

The computed first ligand dissociation free energies reveal that the stability of the complexes increases in the following order: **6** (-2.20 kcal/mol) < **11** (3.81 kcal/mol) < **18** (10.41 kcal/mol). This stability order correlates well with the experimental observations discussed above.

3.4.2 DFT Calculations for the Synthesis of Complexes Starting from **1**

The preparation of air-stable complex **26** from **1** was investigated by computational studies as well (Scheme 28). Here the first step – the reaction between **1** and $P(OPh)_3$ and formation of **24** – suggests an endergonic reaction with a computed free energy of 12.65 kcal/mol. The same reaction with dimethylfumarate instead of $P(OPh)_3$ has a slightly higher computed free energy (15.80 kcal/mol).

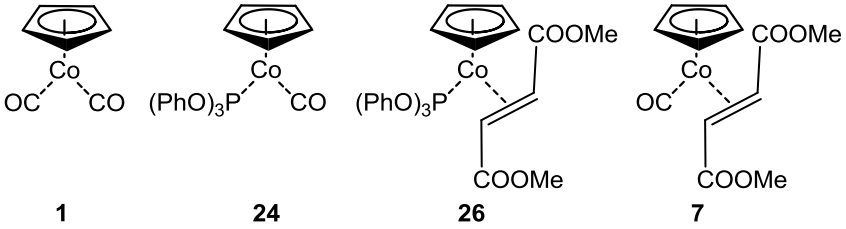

1 **24** **26** **7**

(*i*) Ligand exchange reaction:

1 + $P(OPh)_3$ ⇌ **24** + CO
ΔG = +12.65 kcal/mol

1 + dimethylfumarate ⇌ **7** + CO
ΔG = +15.80 kcal/mol

24 + dimethylfumarate ⇌ **26** + CO
ΔG = +23.35 kcal/mol

(*ii*) Selective ligand dissociation reaction:

A' + $P(OPh)_3$ ⇌ **24** ⇌ **B'** + CO
ΔG = +17.78 kcal/mol **ΔG = +34.87 kcal/mol**

C' + $P(OPh)_3$ ⇌ **26** ⇌ **B'** + dimethylfumarate
ΔG = +3.87 kcal/mol **ΔG = +11.52 kcal/mol**

C' + CO ⇌ **7** ⇌ **A'** + dimethylfumarate
ΔG = +24.08 kcal/mol **ΔG = +14.64 kcal/mol**

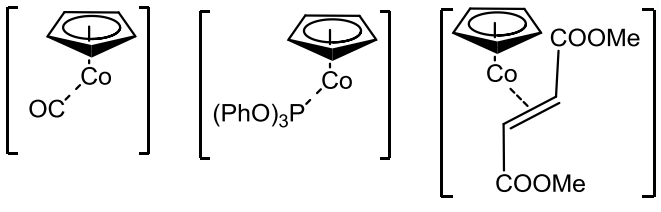

A' **B'** **C'**

Scheme 28: Calculations on the formation of the new complexes **24**, **26** and **7** and free energies of ligand dissociation from **1**, **24**, **26** and **7** at BP86/TZVP level

This is in accordance with the experimental results showing that **24** is formed at ambient temperatures while the formation of **7** requires heating to 70-80 °C and irradiation with light. The calculated energy difference of 3.15 kcal/mol however does not seem to reflect the difference in required activation energy for those two reactions. This difference therefore has to be attributed to dissimilar transition states or rather activation barriers.

The substitution of the second CO ligand and formation of **26** has been found to have a free computed energy of 23.35 kcal/mol. Thus the generation of **26** is less favored than the formation of **24**. This reflects the experimental results which showed that the application of irradiation is required to produce **26**.

The stability of complexes **24**, **26** and **7** towards ligand dissociation has also been computed. Again it can be seen that the phosphite ligand $P(OPh)_3$ has a lower computed dissociation energy in both cases (**24** and **26**) and dissociates before the CO or dimethylfumarate ligand leading to the $16e^-$ complexes **A'** or **C'** respectively.

It is also found that a combination of phosphite and olefin ligand lowers the dissociation energies of both ligands immensely (17.78 kcal/mol vs. 3.87 kcal/mol and 14.64 kcal/mol vs. 11.52 kcal/mol). This is in accordance with the results obtained from the catalytic activity screening experiments, where it was found that a ligand combination of phosphite and olefin is superior to a combination of phosphite-CO or olefin-CO.

The computed ligand dissociation energies suggest an increase in stability in the order: **26** (3.87 kcal/mol) < **7** (14.64 kcal/mol) < **24** (17.78 kcal/mol), which is consistent with the decrease in catalytic activity, yet not the experimentally found stability towards air.

3.4.3 DFT Calculations for the Synthesis of Chelating Complexes Starting from **1**

The syntheses of the two investigated complexes containing (potential) chelating ligands (**17** and **30**) have been studied with DFT calculations as well (Scheme 29). The reactions of **1** with **17** or **30** releasing one CO ligand and yielding **31** and **32** respectively are both endergonic and require energy as indicated by the computed free energies (11.50 kcal/mol and 13.42 kcal/mol respectively). This is surprising since these simple substitution reactions proceed at room temperature without the need of any additional activation.

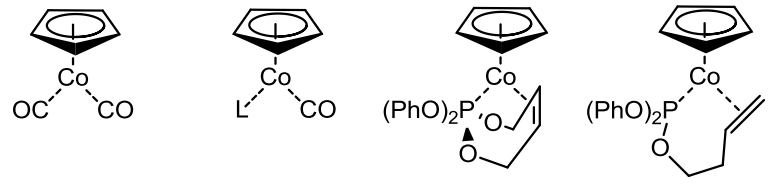

1 **31** (L = **17**) **32** (L = **30**) **33** **34**

(*i*) Ligand exchange reaction:

1 + **17** ⇌ **31** + CO
ΔG = +11.50 kcal/mol

1 + **30** ⇌ **32** + CO
ΔG = +13.42 kcal/mol

31 ⇌ **33** + CO
ΔG = +9.76 kcal/mol

32 ⇌ **34** + CO
ΔG = +16.93 kcal/mol

Scheme 29: Calculations on the formation of the new complexes **31**-**34** from **1, 17** and **30** at BP86/TZVP level

The release of the second CO ligand and the following coordination of the olefin moiety of **17** and **30** to yield the chelated complexes **33** and **34** were computed next. The computed energies required for the chelation are in the range of the first substitution reaction (9.76 kcal/mol and 16.93 kcal/mol respectively), which is interesting since the conversion of neither **31** to **33** nor **32** to **34** can be achieved thermally but only under irradiation with light (at least in the case of **32**).

Additionally it appears that a chelation of the CpCo(I)-fragment with **17** requires much less energy – 7.17 kcal/mol – than a chelation with **30**. This is astonishing since the experimental results show that only **34** can be isolated as a pure compound while **33** or an intermediate beforehand decomposes to **35**.

3.5 *In situ* NMR Spectroscopy of Photocatalytic Cycloaddition Reactions

In situ NMR spectroscopy is a great tool to observe short-lived species during a reaction. However, there are only a few reports on light induced reactions that have been studied using NMR spectroscopy. One example is the photoisomerization of NHC-ruthenium hydride complexes that has been investigated. Because the sample was irradiated outside and afterwards quickly transferred into the NMR, no real *in situ* experiment was performed. [109]

In situ irradiation NMR studies in solution are rare. There are only single reports, for example Linehan et al. studied the photolysis of cymantrene derivatives in supercritical fluids using a high-pressure NMR tube and an optical fibre connected to a HeCd laser inside the NMR. [110] The observation of homolysis of the Mn-R bond and its dependency on the alkyl group in $[Mn(R)(CO)_3(bisimin)]$ compounds has been studied using *in situ* NMR spectroscopy by Rossenaar et al. [111] The photoisomerization of azobenzenes has been studied in an *in situ* experiment as well. Here Jones et al. could only detect the short-lived isomers when a constant irradiation of the solution maintained the concentration of the transient species at a certain level. To achieve this an optical fibre was used to deliver light from a CW argon/krypton laser directly into the sample inside the NMR magnet. [112] A great review on *in situ* photochemistry with NMR detection has been written by Ball focussing on the investigation of organometallic complexes. [113]

Since a large array of the previously described CpCo(I)-complexes has been synthesized via photochemical substitution reactions (see chapters 3.1.2-4), it seemed to be interesting to record a time-resolved progess of the reaction – maybe even to measure kinetics – and to investigate whether one would be able to see a potential intermediate.

The experimental setup for our *in situ* NMR spectroscopy experiments consisted of a sapphire NMR tube which enabled us to connect an optical fiber using a Ti flange. [114] The system was sealed using a Viton o-ring to maintain the inert gas atmosphere. With an inner diameter of 7 mm, the NMR tube provided a cross-section greater than or equal to that which is given by the optical fiber, so that the radiation could penetrate the Ar atmosphere above the liquid without any significant loss of intensity. The refraction index of the sapphire and of the angle of incidence contributed to full reflection of the light that may hit the inner wall of the NMR tube before penetrating the liquid (Figure 14).

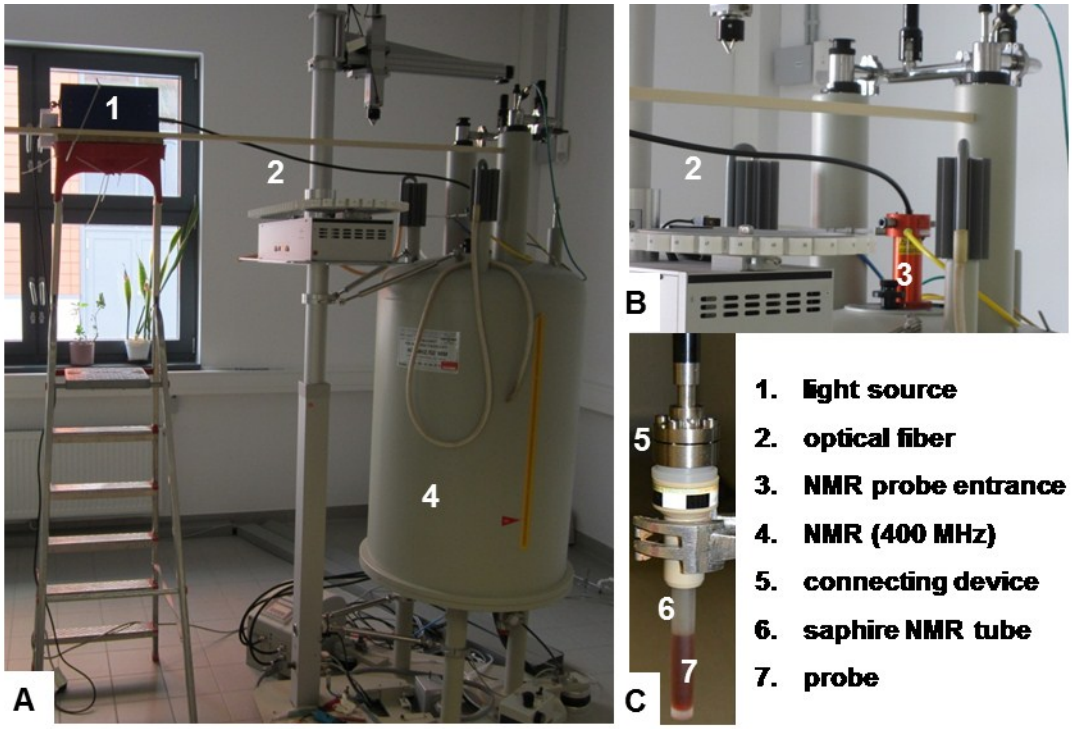

Figure 14: Experimental setup for the *in situ* NMR spectroscopy; **A**: optical fiber connecting NMR spectrometer with the light source; **B**: close-up of the entrance of the NMR; **C**: custom-made NMR tube with reaction mixture and connected optical fiber

In the following three different photochemically-induced ligand substitution reactions (inter- as well as intramolecular) as well as the degradation of the coordinated phosphite ligand **17** in **31** will be investigated and the results discussed.

3.5.1 Reaction of **3** to **18**

The first reaction studied was the reaction of **3** and triphenylphosphite to yield **18**. This simple substitution reaction can easily be monitored via ^{1}H NMR and ^{31}P NMR spectroscopy. The shift in the ^{31}P NMR spectrum using C_6D_6 as a solvent from 127.3 ppm of the free $P(OPh)_3$ to 157.3 ppm of the coordinated phosphorus ligand can be traced straightforwardly. The overlay of the recorded ^{1}H NMR spectra after various irradiation intervals also proves that **18** is formed. The new signals appearing belong to **18** as well as the released and now uncoordinated 1,5-cyclooctadiene (cod) (Figure 15).

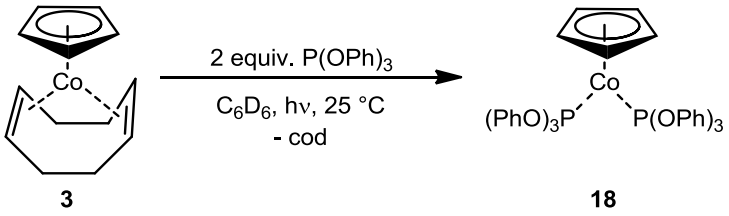

3 **18**

Scheme 30: Substitution reaction of **3**

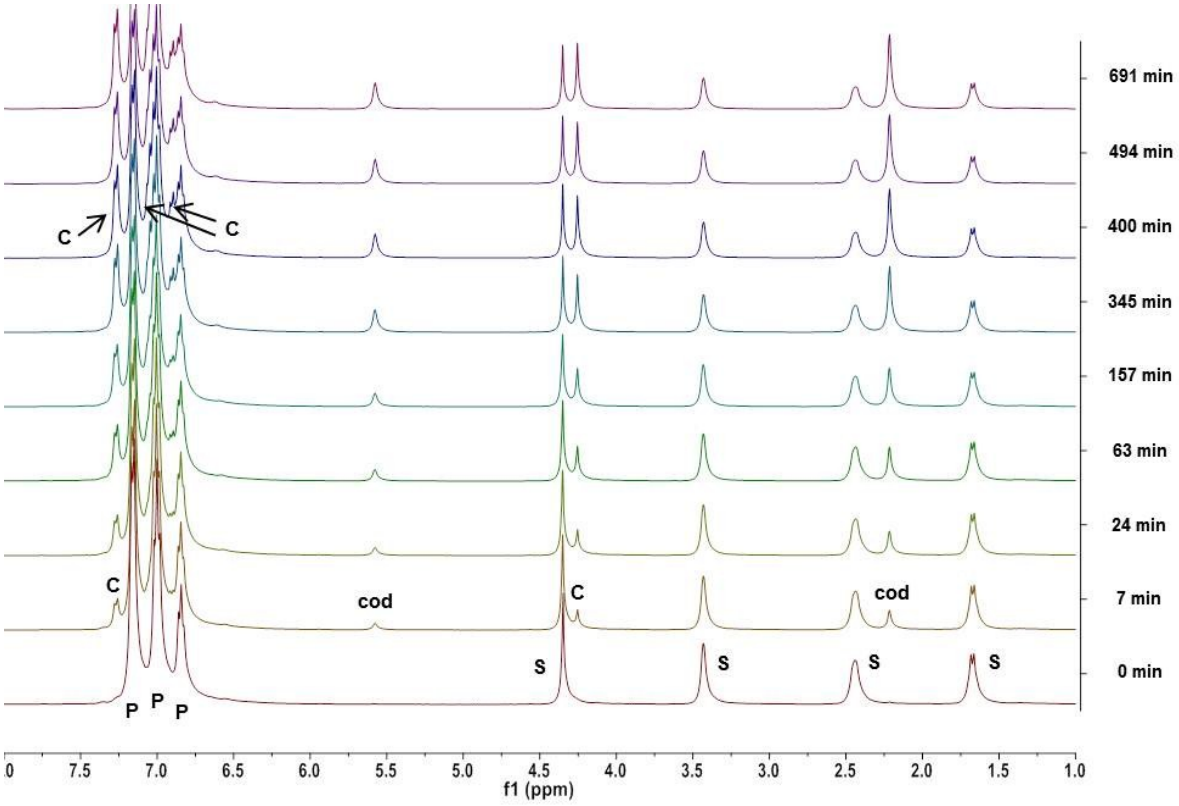

Figure 15: Overlay of the recorded ^{1}H NMR spectra (**S**: [CpCo(cod)] (**3**); **P**: $P(OPh)_3$; **cod**: free cod; **C**: $[CpCo\{P(OPh)_3\}_2]$ (**18**))

The reaction progress is best depicted if the integrals of starting compound and product are plotted against the irradiation time. Since the starting compound **3** is exclusively converted to **18** both complexes can be equalized with the amount of coordinated cod and free cod respectively. Therefore the ^{1}H NMR signals of either the CH or CH_2 groups of coordinated and free cod can be used as a reference for the ratio of **3** to **18**. Both sets of integrals led to the same result. Figure 16 shows the resulting graph for the integration of the CH_2 resonances of the cod exemplarily.

It is interesting that after a very fast initiation phase the conversion of **3** slows down and seems to reach a saturation phase. After irradiation of the solution for 11½ h the reaction was

stopped since further conversion was proceeding very slowly. This stagnation of the reaction can presumably be attributed to the missing stirring of the solution and the difference in light intensity throughout the solution leading to a conversion gradient in the NMR tube.

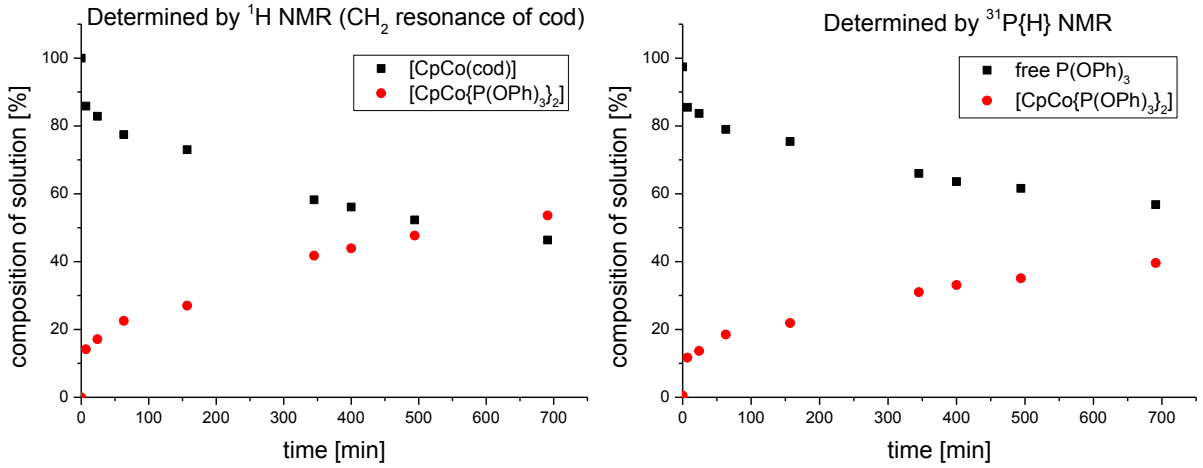

Figure 16: Composition of the reactant solution determined by ^{1}H NMR using the CH_2 resonance of the coordinated and free cod (left) and by ^{31}P{H} NMR (right)

The signals of free and coordinated triphenylphosphite in the ^{31}P{H} NMR can also be used to quantitatively determine the ratio of **3** to **18** (Figure 16, right). However, the results do not equal those obtained from the integration of the ^{1}H NMR spectra. While the trend of the reaction is similar, different ratios and a lower final conversion are established.

3.5.2 Reaction of **23** to **25**

The synthesis of CpCo-olefin-phosphite-complexes through a photochemical substitution reaction as previously described (see chapter 3.1.3) was also studied.

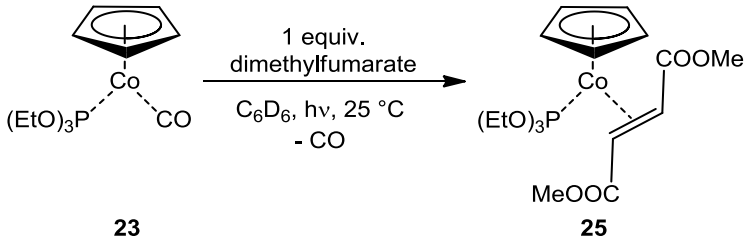

23 **25**

Scheme 31: Substitution reaction of **23**

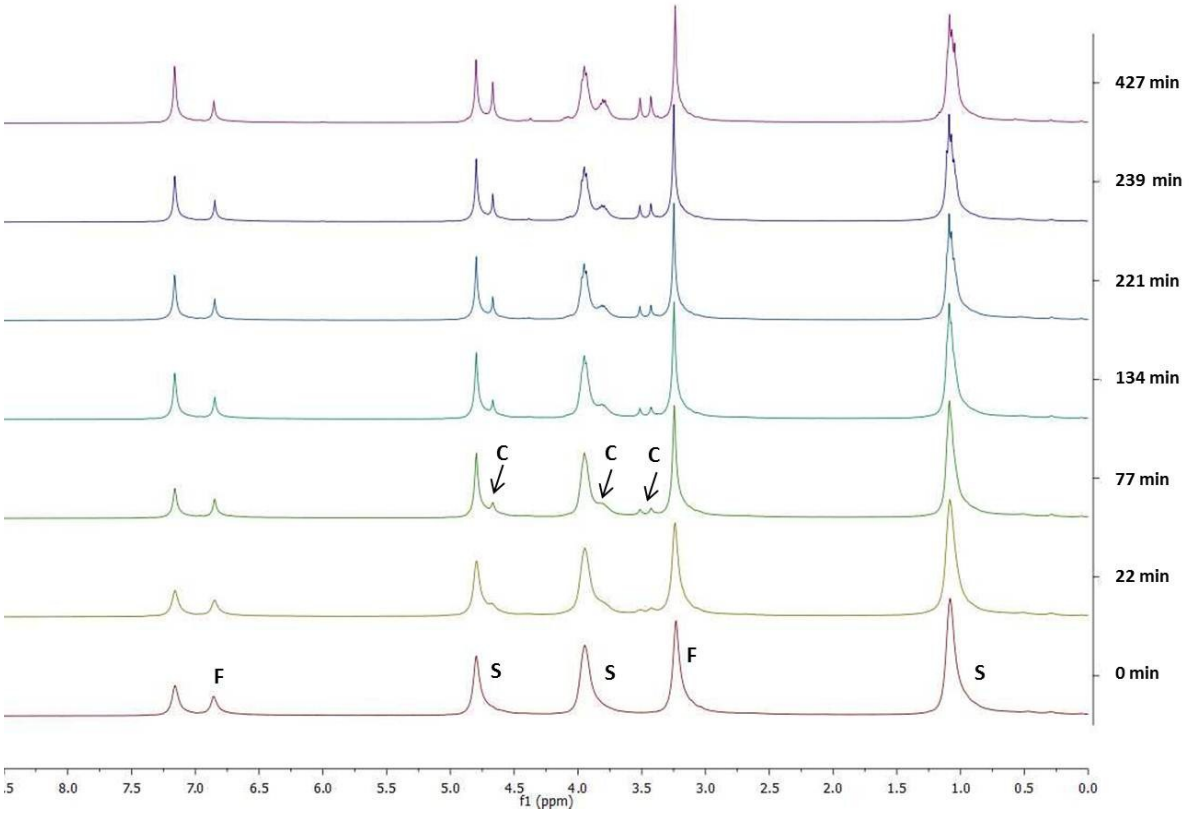

Figure 17: Overlay of the recorded ^{1}H NMR spectra (**S**: [CpCo(CO){P(OEt)$_3$}] (**23**); **F**: free dimethylfumarate; **C**: [CpCo(dimethylfumarate){P(OEt)$_3$}] (**25**))

Here the reaction of **23** with dimethylfumarate to yield **25** was studied exemplarily. Figure 17 shows quite nicely how the new Cp-resonance and the two signals of the methyl groups of the coordinated dimethylfumarate in **25** emerge. Plotting the composition of the reaction mixture against the irradiation time, the generation of **25** from **23** becomes apparent. Again the reaction process can be best monitored if the ^{1}H NMR resonances – here the CH_3 resonances of the free and coordinated dimethylfumarate – are used (Figure 18). The employment of the ^{31}P{H} NMR signals for **23** and **25** results in a similar plot, but depicts lower conversions (Figure 18, right). This resembles the results as described before for the reaction of **3** to **18**.
The low overall conversion of **23** to **25** can again be attributed to the absence of a stirring device.

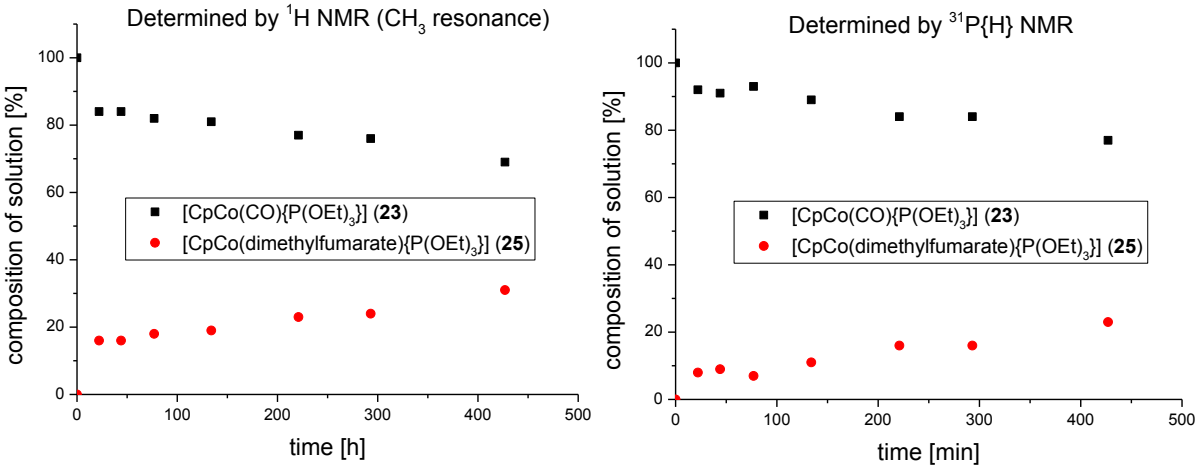

Figure 18: Composition of the reactant solution determined by ^{1}H NMR using the CH_3 resonance of the coordinated and free dimethylfumarate (left) and by ^{31}P{H} NMR (right)

3.5.3 Reaction of **31** to **35**

The decomposition of **31** seemed to be another very interesting reaction to study with *in situ* NMR spectroscopy. Therefore a sample of **31** in deuterated benzene was prepared and irradiated inside the NMR.

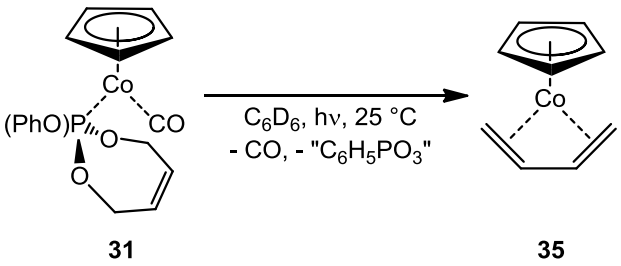

Scheme 32: Photolysis reaction of **31**

Figure 19 shows the recorded ^{1}H NMR spectra over time. As one can easily recognize no change in the reaction mixture can be observed. The experiment was therefore stopped after almost 5 h of irradiation. Upon removal of the NMR tube from the NMR spectrometer it became obvious why no reaction occurred. On top of the solvent a thick black layer had formed. This black residue was always observed in the decomposition reaction of **31** to **35** and consists mainly of phosphorus and cobalt. Usually if the solution is stirred this decomposition product deposits on the ground and can be easily separated. Unfortunately in

the NMR tube the high intensity of the light on the surface of the solution and the absence of stirring resulted in the formation of a thick black layer on top of the solution. This "pellet" hampers the incoming light from entering the reaction mixture and hence no reaction progress can be monitored in the ^{1}H and $^{31}P\{H\}$ NMR spectra. This result clearly marks the disadvantages and limits of the *in situ* NMR spectroscopy for photocatalytic reactions by our approach, especially for conditions that involve only the diffusion of reactants.

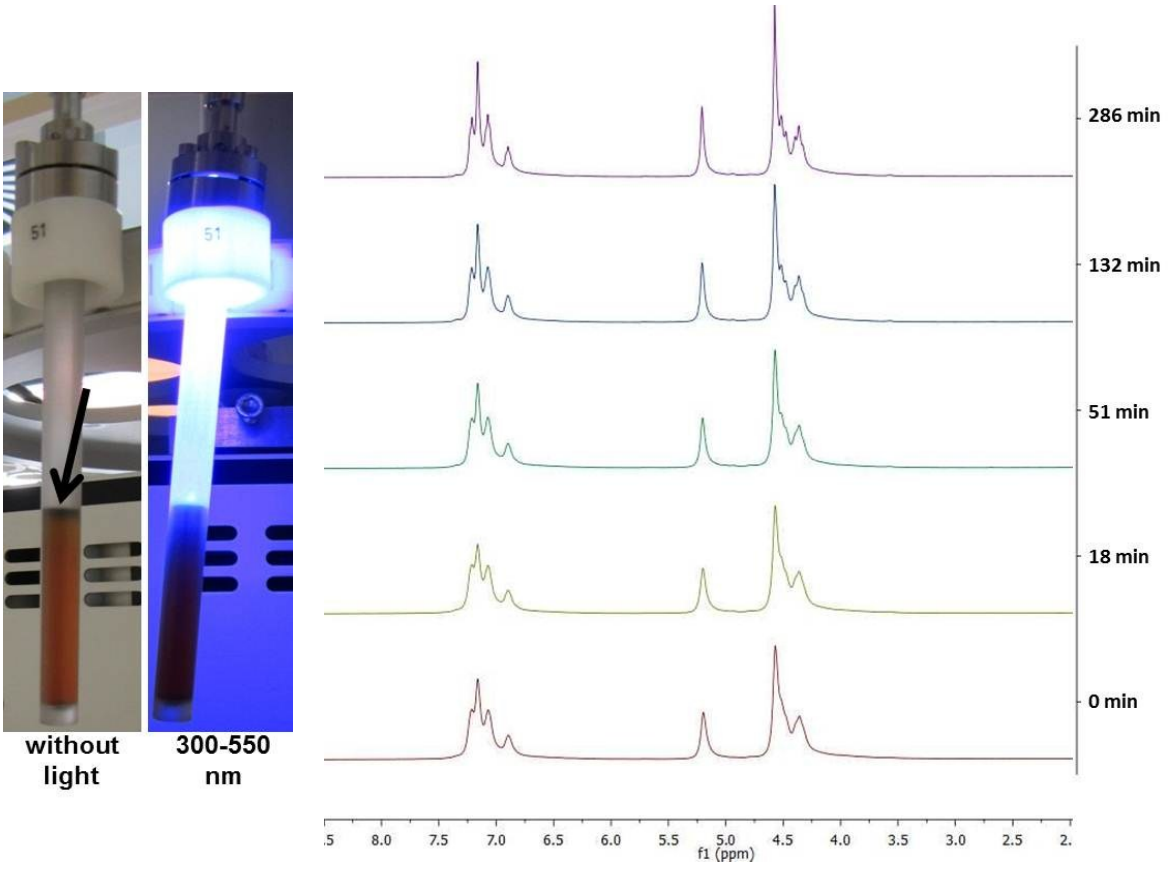

Figure 19: Left: custom-made NMR tube with reaction mixture after irradiation (arrow indicates the black pellet of decomposition products at the surface of the solution); right: overlay of the recorded ^{1}H NMR spectra of **31**

3.5.4 Reaction of **32** to **34**

The final reaction that was studied with *in situ* NMR spectroscopy was the synthesis of **34** containing a chelating phosphite-olefin ligand through irradiation of **32**. Since this reaction is an intramolecular reaction, the absence of stirring should not be of such a great influence. Only the difference in light intensity in the solution (from top to bottom) should affect the reaction.

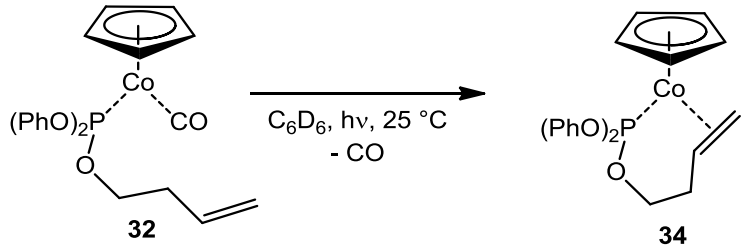

Scheme 33: Substitution reaction and chelatization of **32**

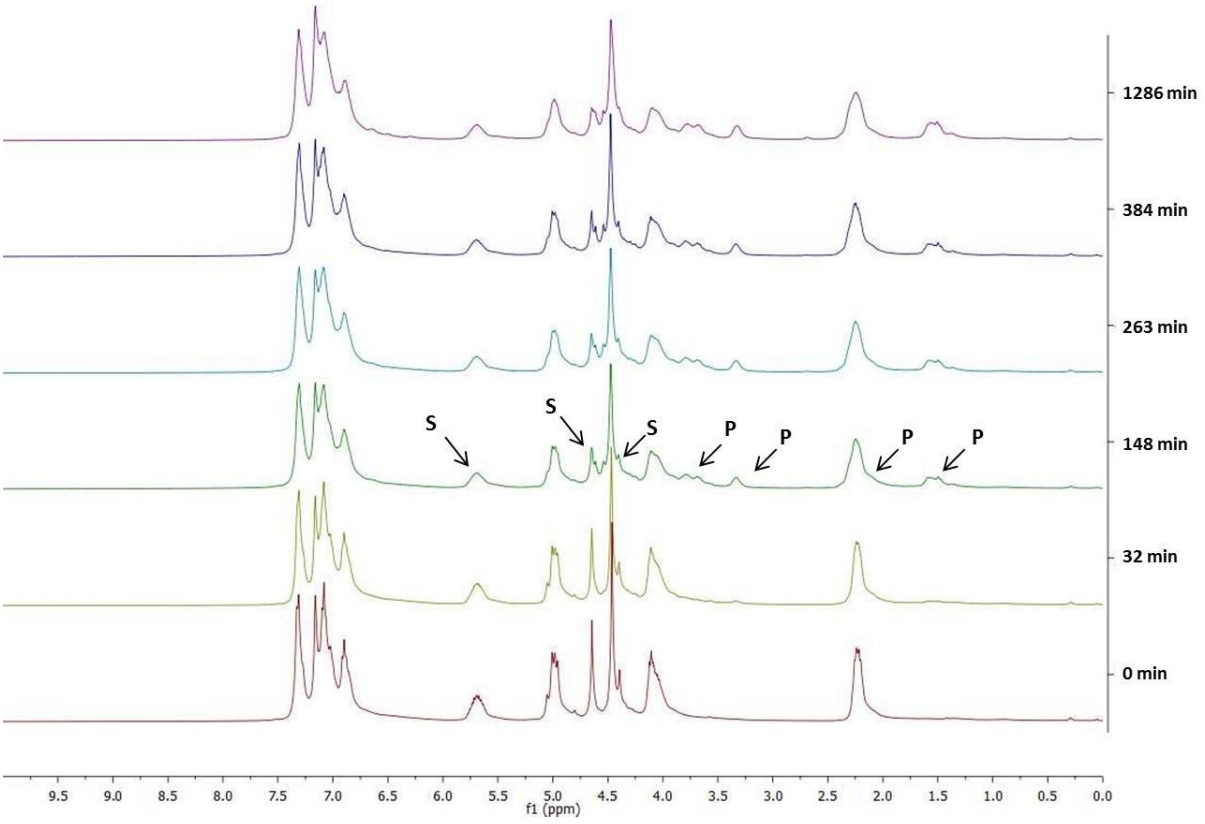

Figure 20: Overlay of the recorded ^{1}H NMR spectra (**S**: [CpCo(CO)(**30**)] (**32**); **P**: [CpCo(**30**)] (**34**))

Indeed, after a first fast transformation phase of **32** to **34** the reaction almost comes to a halt. To check whether longer irradiation times would make up for the absence of a stirring device the probe was irradiated over night, but the long reaction times, as Figure 20 and Figure 21 show, do not improve the yield of **34** to a significant extent.

Nevertheless the progress of the reaction can be easily followed by ^{1}H NMR. The new signals correlating to the coordination of the free olefin moiety of the phosphite ligand and therefore the successful formation of **34** can easily be identified (Figure 20). Again the composition of

the reaction mixture can be plotted against the irradiation time to visualize the reaction progress.

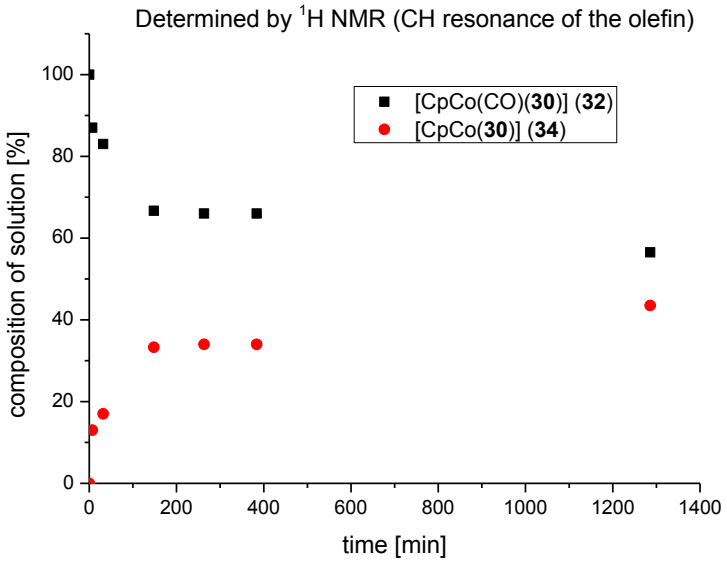

Figure 21: Composition of the reactant solution determined by ^{1}H NMR using the CH resonances of the olefin of substrate and product complex

Exemplarily the results from the integration of the free and coordinated CH resonance of the olefin moiety are shown in Figure 21. The result is illustrated in an identical manner if the CH_2 group of the olefin or one of the CH_2 groups of the linker is used. In this case the ^{31}P NMR spectra could not be used as a second tool for the determination of the reaction mixture's composition, since **32** exists in three different conformers due to different arrangements of the phosphite phenyl groups. Therefore only a shift in the intensity towards the most upfield signal at 163 ppm during the reaction to **34** can be accounted for.

While these four experiments represent some of the few *in situ* irradiation experiments inside the NMR and therefore a novelty themselves, they have also shown how important a sufficient mixing of the solution is for the progess of the photochemically induced reaction even if it is proceeding intramolecularly. The absorption of the light through the solution is another factor that can not be left aside. The longer the distance through the solution the higher the decrease in light intensity. Since the NMR only records the spectrum in a certain small volume, it is necessary to keep the solvent level above this area to a minimum.

3.6 CpCo-Based Solid Phase-Supported Catalysts for the [2+2+2] Cycloaddition Reaction

Up to now only very few examples of polymer-bound complexes have been reported for the use in [2+2+2] cycloaddition reactions as already mentioned before (see chapter 1.3). The only example for a cobalt catalyst linked via a cyclopentadienyl ligand to a support material has been reported by Perkins and Vollhardt, where they described a polystyrene-supported version of $[CpCo(CO)_2]$. However, this complex did not achieve the intended high recyclability, but decomposed quickly affording the desired cycloaddition product in only mediocre yields. [74] The support of one of the newly synthesized air-stable complexes **25** or **26** on a solid phase would therefore represent a big step towards a more conveniently recoverable catalyst for the [2+2+2] cycloaddition reaction.

Polystyrene has been used as a support material to covalently bind cyclopentadienyl complexes of various metals such as titanium, [69b, 115] zirconium, [115b] hafnium, [115b] rhodium, [116] cobalt [74, 116-117] and iron. [118]

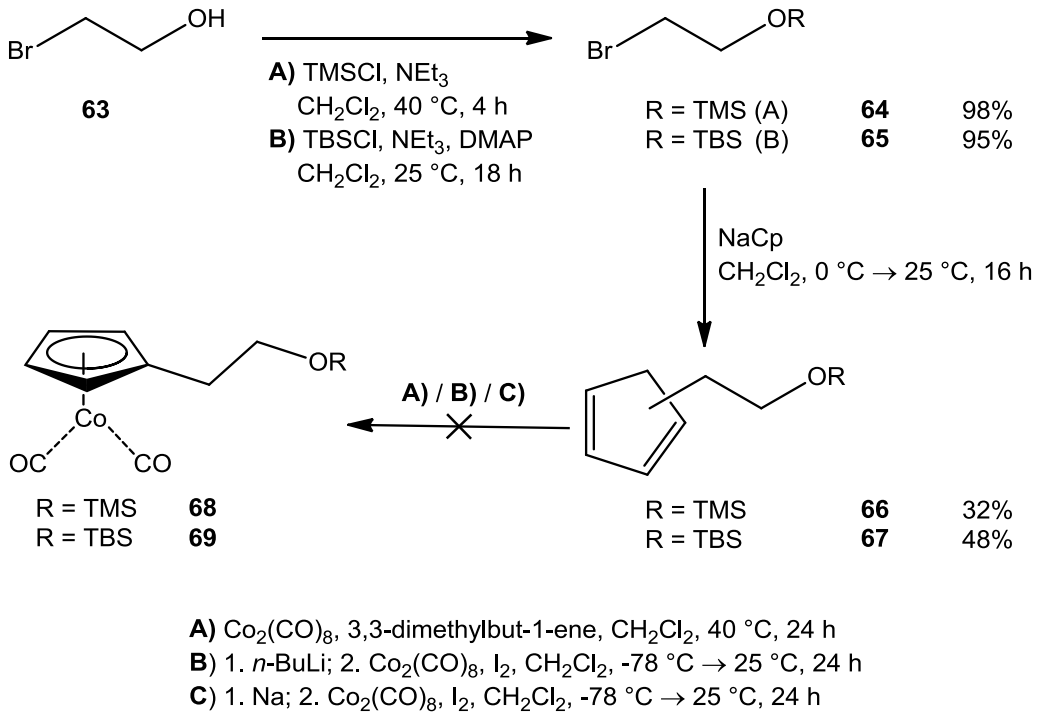

Scheme 34: Synthesis of substituted cyclopentadiene derivatives and attempted synthesis of $Cp^{OR}Co(CO)_2$ complexes

However, the initial idea to support **25** or **26** on Merrifield resin, a copolymer of styrene and chloromethylated divinylbenzene, which offers due to the chloromethyl moiety the possibility to easily connect other functional groups such as hydroxyl moieties, proved to be not successful. The synthesis of hydroxyl-functionalized Cp-derivatives was only accomplished in mediocre yields and especially the synthesis of the respective cobalt(I)-complexes **68**-**69** did not work out as anticipated (Scheme 34). [119] Additionally, the maximum loading of commercially available Merrifield resin with 5.5 mmol Cl/g is by far too low for (elemental) analysis of the final catalyst.

A promising alternative seemed to be sol-gel-supported complexes since there had been reports on similar rhodium(I)-complexes being still active in hydrogenation reactions after being supported on a sol-gel. [120] To covalently bind a complex in these sol-gel matrices a different linker – containing a siloxane moiety – was needed.

3.6.1 Solid Support Material: Sol-Gel – Synthesis of Silyl-Containing Cyclopentadiene Derivatives

Analogously to the previously synthesized substituted cyclopentadiene derivatives (3-bromopropyl)trimethoxysilane (**70**) was reacted with sodium cyclopentadienyl to yield the two regioisomers **71** in 60% yield after bulb-to-bulb distillation of the crude reaction product (hereafter **71** will be abbreviated as HCp^{Si}).

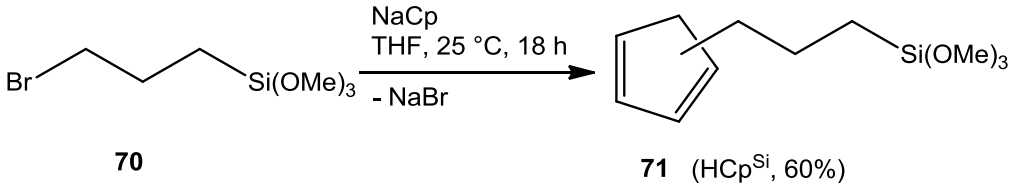

Scheme 35: Synthesis of silylated cyclopentadienyl derivative **71**

3.6.1.1 Synthesis of $Cp^{Si}Co(CO)_2$-Complexes

Following the procedure Blum et al. [120] published for the synthesis of their silyl-substituted CpRh(I)-complexes, **71** was reacted with sodium sand overnight and the evolution of hydrogen gas could be observed. The reaction mixture was then added to a freshly prepared

solution of the Co(I)-source generated by the reaction of $Co_2(CO)_8$ and iodine finally yielding **72** in 17% yield. Because **72** could not be isolated as a pure compound but always contained a significant amounts of free **71**, the earlier described route with 2,2-dimethylbut-1-ene as a hydrogen acceptor was tested as well. [119a] Refluxing $Co_2(CO)_8$, **71** and 2,2-dimethylbut-1-ene in dichloromethane for 72 h resulted after filtration in the deep red, liquid compound **72** in 93% yield (Scheme 36).

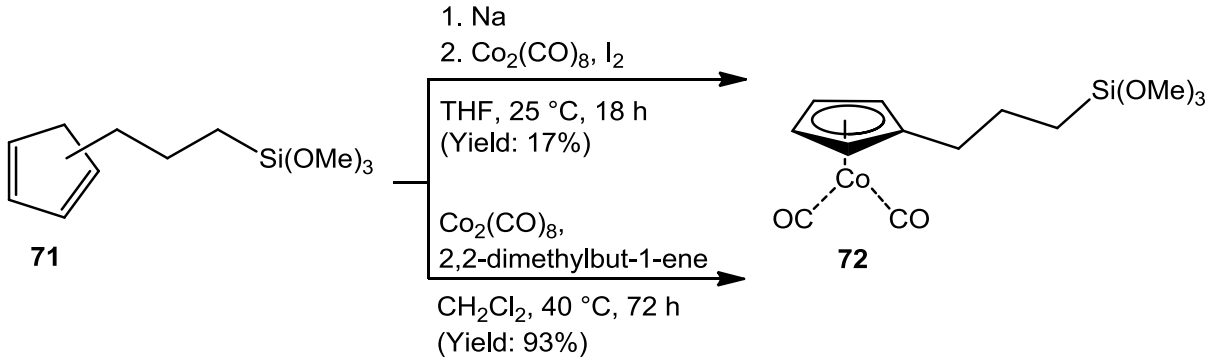

Scheme 36: Synthesis of $[Cp^{Si}Co(CO)_2]$ (**72**)

3.6.1.2 Ligand Substitution of the Silylated $Cp^{Si}Co(CO)_2$-Complex

The substitution of CO ligands of CpCo(I)-complexes with phosphite as well as olefin ligands has already been demonstrated before (chapters 3.1.3 / 3.1.4). In addition there have been some reports on the replacement of a carbonyl ligand in complexes containing substituted cyclopentadienyl derivatives. As an example the thermal replacement of a CO ligand with a phosphine ligand in a $Cp^{sub}Rh(I)$-complex should be mentioned, [54, 121] and a substitution for an alkene ligand was also achieved by irradiation of a $Cp^{sub}Co(I)$-complex. [54] However, there are no reports on the successive replacement of both carbonyl ligands in $[Cp^{sub}Co(CO)_2]$ complexes.

According to the previously described protocol (see chapter 3.1.3) **72** was reacted with triethylphosphite at room temperature to yield **73** in 74% yield (Scheme 37). The addition of one equivalent dimethylfumarate and irradiation of the solution led to the desired complex $[Cp^{Si}Co(MeO_2CCH{=}CHCO_2Me)\{P(OEt)_3\}]$ (**74**) in 51% yield after precipitation from a *n*-pentane solution at -78 °C.

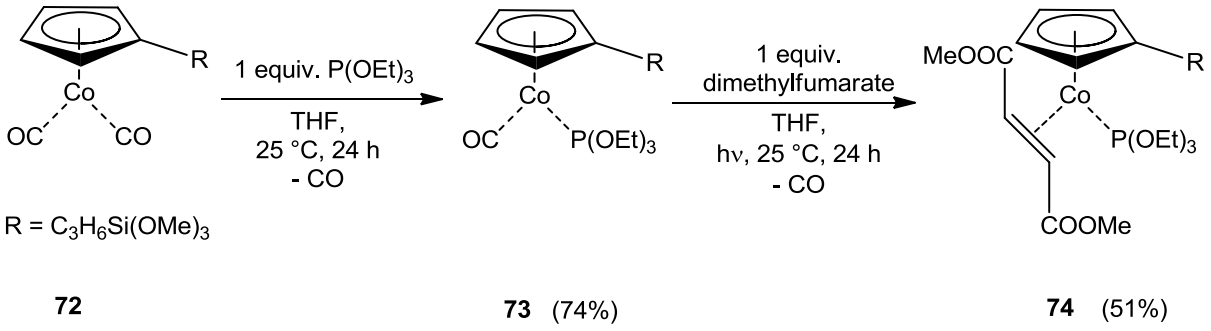

Scheme 37: Substitution of the CO ligands in [$Cp^{Si}Co(CO)_2$] (**72**)

A different route to obtain **74** starts with the generation of [$Cp^{Si}Co(cod)$] (**75**) by reacting [$CoCl(PPh_3)_3$] (**81**) with a freshly prepared sodium derivative of **71**. Cobalt complex **81** is a standard precursor for the generation of Co(I)-complexes with coordinated (substituted) cyclopentadienyl derivatives. [87, 92c, 122] The resulting [$Cp^{Si}Co(PPh_3)_2$]-species can then be converted to **75** by adding cod and stirring the solution at 60 °C over night (Scheme 38). The residual triphenylphosphine is removed according to a procedure published by Lipshutz and Blomgren using Merrifield resin and sodium iodide. [123]

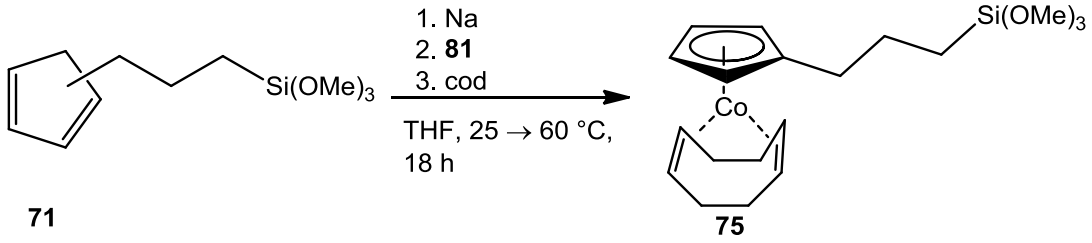

Scheme 38: Synthesis of [$Cp^{Si}Co(cod)$] complex **75**

The substitution of cod in **75** with a triethylphosphite and a dimethylfumarate ligand did not lead to the expected results. **75** was irradiated with light in the presence of 1 equivalent of triethylphosphite and 10 equivalents of dimethylfumarate. Instead of the desired complex **74**, only the respective bis(phosphite) complex [$Cp^{Si}Co\{P(OEt)_3\}_2$] and starting compound could be recovered. This result is in accordance with the previously performed experiment to generate the mixed olefin-phosphite complex **11** starting from **3**, triphenylphosphite (1 equiv.) and trimethylvinylsilane (10 equiv.) yielding only a 2:2:1 mixture of **3**, **18** and **11** after irradiation with light (see chapter 3.1.2).

3.6.1.3 Synthesis of Sol-Gel-Supported [Cp^{Si}Co(dimethylfumarate){$P(OEt)_3$}] (SG-(**74**)) and [Cp^{Si}Co(cod)] (SG-(**75**))

To obtain a solid phase-bound catalyst system the silylated CpCo(I)-complexes **74** and **75** have to be covalently trapped inside a sol-gel matrix. Blum et al. developed a procedure which can also be applied for air-sensitive compounds. [120] Therefore an acidic solution of $Si(OMe)_4$, methanol and the respective cobalt complex was stirred at room temperature before it was neutralized and left to gel. The wet gel was dried under high vacuum over night and washed extensively with dichloromethane to remove any not covalently bound catalyst. SG-(**74**) and SG-(**75**) were obtained as deep red coarse solids.

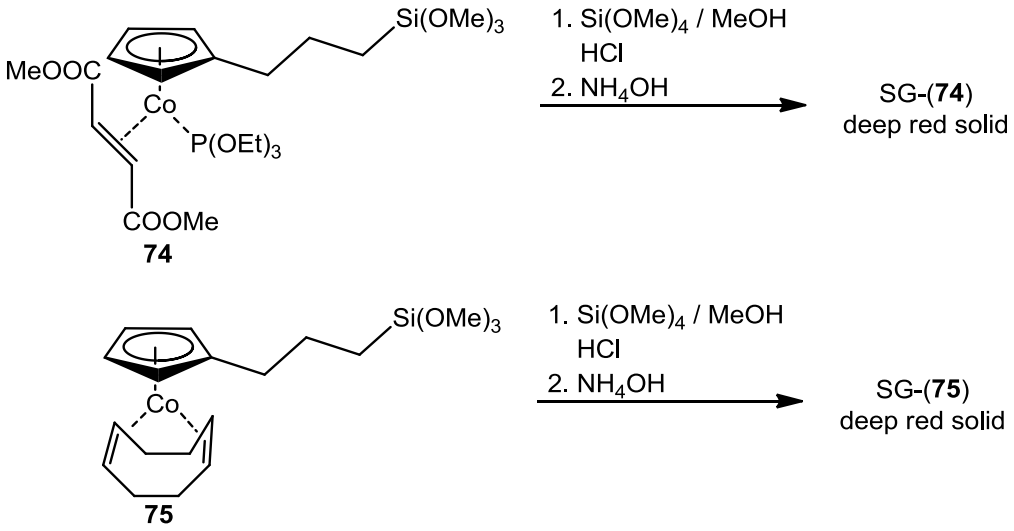

Scheme 39: Synthesis of sol-gel-supported SG-(**74**) and SG-(**75**)

One important discovery was the observation that is was essential that the complex was added to the acidic solution before it was neutralized (method 2) – in contrast to the procedure by Blum et al., who added the complex together with the base (method 1) – because this way ensured a better fixation of the complex. Following the published procedure almost half of the catalyst could be washed out and recovered after the gelation process. The actual catalyst loading has been determined through elemental analysis.

3.6.1.4 Catalytic Screening of Sol-Gel-Supported Catalysts SG-(**74**) and SG-(**75**)

Having successfully synthesized the sol-gel-supported complexes SG-(**74**) and SG-(**75**), both were applied in the [2+2+2] cycloaddition test reaction between **36** and **40** to assess their catalytic activity as well as recoverability and recyclability.

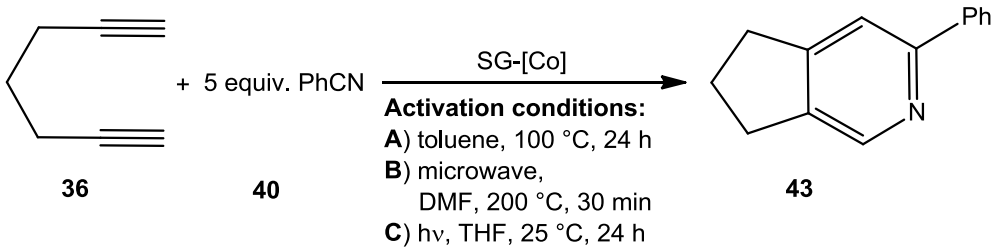

Scheme 40: Catalytic test reaction between 1,6-heptadiyne (**36**) and benzonitrile (**40**)

Table 7: Screening of catalytic activity and recycability of SG-(**74**) and SG-(**75**)

Entry	Catalyst (Preparation)	Catalyst Loading	Activation Conditions	Cycle	Yield [%]	Color of used Catalyst
1	SG-(**74**) (method 1)	5.6 mol%	**A**	1	19	red
				2	5	red-brown
				3	3	red-brown
2	SG-(**74**) (method 1)	5.6 mol%	**B**	1	0	bright green
3	SG-(**74**) (method 2)	5.1 mol%	**A**	1	0	red
				2	0	red
				3	0	red
4	SG-(**75**) (method 1)	3.3 mol%	**A**	1	0	green
5	SG-(**75**) (method 1)	3.3 mol%	**B**	1	0	bright green
6	SG-(**75**) (method 1)	3.3 mol%	**C**	1	7	brown-red
				2	0	bright green

While SG-(**75**) proves to be inactive under thermal, microwave and irradiation conditions (Table 7, entry 4-6), SG-(**74**) shows some activity in toluene at 100 °C even though the yield of **43** with SG-(**74**) is as low as 19% after the first cycle and even decreases in the second and third cycle (Table 7, entry 1). Interestingly, applying either sol-gel catalyst in a catalytic trial within the microwave leads to the immediate decomposition of the catalyst and no conversions at all (Table 7, entry 2 and 5). The solution turns orange, hinting at a solvated complex due to extensive complex leaching, while the support material turns bright green.
Comparing the reactivity of SG-(**74**) synthesized after method 1 and method 2 shows yet another interesting result. SG-(**74**), prepared after method 2, exhibits no activity whatsoever (Table 7, entry 3) whereas SG-(**74**), prepared after method 1, does yield the desired product **43** (Table 7, entry 1). This activity of SG-(**74**) can therefore be attributed to catalyst leaching, suggesting the free and soluble **74** to be the active species and not the sol-gel-supported version. The very tight network of the sol-gel matrix might inhibit the diffusion of the reactants to the catalytic active center and hence be an explanation why the catalyst is inactive under various conditions. While Blum et al. reported on successful hydrogenation experiments, [120] **36** and **40** are extensively larger molecules that have to enter the sol-gel matrix in order to get to the catalysts active site. This might be circumvented if a linker molecule is present between the siloxane moieties of the network, allowing larger pores in the gel.

3.6.1.5 Synthesis of a Linker Containing Sol-Gel-Supported Complex

$[Cp^{Si}Co(dimethylfumarate)\{P(OEt)_3\}]$ (SGL-(**74**))

To achieve the synthesis of a more loosely woven sol-gel, the potential linker has to contain a somewhat rigid unit to allow the generation of larger pores. The commercially available 1,4-bis(trimethoxysilylethyl)benzene seemed to be a good candidate as it has a rigid benzene moiety and additional ethyl spacers. The respective sol-gel was synthesized according to the same procedure as before (method 2). After addition of the basic solution the liquid gelled within one minute. The gel was dried under high vacuum over night and washed extensively with dichloromethane. The desired porose coarse SGL-(**74**) was obtained as a red solid.

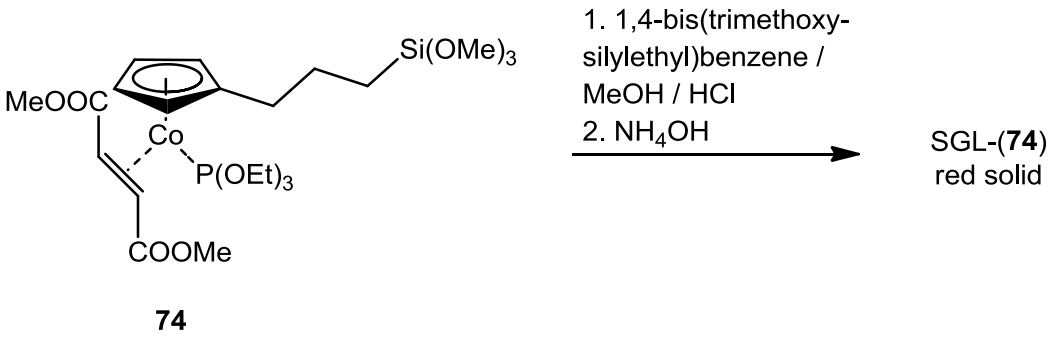

74

Scheme 41: Synthesis of sol-gel-supported SGL-(**74**)

3.6.1.6 Catalytic Screening of Sol-Gel-Supported Catalysts SGL-(**74**)

The SGL-(**74**) was immediately tested in the reaction between **36** and **40** under the same conditions as before (Scheme 40).

Table 8: Screening of catalytic activity and recyclability of SGL-(**74**)

Entry	Catalyst (Preparation)	Catalyst Loading	Activation Conditions	Cycle	Yield [%]	Color of used Catalyst
1	SGL-(**74**) (method 2)	1.6 mol%	**A**	1	4	red-green
				2	0	green

The lack of activity of SGL-(**74**) indicates that the sol-gel matrix is still not sufficient porous to allow the substrates to penetrate the solid material. It is questionable whether the 4% yield of **40** (Table 8) can be attributed to the larger pore size of the gel foundation compared to SG-(**74**) or if it is caused by a leaching of the solid catalyst, even though SGL-(**74**) was prepared after method 2, which reduces the amount of leached catalyst.
Nevertheless, in account of the experimental results, sol-gel appears not to be a suitable solid support for **74** and its application in [2+2+2] cycloaddition reactions.

3.6.2 Solid Support Material: Silica

Next to organic macromolecules and polymers, inorganic surfaces can also act as support materials. Here the catalyst is covalently bound to the surface of the support material. Silica is a widely used support material for different organometallic compounds.

There are various reports on silica-supported palladium catalysts for Heck coupling reactions [124] and hydroformylation reactions have been successfully carried out with rhodium-complexing dendrimers on silica. [125] A silica-bound chiral Co-salen complex for the highly efficient and enantioselective epoxide ring-opening has been reported by Annis and Jacobsen. [117b] There have even been reports on silica gel-supported cobalt dicarbonyl complexes for the use in olefin hydroformylation reactions. [67]

The employment of silica as the solid support material has the additional advantage that **74** can be used without further modifications, since the trimethoxysiloxane moiety can interact with the free hydroxyl groups on the silica surface.

3.6.2.1 Synthesis of Silica-Supported [Cp^{Si}Co(dimethylfumarate){$P(OEt)_3$}] (SiO_2-(**74**))

The simplest procedure to attach Cp^{sub}Co(I)-complexes to silica has been described by Brintzinger et al. who stirred silica and the respective complex in toluene at 80 °C for 12 h. [67a] An alternative preparation method was reported by Booth et al., who first equilibrated the silica with an aqueous sodium hydroxide solution before adding the complex and heating the suspension at 80 °C for 4 h. [67b]

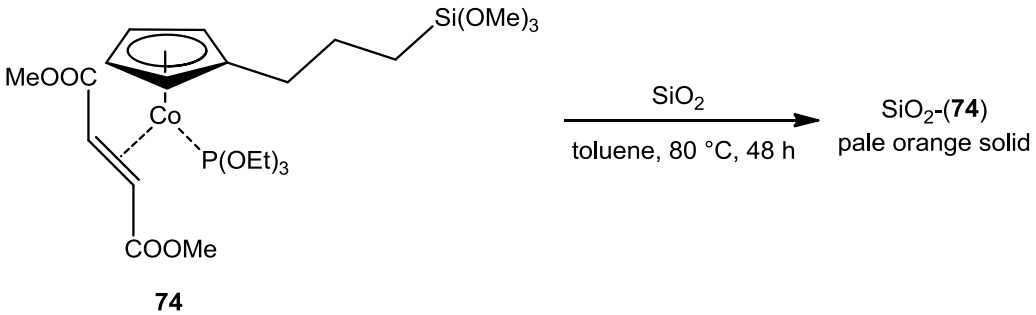

Scheme 42: Synthesis of silica-supported SiO_2-(**74**)

Following Brintzingers procedure SiO_2-(**74**) was synthesized without problems (Scheme 42). The resulting pale orange solid was extracted in a Soxhlet apparatus before it was dried under vacuum. The cobalt loading was determined by elemental analysis as well as inductively coupled plasma atomic emission spectroscopy (ICP-AES).

3.6.2.2 Catalytic Screening of Silica-Supported Catalysts SiO_2-(**74**)

The newly synthesized SiO_2-(**74**) was again tested in the [2+2+2] cycloaddition reaction between **36** and **40**.

In contrast to SG-(**74**) and SGL-(**74**) the silica-based catalyst SiO_2-(**74**) yields 21% of pyridine **43** already after 4 h at 100 °C (Table 9, entry 1). This is roughly one fifth of the yield which is achieved with the homogeneous complex **25** in the same amount of time and under the same conditions. The catalyst can easily be removed from the reactant solution by filtration, but the yield drops in the consecutive two cycles.

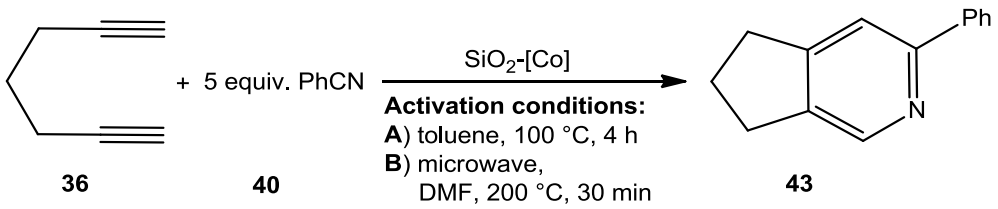

Scheme 43: Catalytic test reaction between 1,6-heptadiyne (**36**) and benzonitrile (**40**)

Table 9: Screening of catalytic activity and recyclability of SiO_2-(**74**)

Entry	Catalyst (Preparation)	Catalyst Loading	Activation Conditions	Cycle	Yield [%]	Color of used Catalyst
1	SiO_2-(**74**)	8.1 mol%	**A**	1	21	pale orange
				2	11	orange-brown
				3	9	brown-orange
2	SiO_2-(**74**)	8.1 mol%	**B**	1	47	pale orange
				2	5	yellow-green

Applying microwave conditions to SiO_2-(**74**) resulted in 47% of **43**, but this very good yield could not be repeated in a second cycle (Table 9, entry 2). Since the reactivity of SiO_2-(**74**) under microwave conditions decreased immensely after the first cycle, different solvents were screened to check whether DMF was deactivating the complex. Unfortunately all other solvents such as xylene, DMSO or water led to even lower yields. In the case of DMSO the solution turned deep red suggesting that **74** was released from the silica support.
Since the Cp-ring is covalently bound to the silica surface it can be presumed that the low yields in the consecutive cycles did not result from catalyst leaching but rather from catalyst decomposition or inhibition.

These results clearly demonstrate that the respective Co(I)-complex has to be bound to the surface of the solid support in order to achieve a conversion of the substrates. However, silica still seems to be not the ideal support material. Just recently an active copper(I)-NHC-catalyst for click chemistry has been reported and dramatic effects towards the recyclability of the compound depending on the support material have been described. [126] While the use of silica flakes and silica nano particles allowed recycling of the catalyst three times, the application of magnetite/silica nanoparticles yielded a supported catalyst that could be recycled up to eleven times with only slight loss in yield. These results suggest that the right supporting material has a rather large effect on the stability as well as recyclability of the catalyst. Maybe in employing slightly different silica-based supporting materials the catalytic activity and recyclability of SiO_2-(**74**) could be improved.

3.7 Enantioselective [2+2+2] Cycloaddition Reactions

After successfully synthesizing a number of active CpCo(I)-bis(phosphite) complexes (see chapter 3.1.2) and demonstrating the positive effect of phosphite ligands in heteroleptic CpCo(I)-systems in homogeneous solution as well as bound to a solid phase (see chapters 3.2 and 3.6), the idea to synthesize chiral Co(I)-complexes with phosphite ligands seemed to be a sensible evolution.

Up to date iridium(I)- [28c-e, 78-80] and rhodium(I)-systems [85-86] predominate the enantioselective [2+2+2] cycloaddition reactions, whereas only a few enantioselective cobalt-catalyzed [2+2+2] cycloadditions are known. While most Ir(I)- and Rh(I)-systems are *in situ* generated by a simple metal precursor and the addition of chiral ligands such as (R)-BINAP [76-77] or MeDUPHOS. [28c-e, 78-79] For cobalt chiral cyclopentadienyl or indenyl complexes are synthesized and isolated beforehand. The perhaps best known complex is the chiral menthyl-derived indenyl-based Co(I)-complex (**10**) reported by Gutnov and Heller et al., [87] which was applied in several of enantioselective cycloaddition reactions. [88-89, 127]

Based on this system a chiral menthyl-derived indenyl-based Co(I)-complex with phosphite ligands should be possible to derive straightforwardly. Nevertheless not only the application of phosphites in defined chiral complexes was supposed to be investigated, but also the application of cobalt(I) for *in situ* systems for enantioselective [2+2+2] cycloaddition reactions. Here not only the application of chiral coordinating ligands was of interest, but rather the extraordinary chiral induction through asymmetric counter anions, which is described by the principle of asymmetric counter anions-directed catalysis (ACDC).

3.7.1 Synthesis of a Defined Chiral Indenyl-Co(I)-Phosphite-Complex

Since CpCo(I)-phosphite complexes were recognized as good catalysts for cyclization reactions at moderate temperatures (50 °C, see chapter 3.2.1.2) the applicaton of phosphite ligands in chiral Co(I)-complexes was targeted next.

As described above Heller et al. established a photochemically activated indenylcobalt(I)-based complex with cod as the neutral ligand. The exchange of the cod ligand for phosphite ligands should not present any problems. Accordingly the synthesis of chiral complex **76** was achieved in very good yield starting from **10** [87] using the same photochemical substitution

reaction as described for **18**-**22** (chapter 3.1.3). The chiral indenyl ligand (Ind*) was not affected by the reaction (Scheme 44).

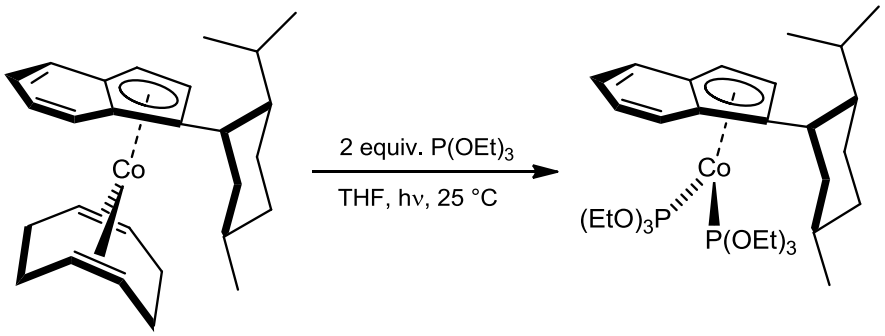

10 **76** (74%)

Scheme 44: Synthesis of the chiral complex **76**

While **10** has already been assessed in the [2+2+2] cycloaddition reaction between diynes and nitriles to form biaryl systems under photochemical conditions, [88] **76** should represent a system that can be activated at mild temperatures, since [CpCo{P(OEt)$_3$}$_2$] (**19**) proved to be very active in the trimerization reaction at 50 °C (see chapter 3.2.1.2).

As a test reaction the cycloaddition between **51** and **40** yielding biaryl **52** with an enantiomeric excess of (*R*)-**52** was chosen (Scheme 45).

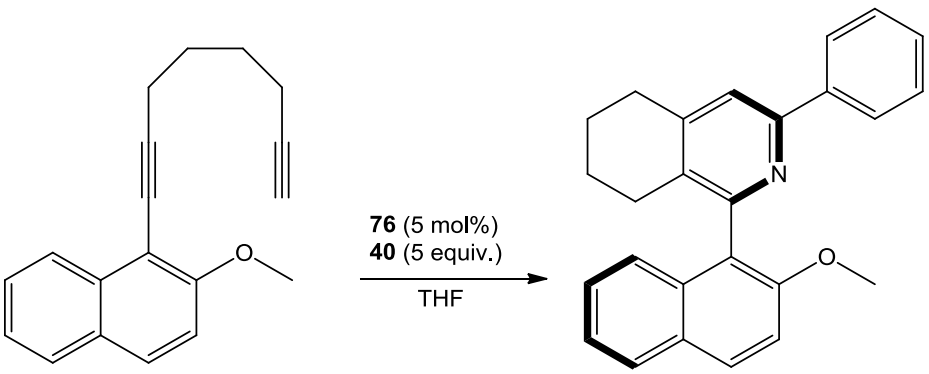

51 **52**

Scheme 45: Test reaction for **76**

The reaction between **51** and **40** in the presence of 5 mol% **76** proceeded very slowly at 50 °C. After reaction times as long as 70 h only 20% of **52** with an enatiomeric excess of 66% *ee* could be obtained. Raising the temperature to 80 °C resulted in higher yields and shorter reaction times, but also in lower *ee* values. The lower *ee* value for the reaction carried out at 80 °C can be attributed to the partial racemization of the biaryl product **52**. Earlier

studies concerning the racemization process of biaryls including **52** showed that racemization occurs at temperatures above 80 °C. [88, 128]

Table 10: Condition screening for **76**

Entry	Solvent	Temperature [°C]	Time [h]	Yield [%]	*ee* [%]
1	THF	50	70	20	66 (*R*)
2	toluene	80	24	54	27 (*R*)
3	THF	-20, hν	24	2	--
4	THF	0, hν	24	18	64 (*R*)

Although **76** only led to low to mediocre yields and *ee* values, these experiments represent the first enantioselective cobalt-catalyzed [2+2+2] cycloaddition with a thermally activated chiral cobalt complex.

3.7.2 *In situ* Systems Containing Chiral Anions

Yet another approach in catalysis is the generation of an active catalyst *in situ* from several precursors. The asymmetric counter anion-directed catalysis (ACDC) – a field primarily pushed forward by List et al. – stands for a principle similar to that of a chiral coordinating ligand, which induces a specific chirality during the reaction and hence in the product. [129]
There are different asymmetric activation modes starting with a) the coordinative interaction of a chiral ligand with a metal center, b) single or multiple hydrogen bonding interaction of a chiral organocatalyst and c) electrostatic interaction between a chiral anion and a cationic reaction intermediate. [129e] The induction of enantioselectivity in a reaction which proceeds through a cationic intermediate by means of ion pairing with a chiral, enantiomerically pure anion is termed asymmetric counter anion-directed catalysis.
Chiral anions can be simple chiral organic acids such as amino acids, mandelic acid or camphorsulfonic acid or various borates, but the most common used chiral anions are phosphoric acid derivatives such as Δ–TRISPHAT (**77**), (*R*)-VAPOL hydrogen phosphate (**78**) and (R)-3,3'-bis(2,4,6-triisopropylphenyl)-1,1'-binaphthyl-2,2'-diyl hydrogen phosphate (**80**) to name a few examples (Scheme 46). [130]

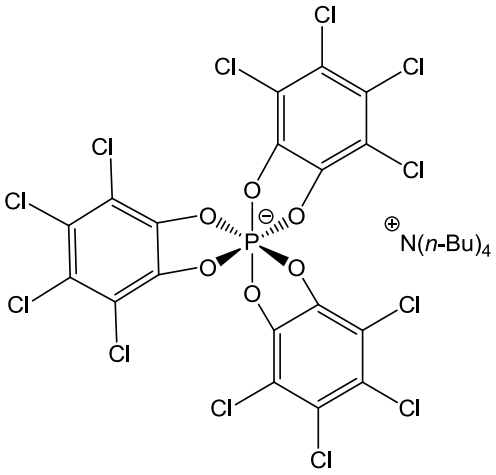

Δ-TRISPHAT tetrabutylammonium salt (**77**)

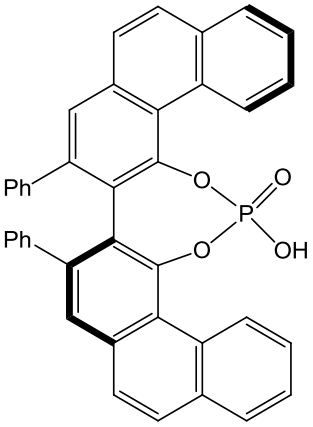

(*R*)-(-)VAPOL hydrogen phosphate (**78**)

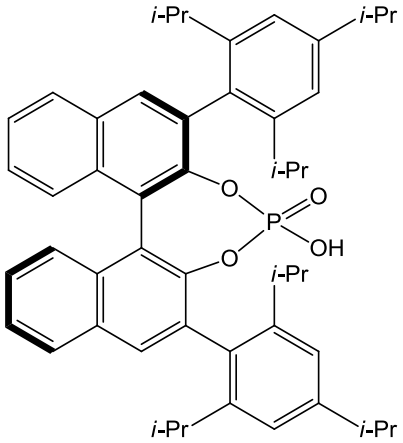

(*R*)-3,3'-bis(2,4,6-triisopropylphenyl)-1,1'-binaphtyl-2,2'-diyl hydrogen phosphate (**80**)

Scheme 46: Examples for chiral anions used in ACDC

Recent examples of asymmetric catalysis by chiral counter ions in combination with transition metals are the ruthenium-catalyzed hydroxyalkylation of butadiene applying chiral phosphates, [131] the epoxidation of alkenes with an achiral manganese(III)-salen complex and a chiral phosphate [132] and the enantioselective intramolecular hydroalkoxylation of allenes by a binuclear gold(I)-complex and the silver salt of a chiral phosphate. [133] The latter reaction only proceeded with good enantiomeric excess if chiral anions were used, while gold(I)-complexes with chiral phosphine ligands led to no enantiomeric excess. In all these reactions the presence of the chiral anion in the vicinity of the positively charged metal center induced the desired enantioselectivity.

Since up to now the effect of chiral anions on Co(I)- or Rh(I)-catalyzed [2+2+2] cycloaddition reactions has not been explored yet, the application of Co(I)- and Rh(I)-precursor complexes in combination with chiral anions – particularly chiral phosphates – seems worthwhile

investigating in greater depth. A potential model substrate has to be either prochiral or contain sterically bulky groups in order to stop a racemization of the product after a successful cyclotrimerization reaction. To compare reactivities and selectivities with established catalytic systems the model substrate was chosen on the basis of Shibata's previous investigations towards Ir(I)-catalyzed intramolecular [2+2+2] cycloaddition reactions and the formation of atropisomers (Scheme 47). [79]

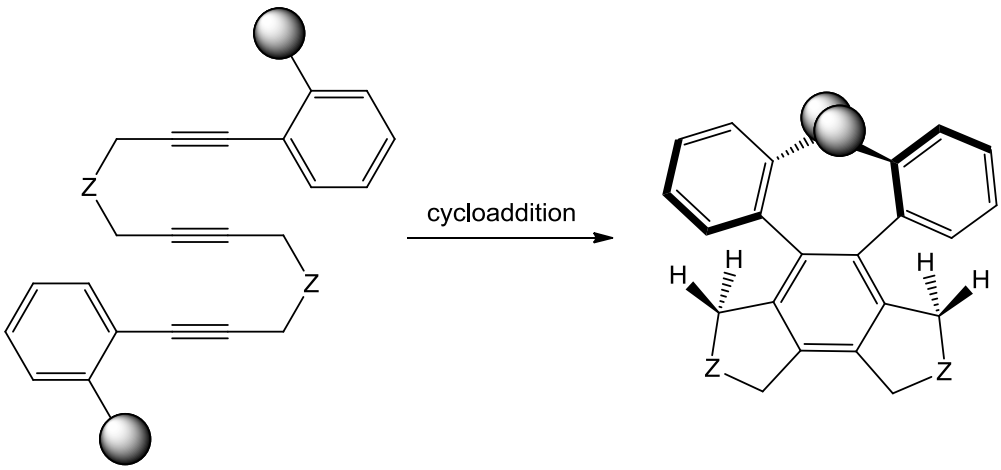

Scheme 47: Generation of chiral atropisomers from a triyne

3.7.2.1 Cobalt

The cobalt(I)-complex $[CoCl(PPh_3)_3]$ (**81**) is a standard precursor for the generation of Co(I)-complexes with η^5-bound cyclopentadienyl derivatives. [87, 92c, 122] There have been some reports on the catalytic activity of **81** in hydrogenation reactions, [134] ethylene dimerization, [135] hydrodimerization of methyl acrylate [136] and cyclodimerization of cyclobutadiene, [137] but there have not been many reports on its catalytic activity in [2+2+2] cycloaddition reactions. Butenschön reported on the trimerization of tolane with 97% yield, [55] but only Chung et al. published a more detailed study on the reactivity of **81** in trimerization reactions. [138] They showed that **81** could cyclotrimerize a number of terminal alkynes as well as internal alkynes with electron-withdrawing groups. Disubstituted alkynes with not sufficiently electron-withdrawing groups such as 2-butyne or 3-phenylpropyne did not form the respective benzene derivatives.

Complex **81** was therefore tested in the intramolecular cyclization of **53** and **54** and was found to yield **55** and **56** in 98% and 85% respectively after 1 min at room temperature with a catalyst loading of 5 mol%. These great results set the foundation for further investigations. In

order to achieve and induce selectivity, a substrate had to be chosen which after a potential stereoselective cyclization reaction would not be able to rotate freely. In the case of triyne **82** the cyclotrimerisation reaction results in the formation of two new atropisomeric bonds leading to stable atropisomers. Triyne **82** with bulky naphthyl-groups was synthesized starting from **53** and 1-iodonaphthalene applying a Sonogashira coupling.

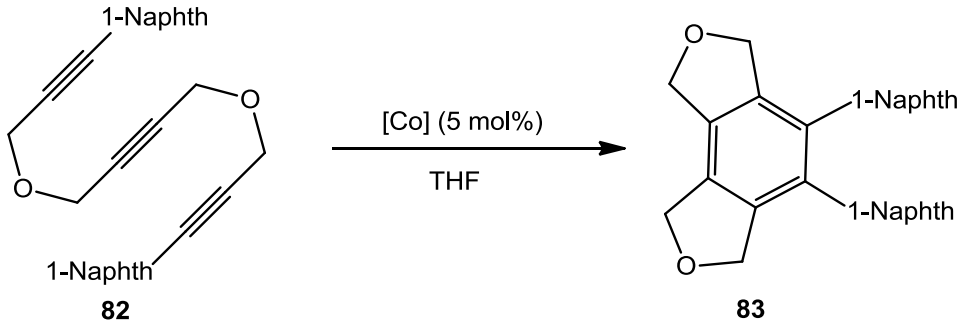

82 **83**

Scheme 48: Test reaction for the *in situ*-generated chiral catalysts

Table 11: Catalyst screening using **81** and various chiral anions

Entry	Catalyst System [a]	Yield [%]	d/l : meso [b]	*ee* [%] [c]
1	no chiral anion	59	1.1:1	0
2	**77**	73	1.3:1	0
3	**77**/ AgOTf	0	--	0
4	**78** / NEt_3	67	1.1:1	0
5	**79** / NEt_3	94	2.2:1	0
6	**80** / NEt_3	76	1.2:1	0
7	$CoBr_2$ / dppe / Zn / ZnI_2 / **78** / NEt_3	41	1:2.2	0

[a] reaction conditions: **81** (5 mol%), 5 mol% chiral anion, 25 °C, 1 h; [b] ratio determined by integration of peak areas in the ^1H NMR; [c] *ee* values determined by chiral HPLC

Because **81** by itself proved to catalyze the cyclotrimerization reaction of **82** in moderate yields (Table 11, entry 1) in just 1 h, it seemed promising to investigate the influence of chiral anions on the reactivity of **81**. Abstraction of the chloride ion with a silver salt to achieve a better influence of the chiral non-coordinating anion resulted only in the catalyst's decomposition and no reaction at all, which was unexpected since there have been reports on the silver-mediated chloride abstraction from **81**. [134b] Therefore in all further experiments the chiral anions had to compete with the coordinated chloride anion.

All chiral anions used (Δ-TRISPHAT tetrabutylammonium salt (**77**), (*R*)-VAPOL hydrogen phosphate (**78**), (*R*)-3,3'-bis[3,5-bis(trifluoromethyl)phenyl]-1,1'-binaphthyl-2,2'-diyl hydrogen phosphate (**79**) and (*R*)-3,3'-bis(2,4,6-triisopropylphenyl)-1,1'-binaphthyl-2,2'-diyl hydrogen phosphate (**80**)) induced no enantiomeric excess, but yielded the racemate. In all cases the *d*/*l*-form of **83** was the major product and the *meso*-form the minor.

Interestingly the application of all chiral anions resulted in higher yields with the reaction of **79** leading to the isolation of 94% of **83**, being a prime example.

Another *in situ* system involving a Co(II)-source and the *in situ* reduction to Co(I) with Zn/ZnI_2 – as Hilt et al. described before – [139] only led to mediocre yields and no enantiomeric excess as well (Table 11, entry 7).

These results led to believe that the chiral anion would be too far away from the active center to have any influence on the reaction, although Gandon et al. reported on an enantioselective Ir(I)-catalyzed carbocyclization of 1,6-enynes by a chiral anion approach, where $[IrCl(CO)(PPh_3)_2]$ in the presence of the chiral anion *(R)*-3,3′-bis(2,4,6-triisopropylphenyl)-1,1′-binaphthyl-2,2′-diyl (**80**) phosphate achieved enantioselectivities up to 93% *ee*. [140]

3.7.2.2 Rhodium

The equivalent of **81** containing a heavier group homolog is represented by the commercially available and widely applied Wilkinson catalyst $[RhCl(PPh_3)_3]$ (**2**). [141] There are a number of reports on its application in [2+2+2] cycloadditions, [141d, 142] some of them taking place at mild conditions and temperatures as low as 20 °C. [17a, 143]

Therefore **2** was tested in the intramolecular cyclization reaction of **82** (Scheme 49). After 4 h at room temperature **2** yielded 52% of **79**, which could even be increased to 70% if silver bis(trifluoromethanesulfonyl)amide, $AgNTf_2$, was added to the solution, abstracting the chloride ion from **2** (Table 12, entry 1-2).

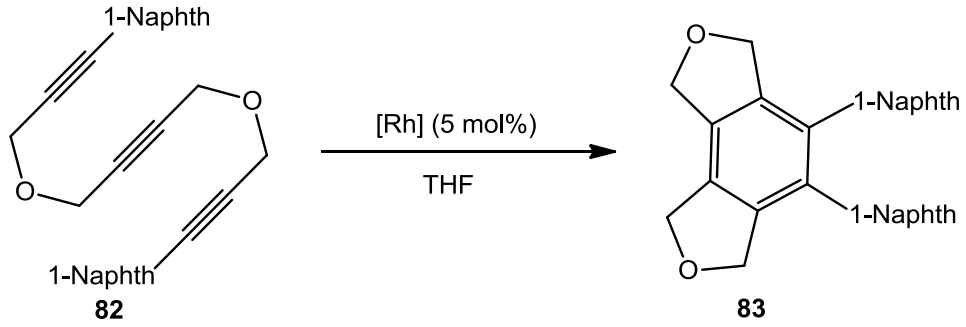

Scheme 49: Test reaction for the *in situ* generated chiral catalysts

Table 12: Catalyst screening using **2** and various chiral anions

Entry	Catalyst System [a]	Yield [%]	d/l : meso [b]	*ee* [%] [c]
1	no chiral anion / no Ag^+ salt	52	1:1.5	0
2	no chiral anion	70	1:1.2	0
3	**77**	53	1:1	0
4	**78** / NEt_3	43	1:1.4	11
5	**79** / NEt_3	49	1:2.1	5
6	**80** / NEt_3	41	1:1.9	0
7	**78** / NEt_3 [d]	12	1:1.3	0
8	**79** / NEt_3 [d]	21	1:4.3	3
9	Ag_2O / **78** / NEt_3 [d]	38	1:2.7	5
10	$[RhCl\{P(OPh)_3\}_2]_2$ [e]	20	1:1.5	0
12	$[Rh(cod)_2]BF_4$ / **78** / NEt_3 [f]	20	1.1:1	0

[a] reaction conditions: **2** (5 mol%), $AgNTf_2$ (5 mol%), 5 mol% chiral anion, 25 °C, 4 h; [b] ratio determined by integration of peak areas in the ^1H NMR; [c] *ee* values determined by chiral HPLC; [d] 10 °C, 23 h; [e] no chiral anion; [f] 24 h

While the addition of **77** or **80** did not lead to any enantiomeric excess at all (Table 12, entry 3+6), **78** and **79** led to low *ee* values of 11% and 5% respectively (Table 12, entry 4-5). The yields are always between 40-50% with the meso form of **83** being the major product and the d/l form being the minor product. If the cyclization reaction was run at 10 °C the yields decreased to around 20% even though the reaction was run for 23 h, with no improvement of the *ee* values (Table 12, entry 7-9).

The use of different Rh(I)-catalysts such as $[RhCl\{P(OPh)_3\}_2]_2$ or $[Rh(cod)_2]BF_4$ led to low yields with no enantiomeric excess at all (Table 12, entry 10-12). $[RhCl(CO)(PPh_3)_2]$ even proved to be absolutely inactive in the test reaction. As these results cleary show, **2** proved to be superior to any other Rh(I)-complex with **78** being the single chiral anion that could induce some enantiomeric excess. Just recently Aubert, Fensterbank and Ollivier et al. reported the use of a preconditioned system containing $[RhCl(cod)]_2$ in combination with Ag-**80** and the bisphosphine ligand 1,4-bis(diphenylphosphino)butane (dppb) – the purpose of the latter being to stabilize the Rh(I)-complex – for the [2+2+2] cycloaddition reaction between diynes and isocyanates. [144] They were able to yield *ee* values up to 82% showing that the chiral anion approach sometimes resulted in better *ee* values that the convential approach with chiral ligands. Thus this displays the great influence of the composition of the catalytic system and the importance of sufficient stabilization of the Rh(I)-fragment (addition of chelating phosphine ligands), but also the still limited application to certain model substrates, in this case the synthesis of pyridones.

However, the usage of **2** in combination with well-known chiral ligands led to moderate to good *ee* values between 42-87%. While *P*,*P*-ligands such as (*R*)-BINAP resulted in no *ee* values worth mentioning (Table 13, entry 1), the use of certain chiral *P*,*N* ligands such as (*R*)-QUINAP or (*R*,*R*)-*O*-PINAP resulted in moderate *ee* values of 49% and 61%, respectively (Table 13, entry 2+7). Only (*R*,*R*)-*N*-PINAP led to mediocre 27% enantiomeric excess (Table 13, entry 5). Accordingly, the (*S*)-derivatives – namely (*S*)-QUINAP, (*R*,*S*)-*N*-PINAP and (*R*,*S*)-*O*-PINAP – led to similar or even better *ee* values of -42%, -87% and -85% repectively, while favoring the other enantiomer (Table 13, entry 4, 6, 8).

Turning to a different, phosphinooxazoline-based *P*,*N*-ligand class (PHOX), which does not contain the chiral information in the backbone structure but in a group close to the nitrogen moiety, high yields and moderate *ee* values of up to -47% could be achieved (Table 13,

entry 9). Remarkably, the (*R*)-configuration of the PHOX ligand induces the formation of the opposite enantiomer compared to the (*R*)-configuration of the biaryl-based ligands.

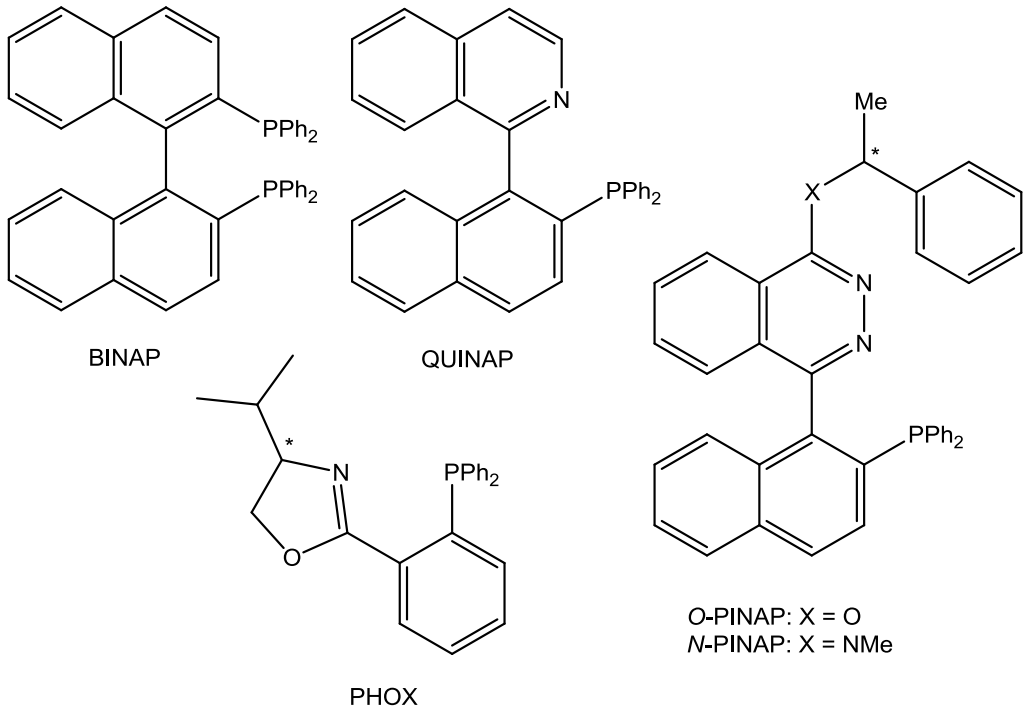

Scheme 50: Chiral bidentate ligands

To alleviate the competition of the triphenylphosphine ligands with the chelating *P*,*N*-ligand **2** was substituted for $[RhCl(C_2H_4)_2]_2$ in a final experiment. Using (*R*)-QUINAP as the chiral ligand moderate yields and a similar selectivity of 42% ee compared to the use of **2** was obtained (Table 13, entry 10).

These results show that while chiral anions in the case of **2** are presumably too far away from the metal center to induce any notable enantioselectivity, chiral *P*,*N*-ligands in combination with **2** as well as $[(C_2H_4)_2RhCl]_2$ lead to moderate to good *ee* values. These *in situ* systems represent the first Rh(I)-based catalysts that do not have to be activated in advance with hydrogen to yield the product as described by Tanaka et al. for all their systems. [76] The here presented results might open the door to the generation of simple *in situ* generated catalysts that can achieve – under modified conditions – high yields and selectivities.

Table 13: Catalyst screening of **2** using various chiral ligands

Entry	Catalyst System [a]	Yield [%]	d/l : meso [b]	*ee* [%] [c]
1	(*R*)-BINAP	83	1:2.4	6
2	(*R*)-QUINAP	41	1:1.4	49
3	(*R*)-QUINAP [d]	37	1:1.5	42
4	(*S*)-QUINAP	48	1:2.3	-47
5	(*R*,*R*)-*N*-PINAP	88	1.3:1	27
6	(*R*,*S*)-*N*-PINAP	62	1.7:1	-87
7	(*R*,*R*)-*O*-PINAP	85	1.2:1	61
8	(*R*,*S*)-*O*-PINAP	94	1.4:1	-85
9	(*R*)-PHOX	78	1:1.2	-45
10	(*R*)-QUINAP [e]	69	1:1.6	42

[a] reaction conditions: **2** (5 mol%), $AgNTf_2$ (5 mol%), 5 mol% chiral ligand, 25 °C, 4 h; [b] ratio determined by integration of peak areas in the ^1H NMR; [c] *ee* values determined by chiral HPLC; [d] 2 equiv. ligand; [e] $[RhCl(C_2H_4)_2]_2$ (2.5 mol%) was used instead of **2**

4. CONCLUSION

The investigation of the influence of the neutral ligands on the ability to activate and/or stabilize the respective CpCo(I)-complexes – with a focus on heteroleptic systems – as well as the application of derived CpCo(I)-catalysts in [2+2+2] cycloadditions was the main focus of this thesis. Modifications to synthesize solid phase-supported CpCo(I)-based catalysts and the implementation of *in situ* generated Rh(I)-based catalysts for the enantioselective [2+2+2] cycloaddition reaction represented further goals of this thesis. Below, the most prominent achievements are summarized:

a) The synthesis and systematic access to a number of different homo- as well as heteroleptic CpCo(I)-complexes containing olefin and/or phosphite ligands has been achieved, including the establishment of novel photochemical routes for their respective syntheses (Scheme 51).

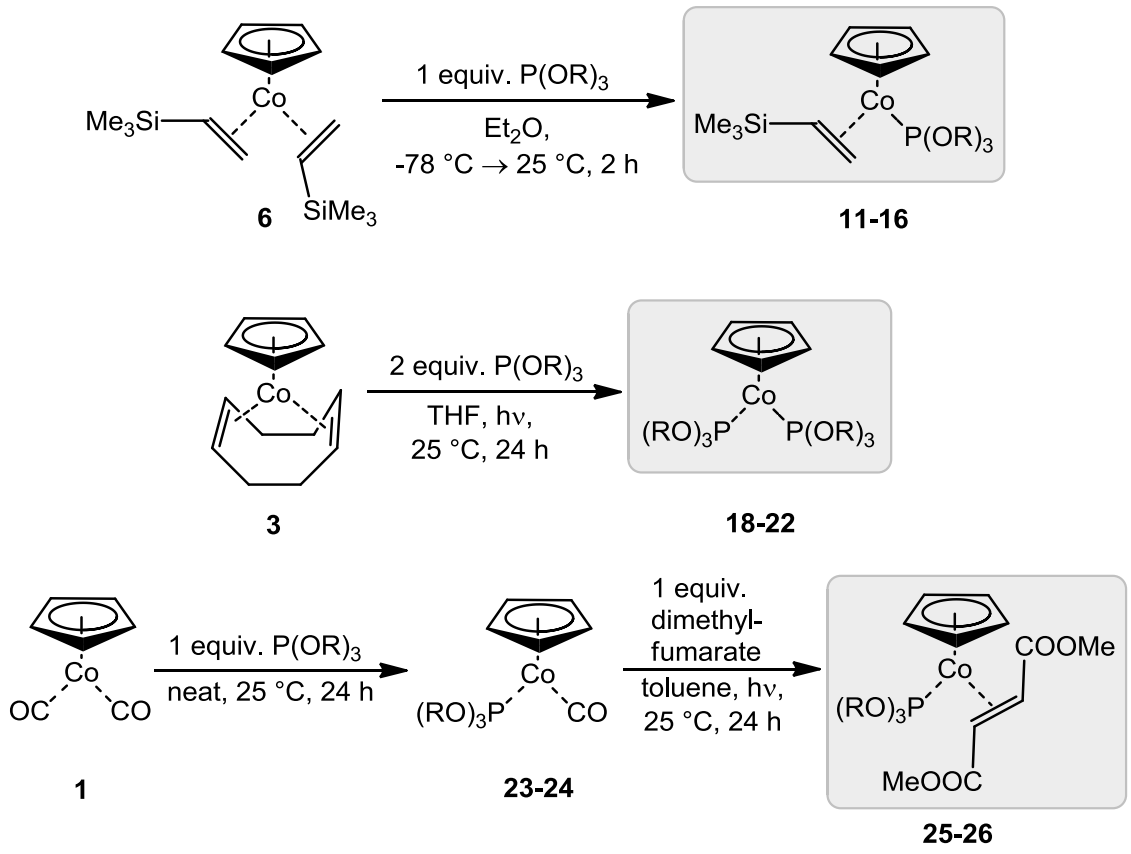

Scheme 51: Novel CpCo(I)-complexes and their newly developed synthetic routes

b) Compared to the thermally instable complex **6** the respective heteroleptic complexes **11-16**, with one trimethylvinylsilane ligand substituted for a phosphite ligand, were stable at room temperature but still exhibited great catalytic activity in [2+2+2] cycloaddition reactions at moderate temperatures.

c) The effect of the electronic properties of the respective phosphite ligand is best recognized in the catalytic screening of complexes **18-22**. The use of electron-rich phosphites such as $P(OEt)_3$ or $P(O\textit{i}\text{-}Pr)_3$ led to highly active catalysts for the [2+2+2] cycloaddition reaction at moderate conditions, while CpCo(I)-complexes containing electron-poor phosphites displayed lower activities.

d) The stabilizing effect of the phosphite ligand has been demonstrated by DFT calculations as well as by a comparative study of the catalytic activity of **6**, **11** and **18** at different temperatures (Scheme 52). The heteroleptic complexes **11-16** therefore do represent an unique compromise between necessary stability and sufficient activity.

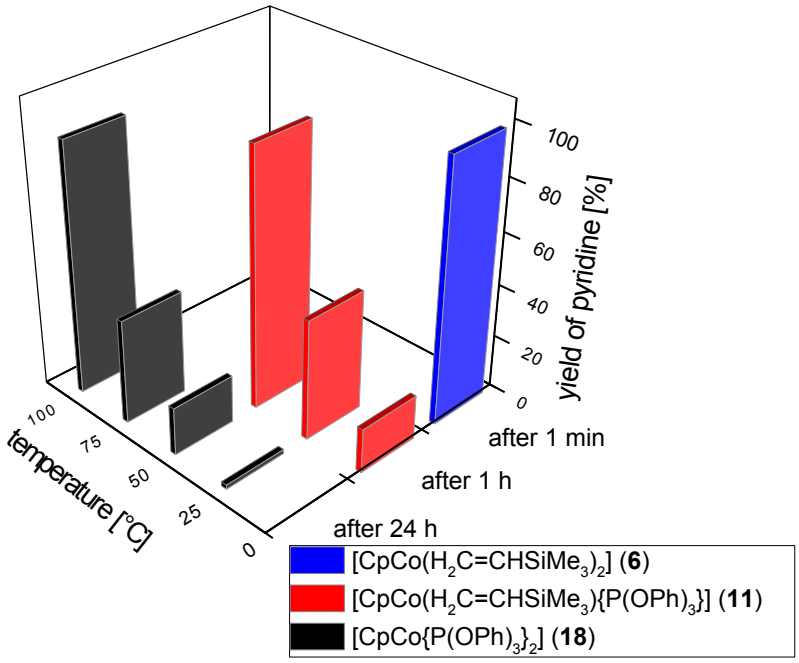

Scheme 52: Temperature-dependent yields of pyridine (**43**) determined for $[CpCo(H_2C{=}CHSiMe_3)_2]$ (**6**, blue), $[CpCo(H_2C{=}CHSiMe_3)\{P(OPh)_3\}]$ (**11**, red) and $[CpCo\{P(OPh)_3\}_2]$ (**18**, black), respectively

e) It was found that CpCo(I)-complexes with one olefin and one phosphite ligand were always superior catalysts compared to CpCo(I)-complexes containing two phosphite ligands or the combination of CO and either olefin or phosphite ligand.

f) The employment of electron-deficient olefins such as dimethylfumarate generated air-stable compounds (**25** and **26**), which can be recycled and handled in air without difficulties, being one of the rare examples of air-stable Co(I)-pre-catalysts.

g) The air-stable complex **25** was successfully modified to incorporate a siloxane linker at the Cp-moiety and the respective complex **74** was then effectively covalently attached to a sol-gel matrix as well as silica to obtain three solid phase-supported CpCo(I)-based catalysts (Scheme 53), which could easily be removed from a reaction mixture by filtration.

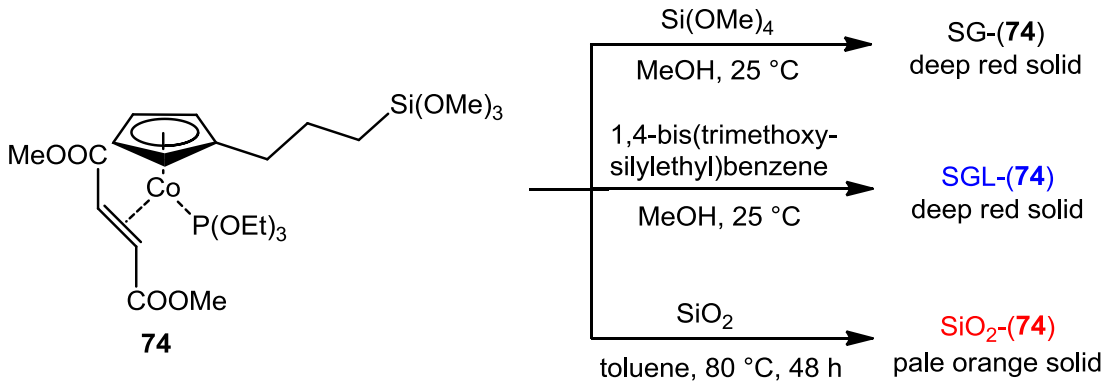

Scheme 53: Solid-supported CpCo(I)-catalysts

h) While the sol-gel-supported catalyst SG-(**74**) and SGL-(**74**) did not display any catalytic activity towards the [2+2+2] cycloaddition test reaction under thermal, photochemical or microwave conditions, the silica-based catalyst SiO_2-(**74**) demonstrated promising catalytic activity in the test cyclization reaction (Scheme 54: 21% yield under thermal conditions, 47% under microwave conditions). Even though SiO_2-(**74**) failed to provide stable catalytic activity over several catalytic cycles, SiO_2-(**74**) represents the first reported CpCo(I)-based catalyst that has been supported on a solid phase material and still maintained to be fairly active in the synthesis of pyridines.

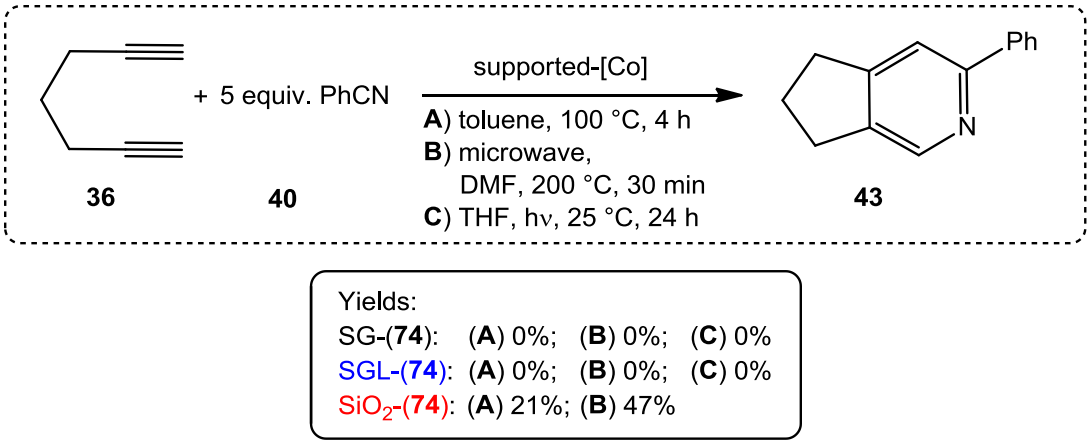

Scheme 54: First solid-supported CpCo(I)-catalyst active in the synthesis of pyridines

i) In search for an *in situ* catalyst system for the enantioselective [2+2+2] cycloaddition reaction the application of chiral anions in combination with $[CoCl(PPh_3)_3]$ (**81**) or $[RhCl(PPh_3)_3]$ (**2**) in the enantioselective cyclization of triyne **82** did not result in the desired high *ee* values. Instead the chiral anions seemed to have no or almost no influence on the [2+2+2] cycloaddition reaction. Only the combination of **2** and **78** led to a low enantiomeric excess of 11% (Scheme 55).

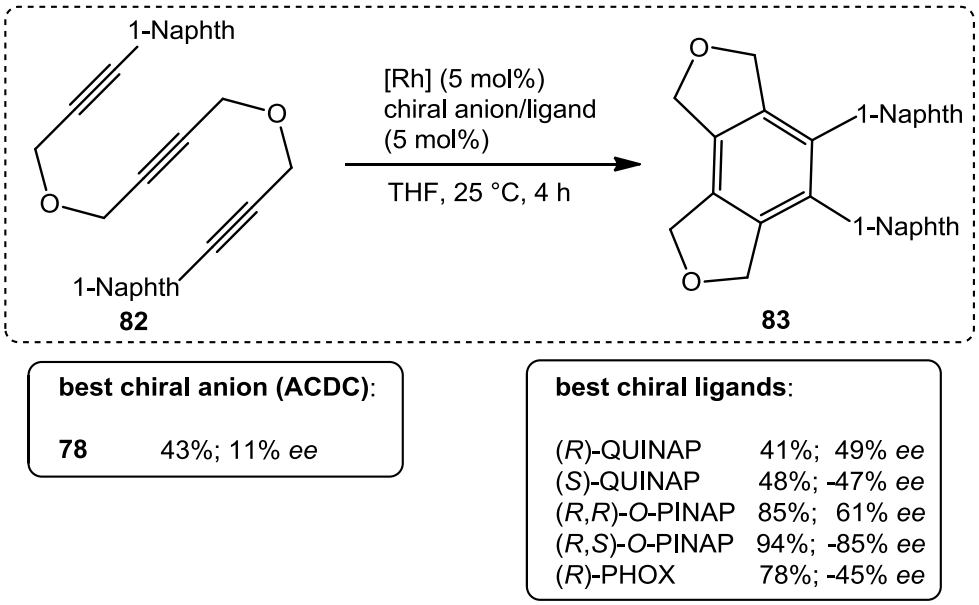

Scheme 55: Chiral induction by chiral anions and chiral ligands in Rh(I)-catalyzed [2+2+2] cycloaddition reactions

j) While the use of chiral *P,P*-ligands for the *in situ* generation of chiral Rh(I)-catalysts resulted in similar *ee* values as those obtained with chiral anions, the application of chiral *P,N*-ligands such as (*R*)-/(*S*)-QUINAP, (*R,R*)-/(*R,S*)-*O*-PINAP, (*R,S*)-*N*-PINAP and (*R*)-

PHOX, which are not as frequently deployed, exhibited promising results with moderate to good *ee* values of 47-85%. Once again the use of ligands with two different coordinating atoms led to better results than the commonly employed *P*,*P*-ligands. Furthermore, in choosing the proper chiral *P*,*N*-ligand the outcome of the reaction and the preference for one enantiomer could be controlled (Scheme 55). While (*R*)-QUINAP and (*R*,*R*)-*O*-PINAP gave the enantiomeric excess of the *d*-enantiomer, (*S*)-QUINAP, (*R*,*S*)-*O*-PINAP and (*R*)-PHOX led to the *l*-enantiomer.

k) These systems represent a promising new class of *in situ* generated chiral Rh(I)-complexes with *P*,*N*-ligands, that do not have to be activated prior the [2+2+2] cycloaddition reaction – as all systems reported by Tanaka et al. require – and still lead to very good yields and moderate to good *ee* values.

APPENDIX

5. EXPERIMENTAL PART

5.1 General Information

The majority of the conducted experiments have been performed with standard Schlenk technic and under an inert gas atmosphere (argon).

5.1.1 Elemental Analysis

Elemental analyses were performed in the analytical department of the Leibniz-Institut für Katalyse e.V. on a Leco C/H/N/S-analyzer 932 and a Perkin-Elmer Lambda 2 (phosphorus).

5.1.2 NMR Spectroscopy

All NMR spectra were recorded on either a Bruker AV 300, AV 400 or Fourier 300 NMR spectrometer. The chemical shift δ is always given in ppm and in the case of ^{1}H and ^{13}C NMR signals relative to the respective deuterated solvent. TopSpin NMR-Software from Bruker BioSpin 2005 as well as MestReNova 8.0 from Mestrelab Research S.L. were used for the evaluation of the spectra. The coupling constant *J* is always given in Hertz (Hz) and characterizes together with the signal multiplicity the structure of the recorded signal.

5.1.3 Mass Spectroscopy

Mass spectra were recorded on a Finnigan MAT 95XP (Thermo Electron) and the ionization occurred through EI (Electron Ionization), CI (Chemical Ionization, with *iso*-butane as reactant gas) or ESI (Electron Spray Ionization).

5.1.4 Gas Chromatography

Qualitative as well as quantitative analyses were performed with an gas chromatograph Agilent 7890A with an FID (flame ionization detector). The calibration for quantitative

analyses was conducted with 1,2,3,4,5,6,7,8,9,10,11,12-dodecahydrotriphenylen (DHT) as internal standard.

5.1.5 X-Ray Structure Analysis

Data for **18** were collected on a STOE IPDS II and for **22**, **25**, **26**, **31** on a Bruker Kappa APEX II Duo diffractometer using graphite-monochromated Mo-K_α radiation. The structures were solved by direct methods (SHELXS-97) [145] and refined by full-matrix least-squares techniques on F^2 (SHELXL-97). [145] XP (Bruker AXS) was used for graphical representations.

5.1.6 Solvents and Reagents

5.1.6.1 Purification and Drying of Solvents

Deuterated as well as non-deuterated solvents used in reactions have been dried following these procedures:

Diethyl ether (Et_2O), **toluene**, ***n*-hexane**, ***n*-pentane** and **tetrahydrofurane** (THF) have been refluxed in the presence of sodium and benzophenone until the solution showed a deep violet color (ketyl generation).

Triethylamine (NEt_3), **dichloromethane** (CH_2Cl_2), **acetone** and **dimethyl formamide** (DMF) have been dried over P_2O_5.

Benzonitrile, **diisopropylamine**, **methanol-*d*$_4$** (CD_3OD), **chloroform-*d*$_1$** ($CDCl_3$), **benzene-*d*$_6$** (C_6D_6), **THF-*d*$_8$** were stirred over molecular sieves.

All respective solvents have been destilled and stored in Schlenk flasks under inert gas atmosphere. Further compounds have been purified according to standard methods. [146]

5.1.6.2 Commercially Available Reagents, Complexes and Salts

The following substances were purchased from various suppliers:

- (*R*)-3,3‘-bis(2,4,6-triisopropylphenyl)-1,1‘-binaphthyl-2,2‘-diyl hydrogen phosphate (Sigma-Aldrich)
- (*R*)-3,3’-bis[3,5-bis(trifluoromethyl)-phenyl]-1,1’-binaphthyl-2,2’-diyl hydrogen phosphate (Sigma-Aldrich)
- (*R*)-BINAP (Strem Chemicals)
- (*R*,*R*)-*N*-PINAP (Strem Chemicals)
- (*R*,*S*)-*N*-PINAP (Strem Chemicals)
- (*R*,*R*)-*O*-PINAP (Strem Chemicals)
- (*R*,*S*)-*O*-PINAP (Strem Chemicals)
- (*R*)-PHOX (Strem Chemicals)
- (*R*)-QUINAP (Strem Chemicals)
- (*S*)-QUINAP (Strem Chemicals)
- (*R*)-VAPOL hydrogen phosphate (Sigma-Aldrich)
- Δ-TRISPHAT tetrabutylammonium salt (Sigma-Aldrich)
- 1,4-bis(trimethoxysilylethyl)benzene (Fluorochem)
- 1,6-heptadiyne (Sigma-Aldrich)
- 1,7-octadiyne (Sigma-Aldrich)
- 1,8-nonadiyne (Sigma-Aldrich)
- 1-iodonaphthalene (Sigma-Aldrich)
- 2-bromoethanol (Sigma-Aldrich)
- 2-butyne (TCI)
- 3,3-dimethylbut-1-ene (TCI)
- cyclopentadienyl cobalt dicarbonyl (Sigma-Aldrich)
- cyclopentadienyl cobalt cyclooctadiene (Convertex)
- dicobalt octacarbonyl (Alfa Aesar / Sigma-Aldrich)
- dimethylfumarate (Sigma-Aldrich)
- dimethylmaleate (Sigma-Aldrich)
- 1,2,3,4,5,6,7,8,9,10,11,12-dodecahydrotriphenylene (Sigma-Aldrich)
- fumarylchloride (Sigma-Aldrich)
- iodine (Sigma-Aldrich)
- isopropylnitrile (Sigma-Aldrich)
- magnesium sulfate (Sigma-Aldrich)
- Merrifield’s resin CAS: 55844-94-5 (Sigma-Aldrich)
- *n*-butyl lithium (Sigma-Aldrich)
- *n*-butylisocyanate (Sigma-Aldrich)
- *n*-propylisocyanate (Acros Organics)
- phenylacetylene (Sigma-Aldrich)
- phosphorus trichloride (Sigma-Aldrich)
- silver(I) bis(trifluoromethanesulfonyl)-amide (Sigma-Aldrich)
- sodium (Acros Organics)
- sodium borohydride (Sigma-Aldrich)
- sodium chloride (Sigma-Aldrich)

- 3-acetylphenylisocyanate (Sigma-Aldrich)
- 3-bromopropyl(trimethoxy)silane (ABCR / Sigma-Aldrich)
- 3-buten-1-ol (TCI)
- 3-hexyne Sigma-Aldrich)
- 4-nitrophenylisocyanate (Sigma-Aldrich)
- 4-trifluoromethylphenol (Sigma-Aldrich)
- 5-hexynenitrile (Alfa Aesar)
- aluminium oxide (Brockman Type I, neutral) (Acros Organics)
- ammonia solution(Merck)
- benzonitrile (Sigma-Aldrich)
- *cis*-cyclooctene (Sigma-Aldrich)
- cobalt(II) chloride hexahydrate (Sigma-Aldrich)
- cobaltocene (Sigma-Aldrich)
- copper(I) iodide (Sigma-Aldrich)
- cyclohexylisocyanate (Sigma-Aldrich)
- 1,5-cyclooctadiene (Sigma-Aldrich)
- sodium cyclopentadienide (2M in THF) (Sigma-Aldrich)
- sodium iodide (Sigma-Aldrich)
- sodium sulfate (Sigma-Aldrich)
- *t*-butyldimethylsilylchloride (Sigma-Aldrich)
- *t*-butylnitrile (Sigma-Aldrich)
- tetrakis(triphenylphosphine) palladium(0) (ChemPur)
- tetramethoxysilane (ABCR)
- tolylisocyanate (Sigma-Aldrich)
- tris(2,2,2-trifluoroethyl)phosphite (Sigma-Aldrich)
- triethylphosphite (Acros Organics)
- triisopropylphosphite (Acros Organics)
- trimethylsilylchloride (TMSCl) (Alpha Aesar / Sigma-Aldrich / Carbolution)
- trimethylvinylsilane (Sigma-Aldrich)
- triphenylphosphite (Acros Organics)
- triphenylphosphine (Acros Organics)

5.2 Synthesis of Phosphite Ligands

5.2.1 Synthesis of 4,7-dihydro-2-phenoxy-1,3,2-dioxaphosphepine (**17**)

The synthesis was performed according to literature and the NMR data were in accordance with the reported data. [99a-d]

5.2.2 Synthesis of (but-3-enyl)diphenylphosphite (**30**)

Synthesized after a modified procedure from Ingenuin et al.[99e]
Sodium (138 mg, 5 mmol) was washed with *n*-hexane (3x) before 3-buten-1-ol (3,3 mL, 38 mmol) was added and gas evolution was observed. Then triphenylphosphite (10 mL, 58 mmol) was added to the solution which turned red-brown and a solid precipitated. This suspension was heated at 100 °C for 2 h before the mixture was allowed to cool to room temperature. The red-brown oil was removed from the white precipitate via syringe and the last residues of phenol were removed by bulb-to-bulb distillation (100 °C, 0.5 mbar). After 6 h at this temperature no more phenol was recovered and the desired phosphite could be distilled at 180 °C and 0.5 mbar.

MW	288.28 g/mol
Formula	$C_{16}H_{17}O_3P$
^{1}H NMR (C_6D_6)	δ = 2.37 (m, 2H), 3.93 (q, *J* = 6.8 Hz, 1H), 4.13 (q, *J* = 6.8 Hz, 1H), 4.98-5.10 (m, 2H), 5.67-5.83 (m, 1H), 6.96-7.11 (m, 6H), 7.17-7.29 (m, 4H)
^{31}P NMR (C_6D_6)	δ = 129.2 (s)
^{13}C NMR (C_6D_6)	δ = 35.2 (s), 61.6 (s), 115.3 (s), 117.3 (s), 120.2 (s), 120.4 (s), 120.8 (s), 123.8 (s), 124.3 (s), 129.6 (s), 129.7 (s), 134.3 (s)

5.2.2 Synthesis of tris(*p*-trifluoromethylphenyl)phosphite (**84**)

Synthesized after a modified procedure from Ingenuin et al. [147]
4-Trifluoromethylphenol (2.25 g, 13.9 mmol) was dissolved in THF (20 mL) and triethylamine (2 mL) was slowly added to the solution. The solution was stirred at room

temperature for 30 min, before a solution of phosphorous trichloride (400 µL, 4.5 mmol) in THF (5mL) was added dropwise. A white solid precipitated immediately and the suspension is stirred for 18 h at room temperature. The solution was filtered and the clear solution reduced in volume, yielding a yellow oil which solidified upon drying in high vacuum. (Yield: 1.605 g, 67%)
The NMR data were in accordance with the reported data. [148]

MW	514.28 g/mol
Formula	$C_{21}H_{12}F_9O_3P$
^{1}H NMR ($CDCl_3$)	δ = 7.23 (d, *J* = 9.0 Hz, 2H), 7.62 (d, *J* = 9.0 Hz, 2H)
^{31}P NMR ($CDCl_3$)	δ = 126.1 (s)
^{19}F NMR ($CDCl_3$)	δ = 61.7 (s)

5.3 Synthesis of Complexes of the Type [CpCo(H_2C=CHSiMe_3)(phosphite)]

General Procedure:
To a solution of [CpCo(H_2C=CHSiMe_3)$_2$] [51] (**6**) in diethyl ether at -78 °C the respective phosphite (1 equiv.) was slowly added. The solution was stirred at -78 °C for 2 h before it was slowly warmed to room temperature. The solution was filtered over a small amount of neutral Al_2O_3 (Brockman Type I), which was washed with THF (10 ml). The solvent was removed under reduced pressure and the resulting red-brown oil dried under vacuum.

5.3.1 Synthesis of [CpCo(H_2C=CHSiMe_3){P(OPh)$_3$}] (**11**)

According to the general procedure [CpCo(H_2C=CHSiMe_3)$_2$] (**6**) in diethyl ether (4 mL, 0.44 mmol) and triphenylphosphite (114 µL, 0.44 mmol) were used. (Yield: 198 mg, 84%)

MW	534.54 g/mol
Formula	$C_{28}H_{32}CoO_3PSi$
^{1}H NMR (C_6D_6)	δ = 0.17 (s, CH_3, 9H), 1.51 (dt, CH, 1H), 2.49 (dd, CH_2, 1H), 2.64 (dd, CH_2, 1H), 4.41 (s, Cp, 5H), 6.86 (t, C_4-CH, 3H), 7.03 (t, $C_{3,5}$-CH, 6H), 7.26 (d, $C_{2,6}$-CH, 6H)
^{31}P NMR (C_6D_6)	δ = 155.1 (bs)
^{13}C NMR (C_6D_6)	δ = 1.1 (s, CH_3), 30.7 (d, *J* = 5.1 Hz), 32.7 (d, *J* = 6.3 Hz), 82.6 (s, Cp), 121.6 (d, *J* = 5.1 Hz), 124.4 (s), 130.0 (s), 152.4 (d, *J* = 6.3 Hz)

CI (Et_2O)	m/z 434 [M^+-(CH_2=$CHSiMe_3$)], 311 [L+H^+], 217 [L^+-OPh], 189 [Cp_2Co^+]
HRMS	not detected, disproportionation into [$CpCo(P(OPh)_3)_2$] (m/z 744.1292) / [$CpCo(P(OPh)_3)$] (m/z 434.0503) and [$(CpCo)_4(HCCSiMe_3)$] (m/z 593.9479)

5.3.2 Synthesis of [$CpCo(H_2C$=$CHSiMe_3)\{P(O(CH_2CF_3)_3\}$] (**12**)

According to the general procedure [$CpCo(H_2C$=$CHSiMe_3)_2$] (**6**) in diethyl ether (2 mL, 0.24 mmol) and tri(2,2,2-trifluoroethyl)phosphite (110 µL, 0.24 mmol) in diethyl ether (1 mL) were used. (Yield: 89 mg, 67%)

MW	552.33 g/mol
Formula	$C_{16}H_{23}CoF_9O_3PSi$
^{1}H NMR (C_6D_6)	δ = 0.11 (s, $SiMe_3$, 9H), 0.74 (m, CH, 1H), 1.96 (dd, CH_2, 1H), 2.31 (t, CH_2, 1H), 3.96 (dsep, CH_2CF_3, 6H), 4.53 (s, Cp, 5H)
^{31}P NMR (C_6D_6)	δ = 175.5 (bs)
^{13}C NMR (C_6D_6)	δ = 0.8 (s, $SiMe_3$), 31.1 (d, *J* = 5.0 Hz, CH), 32.2 (d, *J* = 5.0 Hz, CH_2), 61.4 (q, *J* = 36.6 Hz, CH_2CF_3), 82.6 (d, *J* = 3.15 Hz, Cp), signal for CH_2CF_3 obscured by solvent signal
^{19}F NMR (C_6D_6)	δ = -74.2 (t)
CI (isobutane)	m/z 552 [M^+], 452 [M-(H_2C=$CHSiMe_3$)$^+$], and decomposition to [$(CpCo)_4(H_2C$=$CHSiMe_3)$]$^+$ (m/z 594) and [$(CpCo)_3(H_2C$=$CHSiMe_3)$]$^+$ (m/z 470)
HRMS	not detectable

5.3.3 Synthesis of [$CpCo(H_2C$=$CHSiMe_3)$(**84**)] (**13**)

According to the general procedure [$CpCo(H_2C$=$CHSiMe_3)_2$] (**6**) in diethyl ether (2 mL, 0.24 mmol) and tri(*p*-trifluoromethylphenyl)phosphite (**84**) (122 mg, 0.24 mmol) in diethyl ether (1 mL) were used. (Yield: 93 mg, 53%)

MW	738.54 g/mol
Formula	$C_{31}H_{29}CoF_9O_3PSi$
^{1}H NMR (C_6D_6)	δ = 0.06 (s, CH_3, 9H), 1.27 (dd, CH, 1H), 2.21 (t, CH_2, 1H), 2.54 (d, CH_2, 1H), 4.30 (s, Cp, 5H), 7.03 (d, Ph, 6H), 7.27 (d, Ph, 6H)
^{31}P NMR (C_6D_6)	δ = 153.7 (bs)
^{13}C NMR (C_6D_6)	δ = 0.8 (s, CH_3), 32.6 (d, *J* = 3.8 Hz, CH_2), 33.8 (d, *J* = 5.4 Hz, CH_2), 83.0 (d, *J* = 3.2 Hz, Cp), 121.4 (d, *J* = 5.5 Hz, CH), 127.3 (d, *J* = 3.8 Hz, CH), 154.4 (d, *J* = 5.3 Hz, Ph), signals for CF_3 and CH obscured by solvent signal
^{19}F NMR (C_6D_6)	δ = -61.4 (s)
CI (isobutane)	m/z 738 [M^+], 638 [M-(CH_2=$CHSiMe_3$)$^+$], 531 [O=P(O($C_6H_4CF_3$)$_3^+$], 515 [P(O($C_6H_4CF_3$)$_3^+$], 189 [Cp_2Co^+]
HRMS (ESI)	not detectable

5.3.4 Synthesis of [CpCo(H_2C=$CHSiMe_3$){P(OEt)$_3$}] (**14**)

According to the general procedure [CpCo(H_2C=$CHSiMe_3$)$_2$] (**6**) in diethyl ether (1 mL, 0.24 mmol) and triethylphosphite (41 µL, 0.24 mmol) were used. (Yield: 74 mg, 79%)

MW	390.42 g/mol
Formula	$C_{16}H_{32}CoO_3PSi$
^{1}H NMR (C_6D_6)	δ = 0.25 (s, $SiMe_3$, 9H), 1.01 (t, *J* = 7.0 Hz, CH_3, 9H), 1.16 (t, *J* = 7.0 Hz, CH, 1H), 2.09 (dd, *J* = 10.4 Hz / 5.9 Hz, CH_2, 1H), 2.44 (dd, *J* = 13.6 Hz / 1.9 Hz, CH_2, 1H), 3.83 (m, CH_2, 6H), 4.77 (s, Cp, 5H)
^{31}P NMR (C_6D_6)	δ = 169.5 (bs)
^{13}C NMR (C_6D_6)	δ = 1.3 (s, $SiMe_3$), 16.4 (d, *J* = 7.0 Hz), 27.9 (d, *J* = 5.7 Hz), 29.9 (d, *J* = 7.0 Hz), 59.6 (s), 81.8 (d, *J* = 3.3 Hz, Cp)
CI (isobutane)	m/z 390 [M^+], 290 [M-(H_2C=$CHSiMe_3$)$^+$]
HRMS (ESI)	not detectable

5.3.5 Synthesis of [CpCo(H_2C=$CHSiMe_3$){P(O*i*-Pr)$_3$}] (**15**)

According to the general procedure [CpCo(H_2C=$CHSiMe_3$)$_2$] (**6**) in diethyl ether (1 mL, 0.24 mmol) and triisopropylphosphite (59 µL, 0.24 mmol) were used. (Yield: 62 mg, 60%)

MW	432.50 g/mol
Formula	$C_{19}H_{38}CoO_3PSi$
^{1}H NMR (C_6D_6)	δ = 0.25 (s, $SiMe_3$, 9H), 0.71 (m, CH, 1H), 1.08 (t, *J* = 6.1 Hz, 18H), 2.23 (dd, *J* = 10.1 Hz / 6.1 Hz, 1H), 2.46 (d, *J* = 13.0 Hz, 1H), 4.71 (m, CH, 3H), 4.80 (s, Cp, 5H)
^{31}P NMR (C_6D_6)	δ = 161.2 (bs)
^{13}C NMR (C_6D_6)	δ = 1.3 (s, $SiMe_3$), 24.2 (d, *J* = 4.6 Hz, CH_3), 24.3 (d, *J* = 3.1 Hz, CH_3), 25.6 (d, *J* = 6.7 Hz, CH_2), 30.8 (d, *J* = 6.2 Hz, CH), 68.5 (d, *J* = 5.2 Hz, CH), 81.8 (d, *J* = 3.1 Hz, Cp)
CI (isobutane)	m/z 432 [M^+], 332 [M-(H_2C=$CHSiMe_3$)$^+$]
HRMS (ESI)	not detectable

5.3.6 Synthesis of [CpCo(H_2C=$CHSiMe_3$)(**17**)] (**16**)

According to the general procedure [CpCo(H_2C=$CHSiMe_3$)$_2$] (**6**) in diethylether (4 mL, 0.48 mmol) and 4,7-dihydro-2-phenoxy-1,3,2-dioxaphosphepine (**17**) (89 µL, 0.48 mmol) were used. (Yield: 151 mg, 73%)

MW	434.43 g/mol
Formula	$C_{20}H_{28}CoO_3PSi$
^{1}H-NMR (C_6D_6)	δ = 0.16 (s, CH_3, 9H), 1.20 (m, CH, 1H), 2.16 (dd, *J* = 6.5 Hz / 10.5 Hz, CH_2, 1H), 2.46 (dd, *J* = 2.2 Hz / 13.7 Hz, CH_2, 1H), 4.16 (m, CH_2, 1H), 4.16-4.47 (m, CH_2, 3H), 4.63 (s, Cp, 5H), 5.15 (d, *J* = 2.5 Hz, CH, 2H), 6.95 (t, *J* = 7.5 Hz, Ph, 1H), 7.14 (d, *J* = 8.2 Hz, Ph, 2H), 7.27 (d, *J* = 8.2 Hz, Ph, 2H)
^{31}P-NMR (C_6D_6)	δ = 172.3 (bs)
^{13}C-NMR (C_6D_6)	δ = 1.1 (s, $SiCH_3$), 29.3 (d, *J* = 5.2 Hz), 30.9 (d, *J* = 6.0 Hz), 61.8 (d, *J* = 5.8 Hz, CH_2), 62.0 (d, *J* = 3.9 Hz, CH_2), 82.3 (d, *J* = 2.9 Hz, Cp), 121.9

	(d, *J* = 5.3 Hz, Ph), 124.1 (s, Ph), 128.5 (s, Ph), 128.9 (s, CH), 129.6 (s, CH), 152.9 (s, Ph)
CI (Et_2O)	m/z 434 [M^+], 335 [M-(CH_2=$CHSiMe_3$)+H^+], 211 [cyclo-PO+H^+], 189 [Cp_2Co^+]
HRMS (ESI)	not detectable

5.4 Synthesis of Complexes of the Type [CpCo(phosphite)$_2$]

General Procedure:
A solution of [CpCo(cod)] (**3**) and the respective phosphite (2 equiv.) in THF (6 mL) was irradiated with light for 24 h. The solution was filtered over a small amount of neutral Al_2O_3 (Brockman Type I), which was washed with toluene (10 ml). After removal of the solvent under reduced pressure the resulting residue was washed with *n*-pentane (2 ml) and the resulting deep red solid/oil dried under vacuum.

5.4.1 Synthesis of [CpCo{P(OPh)$_3$}$_2$] (**18**) [92c]

a) Cobaltocene (342 mg, 1.8 mmol) was placed in a Schlenk flask and dissolved in *n*-hexane (15 mL). 2-Butyne (500 µL, 6.5 mmol) and triphenylphosphite (1.1 mL, 4.2 mmol) were added to the red-black solution. After 48 h at 70 °C the solution was filtered, leaving behind a black amorphous solid. The solvent was removed under reduced pressure and the unreacted cobaltocene and triphenylphosphite were removed by sublimation. The residual red-brownish solid was extracted with *n*-pentane. After removal of the solvent the red-brown solid was dried under vacuum. (Yield: 911 mg, 66%) Crystals suitable for X-Ray analysis were obtained from a *n*-pentane/diethyl ether mixture at 4 °C.

b) According to the general procedure [CpCo(cod)] (**3**) (232 mg, 1 mmol) and triphenylphosphite (521 µL, 2 mmol) were used. The resulting deep red solid was dried under vacuum. (Yield: 669 mg, 90%)

MW	744.59 g/mol
Formula	$C_{41}H_{35}CoO_6P_2$
^{1}H-NMR (C_6D_6)	δ = 4.26 (s, Cp, 5H), 6.89 (tt, C_4-CH, 6H), 7.04 (t, $C_{3,5}$-CH, 12H), 7.26 (d, $C_{2,6}$-CH, 12H)
^{31}P-NMR (C_6D_6)	δ = 157.3 (s)
^{13}C-NMR (C_6D_6)	δ = 82.1 (s, Cp), 122.0 (s, Ar-C_2/C_6), 124.0 (s, Ar-C_4), 129.5 (s, Ar-C_3/C_5), 152.9 (t, Ar-C_1)
CI (isobutane)	m/z 744 [M^+], 651[M^+-OPh], 434 [M^+-P(OPh)$_3$], 311 [L+H^+], 217 [L^+-OPh], 189 [Cp_2Co^+]

HRMS (THF)	calc.: m/z 744.1235; found: m/z 744.1251 [M*$^+$]
EA	calc.: C, 66.14%; H, 4.74%; Co, 7.91%; found: C, 65.80%; H, 4.26%; Co, 7.33%

5.4.2 Synthesis of [CpCo{P(OEt)$_3$}$_2$] (**19**)

According to the general procedure [CpCo(cod)] (232 mg, 1 mmol) and triethylphosphite (342 µL, 2 mmol) were used. The resulting deep red oil was dried under vacuum. (Yield: 452 mg, 99%)

MW	456.34 g/mol
Formula	$C_{17}H_{35}CoO_6P_2$
^{1}H-NMR (C_6D_6)	δ = 1.15 (t, *J* = 7.1 Hz, CH_3, 18H), 3.97 (m, *J* = 3.5 Hz, CH_2, 12H), 4.83 (s, Cp, 5H)
^{31}P-NMR (C_6D_6)	δ = 175.4 (bs)
^{13}C-NMR (C_6D_6)	δ = 16.6 (t, *J* = 3.2 Hz, CH_3), 59.3 (s, CH_2), 79.5 (t, *J* = 1.9 Hz, Cp)
CI (isobutane)	m/z 456 [M$^+$], 290 [M-(P(OEt)$_3$)$^+$]
HRMS (ESI)	not detectable

5.4.3 Synthesis of [CpCo{P(O*i*-Pr)$_3$}$_2$] (**20**)

According to the general procedure [CpCo(cod)] (**3**) (232 mg, 1 mmol) and triisopropylphosphite (493 µL, 2 mmol) were used. The resulting deep red oil was dried under vacuum. (Yield: 428 mg, 79%)

MW	540.50 g/mol
Formula	$C_{23}H_{47}CoO_6P_2$
^{1}H-NMR (C_6D_6)	δ = 1.26 (d, *J* = 6.0 Hz, CH_3, 36H), 4.83 (s, Cp, 5H), 4.85 (sep, *J* = 6.0 Hz, 6H)
^{31}P-NMR (C_6D_6)	δ = 172.9 (bs)
^{13}C-NMR (C_6D_6)	δ = 24.7 (s, CH_3), 67.3 (s, CH), 79.8 (s, Cp)
CI (isobutane)	m/z 540 [M$^+$], 332 [M-(P(O-*i*Pr)$_3$)$^+$]
HRMS (ESI)	not detectable

5.4.4 Synthesis of [CpCo{P(OCH$_2$CF$_3$)$_3$}$_2$] (**21**)

According to the general procedure [CpCo(cod)] (**3**) (50 mg, 0.21 mmol) and tris(2,2,2-trifluoroethyl)phosphite (110 µL, 0.24 mmol) were used. The resulting light orange solid was dried under vacuum. (Yield: NMR-yield: quantitative, isolated yield: 131 mg, 80%)

MW	780.17 g/mol
Formula	$C_{17}H_{17}CoF_{18}O_6P_2$
^{1}H-NMR (C_6D_6)	δ = 3.94 (m, *J* = 3.8 Hz / 4.2 Hz, CH_2, 12H), 4.41 (s, Cp, 5H)
^{31}P-NMR (C_6D_6)	δ = 177.1 (bs)
^{13}C-NMR (C_6D_6)	δ = 61.8 (q, *J* = 36.8 Hz, *C*H$_2$CF$_3$), 81.3 (s, Cp), signal for CH$_2$*C*F$_3$ obscured by solvent signal
^{19}F-NMR (C_6D_6)	δ = -74.3 (t, *J* = 9.2 Hz)
CI (isobutane)	m/z 780 [M$^+$], 681 [M-OCH$_2$CF$_3^+$], 452 [M-P(OCH$_2$CF$_3$)$_3^+$], 329 [L+H$^+$]
HRMS (ESI)	not detectable

5.4.5 Synthesis of [CpCo(**84**)$_2$] (**22**)

According to the general procedure [CpCo(cod)] (**3**) (180 mg, 0.78 mmol) and tris(*p*-trifluoromethylphenyl)phosphite (**84**) (800 mg, 1.56 mmol) were used. The resulting red solid was recrystallized from a *n*-pentane/toluene mixture. The orange solid was dried under vacuum. (Yield: 447 mg, 50%)

Crystals suitable for X-Ray analysis were obtained from a *n*-*n*-pentane/toluene mixture at 4 °C.

MW	1152.58 g/mol
Formula	$C_{47}H_{29}CoF_{18}O_6P_2$
^{1}H-NMR (C_6D_6)	δ = 4.13 (s, Cp, 5H), 6.83 (d, *J* = 8.2 Hz, 6H), 6.95 (d, *J* = 8.9 Hz, 6H), 7.27 (d, *J* = 8.9 Hz, 12H)
^{31}P-NMR (THF-d$_8$)	δ = 156.0 (s)
^{13}C-NMR (C_6D_6)	δ = 82.7 (s, Cp), 120.6 (s), 120.7 (s), 121.5 (s), 127.2 (s), 127.3 (s), 152.8 (s)

^{19}F-NMR (THF-d_8)	δ = -62.4 (s)
CI (isobutane)	m/z 1154 [M+2H$^+$], 992 [M-($OC_6H_4CF_3$)$^+$], 638 [M-(P($O(C_6H_4CF_3)_3$)$^+$], 531 [O=P($O(C_6H_4CF_3)_3^+$], 515 [P($O(C_6H_4CF_3)_3^+$], 189 [Cp_2Co^+]
HRMS (ESI)	not detectable
EA	calc.: C, 48.98%; H, 2.54%; Co, 5.11%; found: C, 49.03%; H, 2.58%; Co, 5.12%

Table 14: ^{31}P NMR shifts of the free and coordinating phosphite ligands

L	**L** $\delta(^{31}P)$/ppm	**[CpCo(L)$_2$]** $\delta(^{31}P)$/ppm	**[CpCo(H_2C=CH$SiMe_3$)(L)]** $\delta(^{31}P)$/ppm
P(OPh)$_3$	128.6 ($CDCl_3$)	157.3 (C_6D_6)	155.1 (C_6D_6)
cyclo-PO	130.1 ($CDCl_3$)	-	172.3 (C_6D_6)
P(OCH_2CF_3)$_3$	139.6 ($CDCl_3$)	177.1 (C_6D_6)	175.5 (C_6D_6)
P(OC_6H_4-4-CF_3)$_3$	126.6 (THF-d_8)	156.0 (THF-d_8)	153.7 (C_6D_6)
P(OEt)$_3$	138.9 (C_6D_6)	175.4 (C_6D_6)	169.5 (C_6D_6)
P(O*i*-Pr)$_3$	139.1 (C_6D_6)	172.9 (C_6D_6)	161.2 (C_6D_6)

5.5 Synthesis of Complexes of the Type [CpCo($MeO_2CCH=CHCO_2Me$)(phosphite)]

5.5.1 Synthesis of [CpCo(CO){$P(OEt)_3$}] (**23**) [56]

[$CpCo(CO)_2$] (0.35 mL, 2.5 mmol) and triethylphosphite (0.42 mL, 2.5 mmol) were stirred at room temperature for 24 h, before heated to 60 °C for 3 h. The solution was filtered over a small amount of neutral Al_2O_3 (Brockman Type I), which was washed with THF (20 ml). After removal of the solvent the deep red liquid was dried under vacuum. (Yield: 796 mg, quantitative)

MW	318.19 g/mol
Formula	$C_{12}H_{20}CoO_4P$
^{1}H NMR (C_6D_6)	δ = 1.08 (t, *J* = 7.3 Hz, CH_3, 9H), 3.93 (quin, *J* = 7.3 Hz, CH_2, 6H), 4.78 (s, Cp, 5H)
^{31}P NMR (C_6D_6)	δ = 173.7 (bs)
^{13}C NMR (C_6D_6)	δ = 16.4 (d, *J* = 7.1 Hz, CH_3), 60.6 (s, CH_2), 82.4 (d, *J* = 1.3 Hz, Cp)
CI (isobutane)	m/z 318
HRMS	not detectable
IR	ν_{max} = 936, 1028, 1388, 1934, 2023, 2899, 2931, 2979 cm^{-1}

5.5.2 Synthesis of [CpCo(CO){$P(OPh)_3$}] (**24**) [56]

[$CpCo(CO)_2$] (**1**) (0.35 mL, 2.5 mmol) and triphenylphosphite (0.65 mL, 2.5 mmol) were stirred at room temperature for 24 h, before heating to 60 °C for 3 h. The solution was filtered over a small amount of neutral Al_2O_3 (Brockman Type I), which was washed with THF (10 ml). After removal of the solvent the deep red liquid was dried under vacuum. (Yield: 1.046 g, 91%)

MW	462.32 g/mol
Formula	$C_{24}H_{20}CoO_4P$

^{1}H NMR (C_6D_6)	δ = 4.37 (s, Cp, 5H), 6.84 (t, *J* = 7.3 Hz, CH, 3H), 7.00 (t, *J* = 7.9 Hz, CH, 6H), 7.31 (m, CH, 6H)
^{31}P NMR (C_6D_6)	δ = 162.2 (bs)
^{13}C NMR (C_6D_6)	δ = 82.9 (d, *J* = 2.0 Hz, Cp), 121.8 (d, *J* = 5.1 Hz, CH), 124.7 (s, CH), 129.7 (s, CH), 152.5 (d, *J* = 6.0 Hz, C_q)
CI (isobutane)	m/z 462
HRMS	not detectable
IR (neat)	ν_{max} = 878, 912, 1195, 1488, 1589, 1952, 2021, 3040, 3064 cm^{-1}

5.5.3 Synthesis of [CpCo(MeO$_2$CCH=CHCO$_2$Me){P(OEt)$_3$}] (**25**)

Dimethylfumarate (72 mg, 0.5 mmol) was added to a solution of [CpCo(CO){P(OEt)$_3$}] (**23**) (158 mg, 0.5 mmol) in toluene (6 mL). The red solution was irradiated with light under reduced pressure for a total of 24 h, during which the reactor was vented and partially evacuated one more time. After filtration over a small amount of neutral Al_2O_3 (Brockman Type I), which was eluted with THF (20 ml), the solvent was removed under reduced pressure and the sticky red oil dried under vacuum. (Yield: 166 mg; NMR-yield: 83%, 17% [CpCo(CO){P(OEt)$_3$}] (**23**))

A solution in *n*-pentane at -78 °C afforded the desired product as an orange solid, which was dried under vacuum.

MW	434.31 g/mol
Formula	$C_{17}H_{28}CoO_7P$
^{1}H NMR (C_6D_6)	δ = 1.04 (t, *J* = 7.1 Hz, CH_3, 9H), 3.19 (t, *J* = 10.8 Hz, CH, 1H), 3.43 (s, CH_3, 3H), 3.51 (s, CH_3, 3H), 3.81 (m, CH_2, 6H), 4.10 (dd, *J* = 3.7 Hz / 10.8 Hz, CH, 1H), 4.67 (s, Cp, 5H)
^{31}P NMR (C_6D_6)	δ = 160.8 (bs)
^{13}C NMR (C_6D_6)	δ = 16.1 (s), 16.2 (s), 31.2 (d, *J* = 5.2 Hz), 35.4 (d, *J* = 7.8 Hz), 50.5 (s), 50.7 (s), 60.6 (d, *J* = 2.9 Hz), 85.2 (d, *J* = 2.9 Hz, Cp), 177.1 (s), 178.4 (s)
CI (isobutane)	m/z 435
HRMS	not detectable
IR	ν_{max} = 924, 1016, 1156, 1435, 1689, 2011, 2950 cm^{-1}

EA	calc.: C, 47.01%; H, 6.50%; Co, 13.57%; P, 7.13%; found: C, 46.98%; H, 6.54%; Co, 13.54%; P, 7.23%

5.5.4 Synthesis of [CpCo(MeO_2CCH=$CHCO_2Me$){$P(OPh)_3$}] (**26**)

Dimethylfumarate (55 mg, 0.38 mmol) was added to a solution of [CpCo(CO){$P(OPh)_3$}] (**24**) (175 mg, 0.38 mmol) in toluene (6 mL). The red solution was irradiated with light under reduced pressure for a total of 18 h, during which the reactor was vented and partially evacuated two more times. After filtration over a small amount of neutral Al_2O_3 (Brockman Type I), which was washed with THF (20 ml), the solvent was removed under reduced pressure and the sticky red oil was dried under vacuum. (Yield: 169 mg, 77%)
From a saturated solution in *n*-pentane at 4 °C deep red crystals suitable for X-ray of the desired complex were obtained.

MW	578.44 g/mol
Formula	$C_{29}H_{28}CoO_7P$
^{1}H NMR (C_6D_6)	δ = 3.49 (s, CH_3, 6H), 3.81 (t, *J* = 11.4 Hz, CH, 1H), 4.24 (dd, *J* = 4.0 Hz / 10.3 Hz, CH, 1H), 4.30 (s, Cp, 5H), 6.85 (t, *J* = 7.2 Hz, CH, 3H), 7.04 (t, *J* = 7.5 Hz, CH, 6H), 7.41 (d, *J* = 7.5 Hz, CH, 6H)
^{31}P NMR (C_6D_6)	δ = 150.0 (s)
^{13}C NMR (C_6D_6)	δ = 33.0 (d, *J* = 2.7 Hz), 37.3 (d, *J* = 8.7 Hz), 50.9 (d, *J* = 7.3 Hz), 85.8 (d, *J* = 2.7 Hz, Cp), 121.7 (d, *J* = 5.1 Hz), 124.7 (s), 129.8 (s), 152.1 (d, *J* = 7.1 Hz), 176.2 (d, *J* = 4.0 Hz), 177.8 (s)
CI (isobutane)	m/z 579
HRMS	not detactable
IR	ν_{max} = 1150, 1187, 1483, 1587, 1698, 1949, 2013, 2946 cm^{-1}
EA	calc.: C, 60.22%; H, 4.88%; P, 5.35%; Co, 10.19%; found: C, 60.50%; H, 4.89%; P, 5.35%; Co, 10.10%

5.5.5 Synthesis of [CpCo(H_2C=$CHSiMe_3$){$P(OPh)_3$}] (**11**)

Trimethylvinylsilane (2 mL, 30 equiv.) was added to a solution of [CpCo(CO){$P(OPh)_3$}] (**24**) (216mg, 0.47 mmol) in toluene (6 mL). The red solution was irradiated with light under

reduced pressure for a total of 4 h, during which the reactor was vented and partially evacuated one more time. After filtration over a small amount of neutral Al_2O_3 (Brockman Type I), which was washed with THF (20 ml), the solvent was removed under reduced pressure and the sticky red oil was dried under vacuum. (Yield: 193 mg; NMR-yield: 92% product, 8% [CpCo{P(OPh)$_3$}$_2$] (**18**))

MW	534.54 g/mol
Formula	$C_{28}H_{32}CoO_3PSi$
^{1}H NMR (C_6D_6)	δ = 0.17 (s, CH_3, 9H), 1.51 (dt, CH, 1H), 2.49 (dd, CH_2, 1H), 2.64 (dd, CH_2, 1H), 4.41 (s, Cp, 5H), 6.86 (t, C_4-CH, 3H), 7.03 (t, $C_{3,5}$-CH, 6H), 7.26 (d, $C_{2,6}$-CH, 6H)
^{31}P NMR (C_6D_6)	δ = 155.1 (bs)
^{13}C NMR (C_6D_6)	δ = 1.1 (s, CH_3), 30.7 (d, *J* = 5.1 Hz), 32.7 (d, *J* = 6.5 Hz), 82.6 (s, Cp), 121.6 (d, *J* = 5.1 Hz), 124.4 (s), 130.0 (s), 152.4 (d, *J* = 6.1 Hz)
CI (Et_2O)	m/z 434 [M^+-(CH_2=$CHSiMe_3$)], 311 [L+H^+], 217 [L^+-OPh], 189 [Cp_2Co^+]

5.5.6 Synthesis of [CpCo(coe){P(OEt)$_3$}] (**27**)

cis-Cyclooctene (2 mL, 22 equiv.) was added to a solution of [CpCo(CO){P(OEt)$_3$}] (**24**) (222 mg, 0.69 mmol) in toluene (6 mL). The red solution was irradiated with light under reduced pressure for a total of 24 h. After filtration over a small amount of neutral Al_2O_3 (Brockman Type I), which was washed with THF (20 ml), the solvent was removed under reduced pressure and the red oil dried under vacuum. (Yield: 222 mg, NMR-yield: 70% product, 30% [CpCo(CO){P(OEt)$_3$}] (**24**))

MW	400.38 g/mol
Formula	$C_{19}H_{34}CoO_3P$
^{1}H NMR (C_6D_6)	δ = 1.04 (t, *J* = 7.2 Hz, CH_3, 9H), 1.44 (m, CH_2, 4H), 1.55 (m, CH_2, 2H), 1.75 (m, CH_2, 4H), 2.20 (m, CH_2, 2H), 2.41 (d, CH_2, 2H), 3.86 (quin, *J* = 6.9 Hz, CH_2, 6H), 4.62 (s, Cp, 5H)
^{31}P NMR (C_6D_6)	δ = 170.40 (bs)

^{13}C NMR (C_6D_6)	δ = 16.4 (d, *J* = 6.9 Hz), 25.8 (s), 26.5 (s), 27.1 (s), 29.5 (s), 33.3 (d, *J* = 3.2 Hz), 33.6 (d, *J* = 1.3 Hz), 49.4 (d, *J* = 7.3 Hz), 59.4 (s), 82.9 (d, *J* = 2.6 Hz)
CI (Et_2O)	only decomposition to [CpCo{P(OEt)$_3$}$_2$] (m/z 457)

5.5.7 Synthesis of [CpCo(coe){P(OPh)$_3$}] (**28**)

cis-Cyclooctene (100 µL, 3 equiv.) was added to a solution of [CpCo(CO){P(OPh)$_3$}] (**24**) (108 mg, 0.23 mmol) in toluene (6 mL). The red solution was irradiated with light under reduced pressure for a total of 24 h. After filtration over a small amount of neutral Al_2O_3 (Brockman Type I), which was washed with THF (20 ml), the solvent was removed under reduced pressure and the sticky red oil was dried under vacuum. (Yield: 77 mg, NMR-yield: 41% product (**28**), 45% [CpCo{P(OPh)$_3$}$_2$] (**18**), 13% [CpCo(CO){P(OPh)$_3$}] (**24**))

MW	544.51 g/mol
Formula	$C_{31}H_{34}CoO_3P$
^{31}P NMR (C_6D_6)	δ = 153.78 (bs)

5.5.8 Synthesis of [CpCo(*cis*-MeO$_2$CCH=CHCO$_2$Me){P(OEt)$_3$}] (**29**)

Dimethylmaleate (118 µL, 0.95 mmol) was added to a solution of [CpCo(CO){P(OEt)$_3$}] (302 mg, 0.95 mmol) in toluene (6 mL). The red solution was irradiated with light under reduced pressure for a total of 24 h. After filtration over a small amount of neutral Al_2O_3 (Brockman Type I), which was washed with THF (20 ml), the solvent was removed under reduced pressure and the sticky red oil dried under vacuum. (Yield: 415 mg; NMR-yield: 59% product (**29**), 17% [CpCo{P(OEt)$_3$}$_2$] (**19**, *****), 6% [CpCo(dimethylfumarate){P(OEt)$_3$}] (**25**, **§**), 17% dimethylmaleate (#))

MW	434.31 g/mol
Formula	$C_{17}H_{28}CoO_7P$
^{1}H NMR (C_6D_6)	δ = 0.94 (t, *J* = 7.0 Hz, 9H), 2.48 (s, 1H), 2.50 (s, 1H), 3.58 (s, 6H), 3.72 (quin, *J* = 7.0 Hz, 6H), 4.87 (s, Cp, 5H)
^{31}P NMR (C_6D_6)	δ = 163.80 (bs)

^{1}H NMR

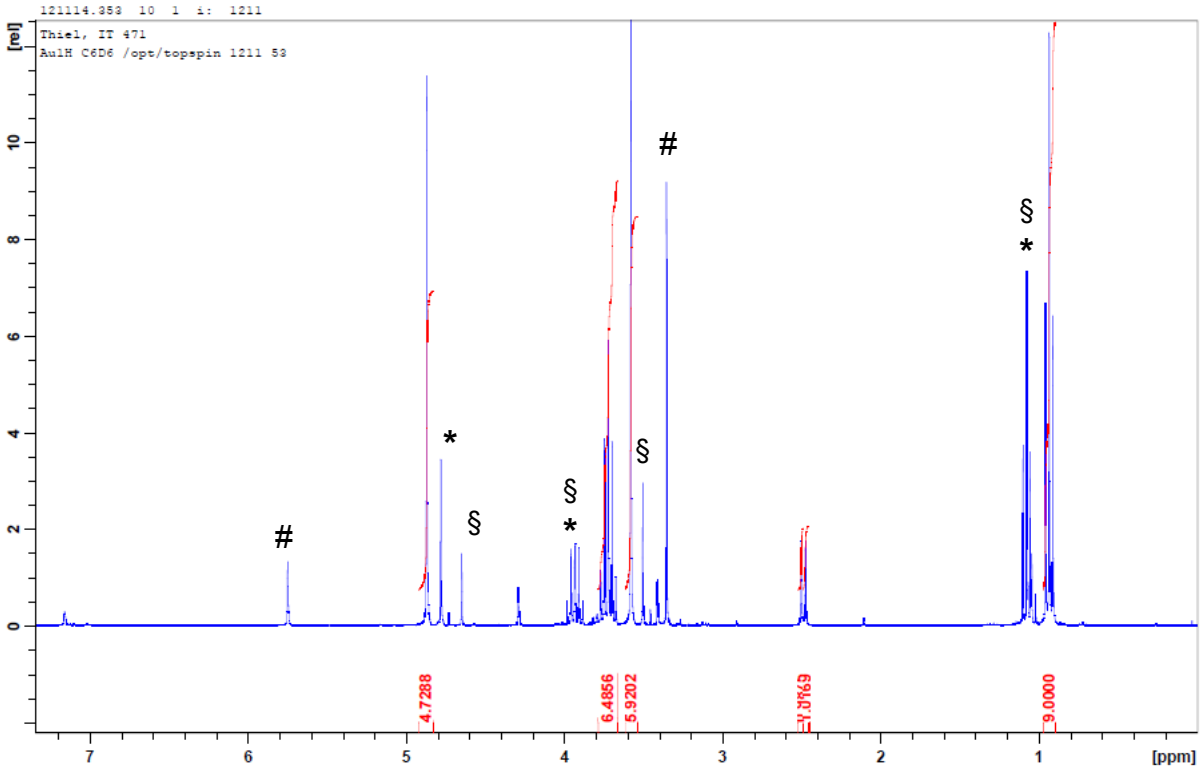

5.5.9 Synthesis of [CpCo(CO)(**17**)] (**31**)

[$CpCo(CO)_2$] (**1**) (0.14 mL, 1 mmol) and 2-phenoxy-4,7-dihydro-1,3,2-dioxaphosphephine (**17**) (0.19 mL, 1 mmol) were stirred at room temperature for 24 h. The solution was filtered over a small amount of neutral Al_2O_3 (Brockman Type I), which was washed with THF (10 ml). After removal of the solvent the deep red liquid was dried under vacuum. A solution in *n*-pentane at 4 °C afforded the desired compound as a red solid. (Yield: 306 mg, 85%)

MW	362.20 g/mol
Formula	$C_{16}H_{16}CoO_4P$
^{1}H NMR (C_6D_6)	δ = 4.35 (m, CH_2, 1H), 4.40 (m, CH_2, 1H), 4.46 (m, CH_2, 1H), 4.51 (m, CH_2, 1H), 4.57 (s, Cp, 5H), 5.19 (t, *J* = 2.0 Hz, CH, 2H), 6.90 (m, Ph, 1H), 7.07 (t, *J* = 7.9 Hz, Ph, 2H), 7.22 (m, Ph, 2H)
^{31}P NMR (C_6D_6)	δ = 177.68 (bs)
^{13}C NMR (C_6D_6)	δ = 62.5 (d, *J* = 5.1 Hz), 82.6 (d, *J* = 2.0 Hz), 122.3 (d, *J* = 5.4 Hz), 124.4 (d, *J* = 2.0 Hz), 128.6 (s), 129.6 (s), 152.7 (s)
CI (isobutane)	m/z 362 [M^+], 334 [M-$(CO)^+$]

EA	calc.: C, 53.06%; H, 4.45%; found: C, 52.91%; H, 4.45%
IR (neat)	ν_{max} = 763, 886, 1021, 1204, 1485, 1588, 1934, 2926 cm^{-1}

5.5.10 Synthesis of [CpCo(CO)(**30**)] (**32**)

$[CpCo(CO)_2]$ (**1**) (0.21 mL, 1.5 mmol) and (but-3-enyl)diphenylphosphite (**30**) (0.42 mL, 1.5 mmol) were stirred at room temperature for 24 h. The solution was filtered over a small amount of neutral Al_2O_3 (Brockman Type I), which was eluted with THF (10 ml). After removal of the solvent the deep red liquid was dried under vacuum. (Yield: 673 mg, quant.)

MW	440.31 g/mol
Formula	$C_{22}H_{22}CoO_4P$
^{31}P NMR (C_6D_6)	δ = 162.1 (bs), 166.2 (bs), 170.5 (bs)
IR (neat)	ν_{max} = 687, 756, 870, 984, 1193, 1486, 1586, 1937, 2895, 2954, 3073 cm^{-1}

→ Mixture of three conformers! Three sets of signals in the ^1H NMR (Cp resonances), ^{13}C NMR and ^{31}P NMR spectrum

^1H NMR

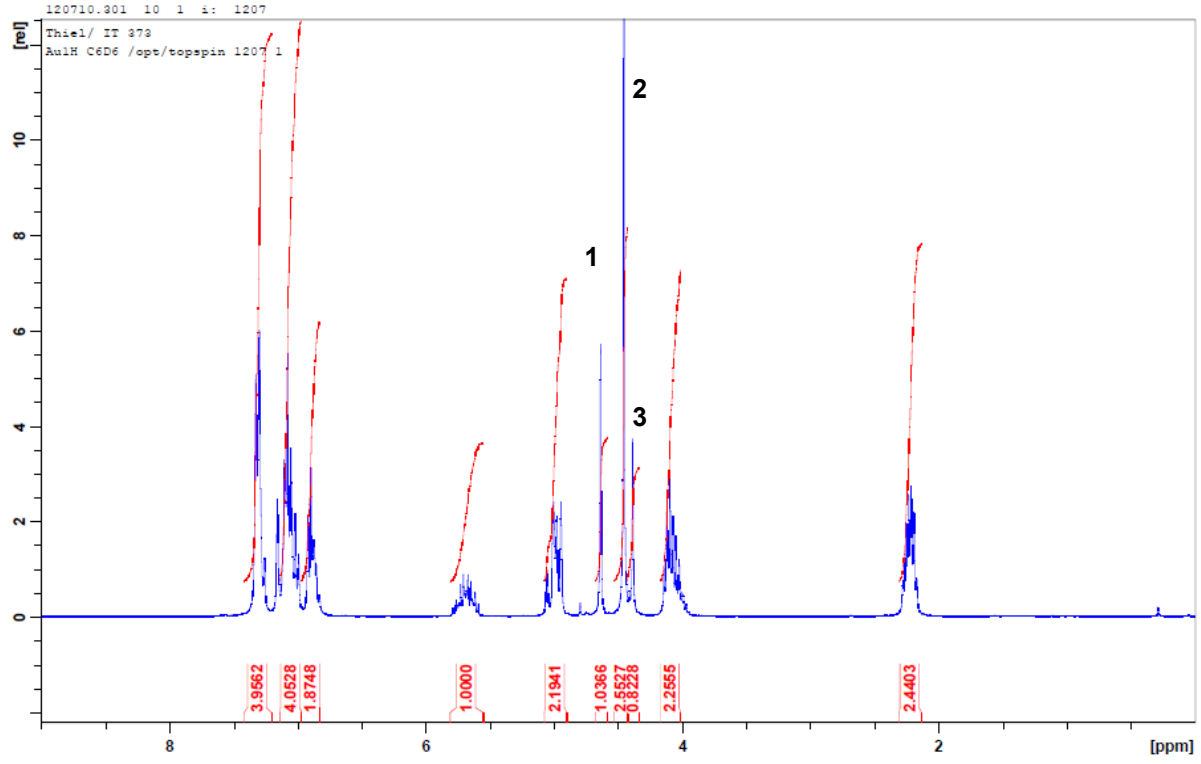

5.5.11 Synthesis of [CpCo(**30**)] (**34**)

Without further purification the mixture (178 mg) was dissolved in toluene (6 mL). The red solution was irradiated with light under reduced pressure for a total of 18 h. After filtration over a small amount of neutral Al_2O_3 (Brockman Type I), which was eluted with THF (20 ml), the solvent was removed under reduced pressure and the red oil dried under vacuum. (Yield: 126 mg, 76%)

MW	412.30 g/mol
Formula	$C_{21}H_{22}CoO_3P$
^{1}H NMR (C_6D_6)	δ = 1.45 (t, *J* = 10.8 Hz, 1H), 1.54 (m, 1H), 2.25 (m, 2H), 3.28 (m, 1H), 3.54-3.79 (m, 2H), 4.42 (s, Cp, 5H), 6.85 (m, 2H), 6.95-7.13 (m, 4H), 7.26 (t, *J* = 7.0 Hz, 4H)
^{31}P NMR (C_6D_6)	δ = 163.1 (bs)
^{13}C NMR (C_6D_6)	δ = 23.0 (d, *J* = 6.8 Hz), 31.1 (d, *J* = 10.5 Hz), 36.5 (d, *J* = 10.5 Hz), 65.1 (d, *J* = 1.9 Hz), 83.4 (d, *J* = 3.2 Hz), 121.34 (d, *J* = 5.1 Hz), 122.6 (d, *J* = 4.6 Hz), 124.0 (s), 124.3 (d, *J* = 1.3 Hz), 129.4 (d, *J* = 1.2 Hz), 129.6 (s), 152.51 (d, *J* = 3.2 Hz), 152.8 (d, *J* = 11.7 Hz)
CI (isobutane)	m/z 412
IR (neat)	ν_{max} = 687, 755, 863, 1022, 1188, 1485, 1588, 1947, 2896, 2969 cm^{-1}

5.5.12 Degradation of **31** to [CpCo(1,3-butadiene)] (**35**)

[CpCo(CO)(**17**)] (177 mg, 0.49 mmol) was dissolved in THF (6 mL) and irradiated at 25 °C for 6 h. A short filtration over neutral aluminium oxide with THF results in a red solution, which was carefully reduced under vacuum at low temperatures of -20 °C (the resulting red solid was volatile). (Yield: 36 mg, 41%)

MW	178.02 g/mol
Formula	$C_9H_{11}Co$
^{1}H NMR (C_6D_6)	-0.31 (ddt, *J* = 8.2 Hz / 1.6 Hz / 0.7 Hz, 2H), 1.75 (dd, *J* = 7.6 Hz / 1.6 Hz, 2H), 4.59 (s, 5H), 4.92 (m, 2H)
^{13}C NMR (C_6D_6)	31.3 (s), 78.5 (s), 79.7 (s)

CI (isobutane)	m/z 178

5.5.13 Synthesis of (–)-(p*S*)-bis(triethylphosphite)(η^5-1-neomenthylindenyl)cobalt ([Ind*Co{P(OEt)$_3$}$_2$]) (**76**)

A solution of [Ind*Co(cod)] (**10**) (226 mg, 0.5 mmol) and triethylphosphite (172 µL, 1 mmol) in THF (6 mL) was irradiated with light for 24 h. The solution was filtered over a small amount of neutral Al_2O_3 (Brockman Type I), which was washed with THF (10 ml). After removal of the solvent under reduced pressure the resulting deep red oil was dried under vacuum. (Yield: 258 mg, 74%)

MW	644.65 g/mol
Formula	$C_{31}H_{55}CoO_6P_2$
^{1}H-NMR (C_6D_6)	δ = 0.46 (d, *J* = 5.4 Hz, 3H), 0.95 (d, *J* = 5.4 Hz, 3H), 1.09 (d, *J* = 5.4 Hz, 3H), 1.15 (t, *J* = 7.2 Hz, 18H), 1.64 (d, *J* = 7.2 Hz, 4H), 1.97 (d, *J* = 11.3 Hz, 1H), 2.16 (m, 1H), 2.71 (d, *J* = 12.4 Hz, 1H), 3.57 (s, 2H), 3.79 (m, 12H), 4.47 (s, 1H), 5.61 (s, 1H), 6.85 (t, *J* = 7.3 Hz, 1H), 7.00 (t, *J* = 7.2 Hz, 1H), 7.45 (dd, *J* = 14.1 Hz / 14.5 Hz, 2H)
^{31}P-NMR (C_6D_6)	δ = 169.4 (bs), 173.9 (bs)
^{13}C-NMR (C_6D_6)	δ = 16.6 (d, *J* = 6.6 Hz), 19.4 (s), 23.3 (s), 23.5 (s), 24.1 (s), 28.4 (s), 29.2 (s), 29.7 (s), 34.0 (s), 35.9 (s), 44.3 (s), 48.2 (s), 59.3 (s), 66.4 (s), 88.4 (s), 96.3(s), 103.2 (s), 103.5 (s), 119.1 (s), 121.9 (s), 122.0 (s)
CI (isobutane)	m/z 644 [M^+]
HRMS (ESI)	not detectable

5.6 Synthesis of Substrates for the [2+2+2] Cycloaddition Reactions

5.6.1 Synthesis of **53**

53 was synthesized after a published protocol and the analytical data was in accordance with the reported data. [46, 52]

5.6.2 Synthesis of **54**

54 was synthesized after a published protocol and the analytical data was in accordance with the reported data. [46, 52]

5.6.3 Synthesis of **51**

51 was synthesized after a published protocol and the analytical data was in accordance with the reported data. [88-89]

5.6.4 Synthesis of **82**

53 (1.0 g, 6.2 mmol), $Pd(PPh_3)_4$ (713 mg, 0.62 mmol) and copper(I) iodide (235 mg, 1.2 mmol) were dissolved in toluene (30 mL). A solution of 1-iodonaphthalene (3.3 g, 13.0 mmol) in toluene (10 mL) was added to the solution before diisopropylamine (4.4 mL, 31 mmol) was slowly added. The solution was stirred at room temperature for 4 h during which a solid precipitated. The solvent was removed and the residue taken up in diethyl ether. Filtration and further washing of the residue with diethyl ether led after removal of the solvent to the crude product as a deep yellow oil. Purification via column chromatography (eluent: *n*-hexane/ethyl acetate 6:1, v/v) yielded the desired product as a viscous yellow oil. (Yield: 2.077 g, 81%)
The analytical data were in accordance with the reported data. [79]

5.7 Catalytic Screening of the Complexes

5.7.1 General Experimental Setup for the Screening of **11**-**16** and **18**-**22**

1,6-Heptadiyne (114 µL, 1 mmol), benzonitrile (515 µL, 5 mmol) and DHT (36 mg, 0.15 mmol) as internal standard were dissolved in THF (2 mL). A solution of the respective complex (5 mol% regarding the diyne) in THF (1 mL) was added and the reaction mixture stirred at 50 °C. At given times small aliquots of the reaction mixture (0.1 mL) were taken for GC analysis.

5.7.2 General Experimental Setup for the Screening of **23**-**26** and **27**

1,6-Heptadiyne (114 µL, 1 mmol), benzonitrile (515 µL, 5 mmol) and DHT (36 mg, 0.15 mmol) as internal standard were dissolved in THF (2 mL). A solution of the respective complex (5 mol% regarding the diyne) in THF (1 mL) was added and the reaction mixture stirred at 100 °C. At given times small aliquots of the reaction mixture (0.1 mL) were taken for GC analysis.

5.7.3 General Procedure for the Substrate Screening

5.7.3.1 Intermolecular Cyclotrimerization (diyne and nitrile)

Diyne (1 mmol), nitrile (5 mmol) and the respective complex (**11**, 26 mg, 5 mol% / **25**, 22 mg, 5 mol%) were dissolved in dry THF (3 mL). The solution was stirred at 50 °C / 100 °C for 3 h before the solvent was removed under reduced pressure. Column chromatography (*n*-hexane/ethyl acetate 6:1, v/v) afforded the respective pyridines as white solids or clear oils. The compounds were identified by NMR and MS and comparison of the obtaine dadata with reported data.

5.7.3.2 Intermolecular Cyclotrimerization (two alkynes and nitrile)

Alkyne (2 mmol), benzonitrile (5 mmol) and (**11**, 26 mg, 5 mol%/ **25**, 22 mg, 5 mol%) were dissolved in dry THF (3 mL). The solution was stirred at 50 °C / 100 °C for 3 h before the

solvent was removed under reduced pressure. Column chromatography (*n*-hexane/ethyl acetate 6:1, v/v) afforded the respective pyridines as a clear oil. The compound was identified by NMR and MS and comparison with reported data.

5.7.3.3 Intramolecular Cyclotrimerization

The respective triyne (1 mmol) and complex (5 mol% regarding the triyne) were dissolved in dry toluene (3 mL). The solution was stirred at 100 °C for 18 h before the solvent was removed under reduced pressure. Column chromatography (*n*-hexane/ethyl acetate 1:1, v/v) afforded the respective benzenes as white solids. The compounds were identified by NMR and MS and comparison with reported data.

5.7.4 General Procedure for the Substrate Screening in Enantioselective Cycloaddition Reactions

The synthesis of $[CoCl(PPh_3)_3]$ (**81**) was carried out according to the published procedure of Aresta et al. using $CoCl_2 \cdot 6\ H_2O$, triphenylphosphine and $NaBH_4$. [149]

5.7.4.1 Enantioselective Intermolecular Cyclotrimerization (diyne and nitrile)

The respective diyne (0.5 mmol) and nitrile (5 equiv. with regard to the diyne) were dissolved in THF (3 mL). A solution of **76** (5 mol% in regard to the diyne) in THF was added to the reaction mixture and the solution was stirred at the respective temperature.
At the end of the reaction, the solvent was removed under reduced pressure and the residue purified by column chromatography (*n*-hexane/ethyl acetate 6 : 1 or 10 : 1, v/v respectively) to yield the biaryls. The *ee* values were determined by chiral HPLC-analysis (Reprosil 100, *n*-heptane/ethanol 99 : 1, v/v, flow 0.5 ml/min).
The compounds were identified by NMR and MS and by their comparison with reported data.

5.7.4.2 Enantioselective Intramolecular Cyclotrimerization with **81** (triyne)

(A) Chiral Anion

The respective triyne (1 mmol), $[CoCl(PPh_3)_3]$ (**81**) (5 mol% in regard to the triyne) and the respective chiral anion (5 mol% with regard to the triyne) were dissolved in THF (3 mL). NEt_3 (3 drops) was added to the reaction mixture before the solution was stirred at room temperature for 1 h.

At the end of the reaction, the solvent was removed under reduced pressure and the residue purified by column chromatography (*n*-hexane/ethyl acetate 1 : 1, v/v) to yield the benzene derivative. The *ee* values were determined by chiral HPLC-analysis (Cellulose 2, *n*-heptane/isopropanol 95:5, v/v, 1 mL/min or Cellulose 4, *n*-heptane/ethanol 98:2, v/v, 1 mL/min).

The compounds were identified by NMR and MS and comparison with reported data.

5.7.4.3 Enantioselective Intramolecular Cyclotrimerization with **2** (triyne)

(A) Chiral Anion

The respective triyne (1 mmol), $[RhCl(PPh_3)_3]$ (**2**) (5 mol% in regard to the triyne), the respective chiral anion (5 mol% in regard to the triyne) and $AgNTf_2$ (5 mol% in regard to the triyne) were dissolved in THF (3 mL). NEt_3 (3 drops) was added to the reaction mixture before the solution was stirred at room temperature for 4 h.

At the end of the reaction, the solvent was removed under reduced pressure and the residue purified by column chromatography (*n*-hexane/ethyl acetate 1 : 1, v/v) to yield the benzene derivative. The *ee* values were determined by chiral HPLC-analysis (Cellulose 2, *n*-heptane/isopropanol 95:5, v/v, 1 mL/min or Cellulose 4, *n*-heptane/ethanol 98:2, v/v, 1 mL/min).

The compounds were identified by NMR and MS and comparison with reported data.

(B) Chiral Ligand

The respective triyne (1 mmol), $[RhCl(PPh_3)_3]$ (**2**) (5 mol% in regard to the triyne), the respective chiral ligand (5 mol% in regard to the triyne) and $AgNTf_2$ (5 mol% in regard to the triyne) were dissolved in THF (3 mL) and the solution was stirred at room temperature for 4 h.

At the end of the reaction, the solvent was removed under reduced pressure and the residue purified by column chromatography (*n*-hexane/ethyl acetate 1 : 1, v/v) to yield the benzene derivative. The *ee* values were determined by chiral HPLC-analysis (Cellulose 2, *n*-heptane/isopropanol 95:5, v/v, 1 mL/min or Cellulose 4, *n*-heptane/ethanol 98:2, v/v, 1 mL/min).
The compounds were identified by NMR and MS and comparison with reported data.

5.8 Recycling Experiments

5.8.1 Recycling Experiments with **25**

(A) Thermal Conditions
1,6-Heptadiyne (114 µL, 1 mmol) and benzonitrile (515 µL, 5 mmol) were dissolved in toluene (2 mL). A solution of **25** (22 mg, 5 mol%) in toluene (1 mL) was added and the reaction mixture stirred at 100 °C for 3 h.
The product was isolated via column chromatography (*n*-hexane/ethyl acetate 6:1, v/v) and the complex isolated as a red fraction by elution with pure ethyl acetate. Both samples were dried under high vacuum. ^{1}H and ^{31}P NMR proved that **25** was still intact and pure. The isolated **25** was reused in the next cyle.

(B) Photochemical Conditions
1,6-Heptadiyne (114 µL, 1 mmol) and benzonitrile (515 µL, 5 mmol) were dissolved in THF (5 mL). A solution of **25** (22 mg, 5 mol%) in THF (1 mL) was added and the reaction mixture irradiated with light at 25 °C for 3 h.
The product was isolated via column chromatography (*n*-hexane/ethyl acetate 6:1, v/v) and the complex isolated as a red fraction by elution with pure ethyl acetate. Both samples were dried under high vacuum. ^{1}H and ^{31}P NMR proved that **25** was still intact and pure. The isolated **25** was reused in the next cyle.

5.8.2 Experiments with Deuterated Dimethylfumarate

5.8.2.1 Synthesis of $D_3COOCCH=CHCOOCD_3$

The deuterated dimethylfumarate was prepared based on a procedure published by Thunberg and Allenmark. [150]

Fumaryl chloride (706 µL, 6.5 mmol) was dissolved in toluene (6 mL) before methanol-d_4 (2.5 mL, > 10 equiv.) was added to the solution. The solution was stirred at 60 °C for 22 h before it was allowed to cool to room temperature. Extraction of the organic phase with water (2 x 10 mL) and aqueous NaOH (1M, 1 x 10 mL), drying over $MgSO_4$ and removal of the organic solvent under reduced pressure led to a crystalline white solid. (Yield: 737 mg, 76%)

MW	150.16 g/mol
Formula	$C_6H_2D_6O_4$
^{1}H NMR ($CDCl_3$)	6.86 (s, 2H)
^{13}C NMR ($CDCl_3$)	51.8 (s), 133.5 (s), 165.5 (s)
GC-MS	m/z 150 (< 5%), 116 [M-CD_3O^+]
HRMS (EI)	calc.: m/z 150.0794; found: m/z 150.0796
mp	104-105°C
EA	calc.: C, 47.99%; H/D, 9.39%; found: C, 47.93%; H, 5.55% (No discrimination between H and D possible, therefore the found value of H has to be in accordance with the not deuterated species $C_6H_8O_4$ with calc.: H, 5.59%.)

5.8.2.2 Catalytic Trial in the Presence of Deuterated Dimethylfumarate

1,6-Heptadiyne (114 µL, 1 mmol), benzonitrile (515 µL, 5 mmol) and deuterated dimethylfumarate-d_6 (15 mg, 0.1 mmol) were dissolved in toluene (2 mL). A solution of **25** (22 mg, 0.05 mmol) in toluene (1 mL) was added and the reaction mixture stirred at 100 °C for 3 h. The solvent was removed under vacuum and the residue purified by column chromatography (*n*-hexane/ethyl acetate, v/v 6 : 1) yielding the product (129 mg, 66%) before the red band was collected by flushing the column with an eluent mixture of *n*-hexane/ethyl

acetate 1 : 1, v/v. The solvents were removed under reduced pressure yielding the complex as a red solid (quant.).

^{1}H NMR analysis shows that 40% of the original dimethylfumarate had been substituted by the deuterated analog.

CI (isobutane) m/z 441 [M+H$^+$] (deuterated analog), 435 [M+H$^+$]

^{1}H NMR

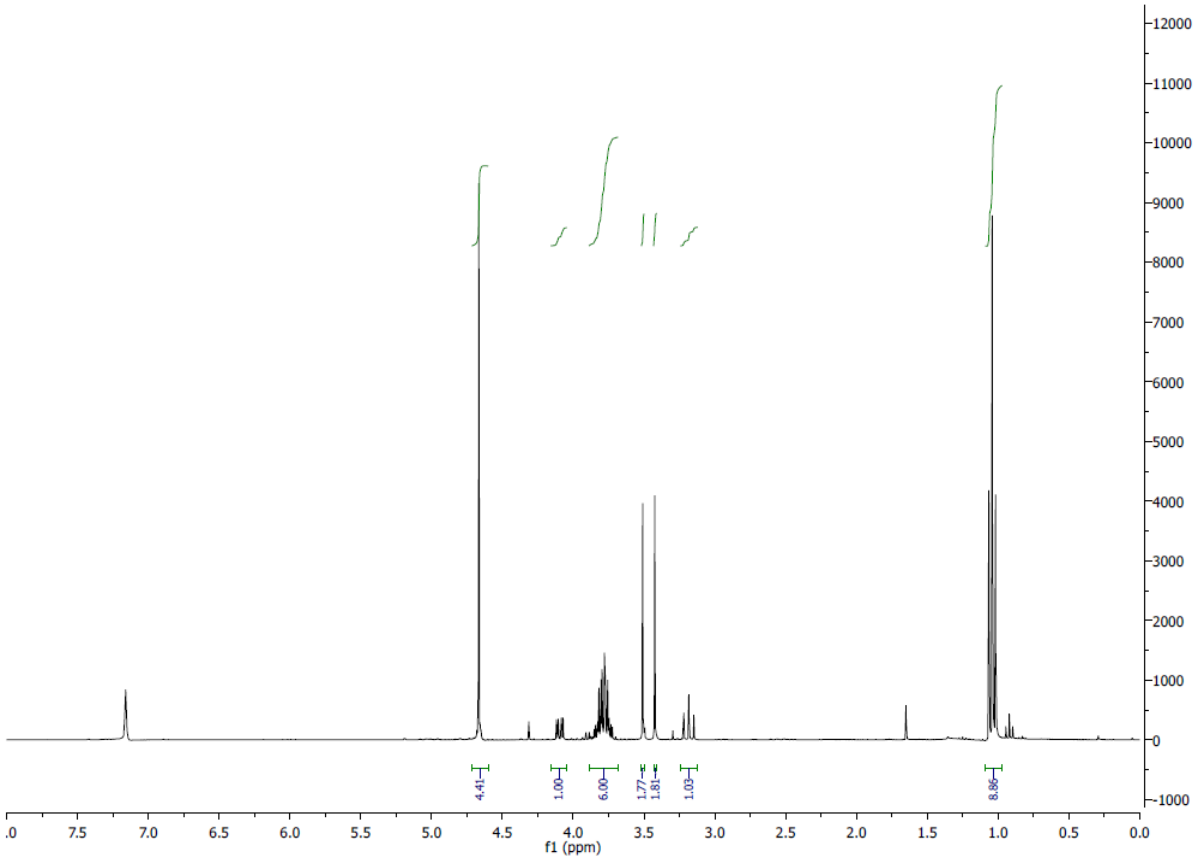

5.6.2.3 Control Experiment

Deuterated dimethylfumarate-d_6 (15 mg, 0.1 mmol) and **25** (22 mg, 0.05 mmol) were dissolved in toluene (3 mL) and the reaction mixture stirred at 100 °C for 3 h. The solvent was removed under vacuum and the residue purified by column chromatography (*n*-hexane/ethyl acetate, v/v 1 : 1). The red band was collected and the solvents removed under reduced pressure yielding the complex as a red solid (quant.).

^{1}H NMR analysis shows that 53% of the original dimethylfumarate had been substituted by the deuterated analog.

CI (isobutane) m/z 441 [M+H$^+$] (deuterated analog), 435 [M+H$^+$]

^{1}H NMR

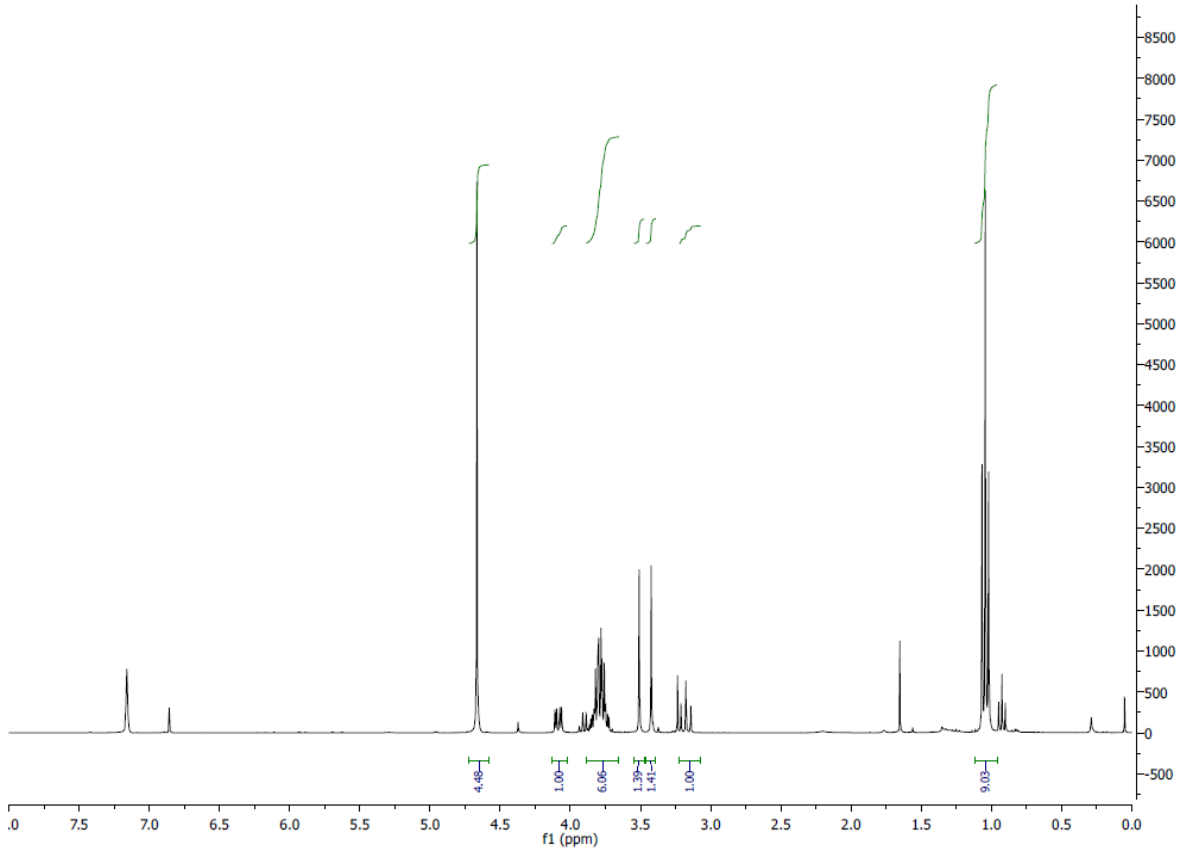

5.9 Characterization of Products of the [2+2+2] Cycloaddition Reaction

NMR data of compounds **43-46**, [51] **47-50**, [151] **52**, [88-89] **55-56** [52] and **83** [79] corresponded to the reported data in literature.

5.9.1 Characterization of **43**

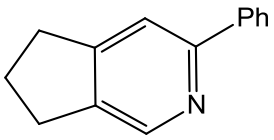

^{1}H NMR ($CDCl_3$) δ = 2.15 (qt, *J* = 7.24 Hz, 2H), 2.98 (t, *J* = 7.62 Hz, 4H), 7.36-7.41 (m, 1H), 7.367.43-7.48 (m, 2H), 7.61 (s, 1H), 7.94-7.98 (m, 2H), 8.54 (s, 1H)

^{13}C NMR ($CDCl_3$) δ = 25.1 (s), 30.1 (s), 33.0 (s), 117.5 (s), 127.2 (s), 128.9 (s), 129.1 (s), 139.7 (s), 143.9 (s), 154.6 (s), 156.7 (s)

5.9.2 Characterization of **44**

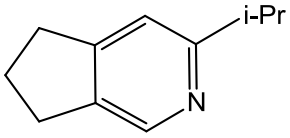

^{1}H NMR ($CDCl_3$) δ = 1.29 (d, *J* = 6.98 Hz, 6H), 2.08 (qt, *J* = 7.44 Hz, 2H), 2.88 (ddd, *J* = 2.82 / 7.53 Hz, 4H), 3.03 (sept, *J* = 6.72 Hz, 1H), 7.06 (s, 1H), 8.37 (s, 1H)

^{13}C NMR ($CDCl_3$) δ = 23.0 (s), 25.3 (s), 30.0 (s), 32.8 (s), 36.3 (s), 116.8 (s), 137.5 (s), 144.8 (s), 154.4 (s), 165.0 (s)

5.9.3 Characterization of **45**

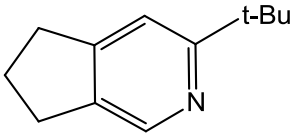

^{1}H NMR ($CDCl_3$) δ = 1.34 (s, 9H), 2.06 (qt, *J* = 7.48 Hz, 2H), 2.87 (t, *J* = 7.48 Hz, 4H), 7.22 (s, 1H), 8.40 (s, 1H)

^{13}C NMR ($CDCl_3$) δ = 25.2 (s), 30.0 (s), 30.5 (s), 32.9 (s), 37.2 (s), 115.3 (s), 138.0 (s), 144.4 (s), 154.0 (s), 167.0 (s)

5.9.4 Characterization of **46**

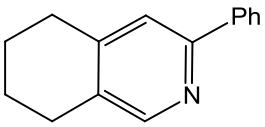

^{1}H NMR ($CDCl_3$) δ = 1.85 (qt, *J* = 3.33 Hz, 4H), 2.80 (m, 4H), 7.33-7.49 (m, 4H), 7.93 (m, 1H), 7.94 (s, 1H), 8.38 (s, 1H)

^{13}C NMR ($CDCl_3$) δ = 22.6 (s), 22.8 (s), 26.2 (s), 29.1 (s), 120.9 (s), 126.8 (s), 128.5 (s), 128.8 (s), 131.9 (s), 139.8 (s), 147.0 (s), 150.3 (s), 154.5 (s)

5.9.5 Characterization of **47**

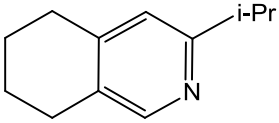

^{1}H NMR ($CDCl_3$) δ = 1.27 (d, *J* = 6.87 Hz, 6H), 1.80 (qt, *J* = 3.28 Hz, 4H), 2.71 (m, 4H), 2.97 (sept, *J* = 6.99 Hz, 1H), 6.85 (s, 1H), 8.22 (s, 1H)

^{13}C NMR ($CDCl_3$) δ = 22.7 (s), 22.8 (s), 22.9 (s), 26.1 (s), 29.0 (s), 35.9 (s), 120.3 (s), 120.6 (s), 125.7 (s), 130.0 (s), 130.4 (s), 146.6 (s), 149.7 (s)

GC-MS (EI) m/z 174

HRMS (ESI) calc.: m/z 176.1433 [M+H$^+$]; found: m/z 176.1435 [M+H$^+$]

5.9.6 Characterization of **48**

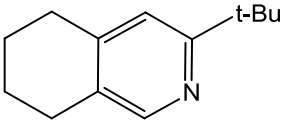

^{1}H NMR ($CDCl_3$) δ = 1.34 (s, 9H), 1.80 (qt, *J* = 3.36 Hz, 4H), 2.71 (m, 4H), 7.00 (s, 1H), 8.26 (s, 1H)

^{13}C NMR ($CDCl_3$) δ = 22.6 (s), 22.9 (s), 26.0 (s), 29.1 (s), 30.4 (s), 36.9 (s), 119.1 (s), 129.9 (s), 146.1 (s), 149.3 (s), 166.0 (s)

GC-MS (EI) m/z 188

HRMS (ESI) calc.: m/z 190.1590 [M+H$^+$]; found: m/z 190.1594 [M+H$^+$]

5.9.7 Characterization of **50**

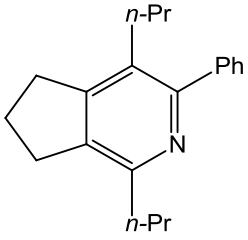

^{1}H NMR ($CDCl_3$) δ = 0.81 (t, *J* = 7.44 Hz, 3H), 0.98 (t, *J* = 7.44 Hz, 3H), 1.44 (sext, *J* = 7.89 Hz, 2H), 1.71 (sext, *J* = 7.89 Hz, 2H), 2.07 (qt, *J* = 7.35 Hz, 2H), 2.50 (m,

2H), 2.73 (m, 2H), 2.95 (m, 4H), 7.31-7.44 (m, 5H)

^{13}C NMR ($CDCl_3$) δ = 14.3 (s), 14.4 (s), 22.7 (s), 22.3 (s), 23.3 (s), 24.8 (s), 30.8 (s), 31.7 (s), 38.2 (s), 112.6 (s), 119.0 (s), 127.3 (s), 129.4 (s), 126.5 (s), 153.3 (s), 154.5 (s), 156.5 (s)

GC-MS (EI) m/z 279

HRMS (ESI) calc.: m/z 280.2060 [M+H$^+$]; found: m/z 280.2062 [M+H$^+$]

5.9.8 Characterization of **52**

^{1}H NMR ($CDCl_3$) δ = 1.65-1.76 (m, 1H), 1.77-1.84 (m, 1H), 1.84-1.91 (m, 2H), 2.28 (d, *J* = 17.4 Hz, 1H), 2.57 (m, 1H), 2.99 (dt, *J* = 6.1 Hz / 2.8 Hz, 2H), 3.90 (s, 3H), 7.38-7.45 (m, 5H), 7.46-7.52 (m, 2H), 7.60 (s, 1H), 7.90-7.94 (m, 1H), 7.99 (d, *J* = 9.0 Hz, 1H), 8.08-8.12 (m, 2H)

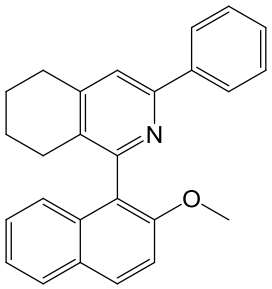

^{13}C NMR ($CDCl_3$) δ = 22.4 (s), 23.1 (s), 25.5 (s), 29.8 (s), 56.7 (s), 113.8 (s), 120.4 (s), 123.7 (s), 123.8 (s), 124.9 (s), 126.5 (s), 127.2 (s), 128.0 (s), 128.3 (s), 128.5 (s), 129.3 (s), 129.7 (s), 132.1 (s), 133.4 (s), 140.1 (s), 146.9 (s), 153.8 (s), 154.1 (s), 155.9 (s)

5.9.9 Characterization of **55**

^{1}H NMR ($CDCl_3$) δ = 5.00 (s, 4 H), 5.10 (s, 4 H), 7.12 (s, 2 H)

^{13}C NMR ($CDCl_3$) δ = 72.2 (s), 73.4 (s), 119.9 (s),132.3 (s), 138.6 (s)

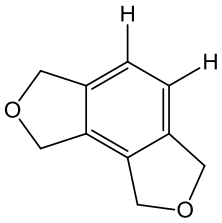

5.9.10 Characterization of **56**

^{1}H NMR ($CDCl_3$) δ = 5.00 (s, 4 H), 5.15 (s, 4 H), 7.01–7.04 (m, 4 H), 7.15–7.19 (m, 6 H)

^{13}C NMR ($CDCl_3$) δ = 72.9 (s), 73.8 (s), 127.0 (s), 128.1 (s), 129.6 (s), 131.4 (s),134.3 (s), 138.6 (s), 138.9 (s)

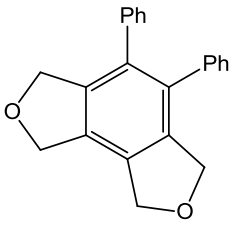

5.9.11 Characterization of **59**

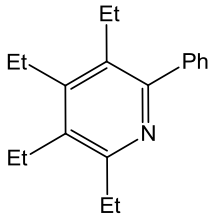

^{1}H NMR ($CDCl_3$)	δ = 0.90 (t, *J* = 7.18 Hz, 3H), 1.13 (t, *J* = 7.39 Hz, 3H), 1.14 (t, *J* = 7.39 Hz, 3H), 1.19 (t, *J* = 7.39 Hz, 3H), 2.47 (q, *J* = 7.61 Hz, 2H), 2.62 (dq, *J* = 7.61 Hz / 0.91 Hz, 4H), 2.73 (q, *J* = 7.61 Hz, 2H), 7.27 (m, 1H), 7.30 (m, 2H), 7. 32 (m, 2H)
^{13}C NMR ($CDCl_3$)	δ = 14.8 (s), 15.5 (s), 15.6 (s), 15.7 (s), 21.6 (s), 21.9 (s), 22.1 (s), 28.5 (s), 127.3 (s), 128.1 (s), 129.0 (s), 132.6 (s), 133.5 (s), 142.5 (s), 149.4 (s), 156.7 (s), 158.3 (s)
GC/MS (EI)	m/z 266
HRMS (EI)	calc.: m/z 266.1903; found: m/z 266.1901

5.9.12 Characterization of **60**

MW	307.39 g/mol
Formula	$C_{23}H_{17}N$
GC/MS (EI)	4 signals with each m/z 306 or m/z 307 (4 stereoisomers)

5.9.13 Characterization of **83**

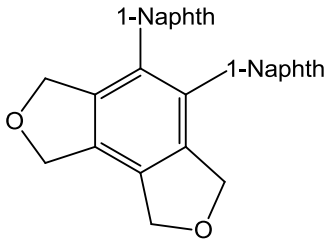

^{1}H-NMR ($CDCl_3$)	δ = 4.71 (d, *J* = 4.7 Hz, 2H), 4.76 (bs, 2H), 5.25 (s, 5H), 6.86 (m, 1H), 6.97 (m, 1H), 7.15 (m, 1H), 7.24 (m, 1H), 7.43-7.64 (m, 6H), 7.70 (m, 1H), 7.77 (m, 1H)
^{13}C-NMR ($CDCl_3$)	δ = 73.0 (s), 73.1 (s), 73.8 (s), 73.9 (s), 77.4 (s), 124.7 (s), 125.1 (s), 125.6 (s), 125.7 (s), 125.8 (s), 125.9 (s), 126.1 (s), 126.4 (s), 127.7 (s), 128.1 (s), 128.5 (s), 130.9 (s), 131.4 (s), 131.5 (s), 131.6 (s), 133.3 (s), 133.4 (s), 133.5 (s), 133.6 (s), 135.6 (s), 136.0 (s), 140.0 (s), 140.1 (s)

5.9.14 Characterization of **62**

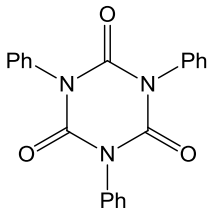

^{1}H-NMR ($CDCl_3$)	δ = 1.55 (s), 7.37-7.43 (m, 6H), 7.44-7.53 (m, 9H)
^{13}C-NMR ($CDCl_3$)	δ = 128.55 (s), 129.50 (s), 133.74 (s), 148.83 (s)
HRMS (ESI)	calc.: m/z 357.11134; found: m/z 358.11898 [M+H^+], m/z 380.10116 [M+Na^+]

5.10 *In situ* NMR Experiments

^{1}H and $^{31}P\{H\}$ NMR spectra were recorded on the Bruker AV 400 spectrometer. As a light source a Lumatec Superlite 400 with a mercury vapor lamp was used. The probe was irradiated with light the wavelength 320–500 nm (UVA and blue light) with an efficient energy output of 3.3 W. The charging of the NMR tube was carried out under standard Schlenk line techniques.

For the *in situ* NMR spectroscopy, a sapphire NMR tube was used to which an optical fiber was connected using a Ti flange. [114] The system was sealed using a Viton o-ring to maintain the inert gas atmosphere. With an inner diameter of 7 mm, the NMR tube provided a cross section greater than or equal to that which is given by the optical fiber, so that the radiation could penetrate the Ar atmosphere above the liquid without any significant loss of intensity. The refraction index of the sapphire and of the angle of incidence contribute to full reflection of the light that may hit the inner wall of the NMR tube before penetrating the liquid.

5.10.1 Reaction of **3** to **18**

The sapphire NMR tube was evacuated three times before [CpCo(cod)] (**3**) (30 mg, 0.13 mmol) and triphenylphosphite (67 µL, 0.26 mmol) were dissolved in C_6D_6 (2 mL).

As long as the probe is irradiated with light the temperature of the solution increases slowly over hours from 297.0 K to 300.5 K, remaining at this temperature for the rest of the experiment's time.

5.10.2 Reaction of **23** to **25**

The sapphire NMR tube was evacuated three times before [CpCo(CO){$P(OEt)_3$}] (**23**) (30 mg, 0.09 mmol) and dimethylfumarate (13.5 mg, 0.09 mmol) were dissolved in C_6D_6 (2 mL).

As long as the probe is irradiated with light the temperature of the solution increases slowly over hours from 297.0 K to 300.5 K, remaining at this temperature for the rest of the experiment's time.

5.10.3 Reaction of **31** to **35**

The sapphire NMR tube was evacuated three times before [CpCo(CO)(**17**)] (**31**) (25 mg, 0.07 mmol) was dissolved in C_6D_6 (2 mL).
As long as the probe is irradiated with light the temperature of the solution increases slowly over hours from 297.0 K to 300.5 K, remaining at this temperature for the rest of the experiment's time.

5.10.4 Reaction of **32** to **34**

The sapphire NMR tube was evacuated three times before [CpCo(CO)(**30**)] (**32**) (58 mg, 0.13 mmol) was dissolved in C_6D_6 (2 mL).
As long as the probe is irradiated with light the temperature of the solution increases slowly over hours from 297.0 K to 300.5 K, remaining at this temperature for the rest of the experiment's time.

5.11 Solid phase-Supported Catalysts

5.11.1 Synthesis of Cyclopentadiene Derivatives

5.11.1.1 Synthesis of **64**

2-Bromoethanol (3 mL, 42 mmol) was dissolved in dichloromethane (50 mL). Triethylamine (6.5 mL, 1.1 equiv.) was added to the solution and stirred for 10 min at room temperature before TMSCl (5.4 mL, 42 mmol) was slowly added via a syringe. A white solid precipitated. The suspension was stirred at room temperature for 3 h before it was heated to 40 °C for an additional hour. The solution was filtered and washed with water two times. The combined aqueous phase was washed with dichloromethane. The combined organic phase was dried over $MgSO_4$, filtered and the solvent removed under vacuum. The clear oil was dried under vacuum at low temperatures (0 °C). (Yield: 8.26 g, 98%)

MW	197.15 g/mol
Formula	$C_5H_{13}BrOSi$
^{1}H NMR ($CDCl_3$)	δ = 0.14 (s, TMS, 9H), 3.39 (t, *J* = 6.6 Hz, 2H), 3.8 (t, *J* = 6.6 Hz, 2H)
^{13}C NMR ($CDCl_3$)	δ = 0.06 (s), 33.2 (s), 63.1 (s)

5.11.1.2 Synthesis of **65**

TBSCl (5.33 g, 35 mmol) was dissolved in dichloromethane (40 mL). Triethylamine (5 mL, 1.1 equiv.), DMAP (42 mg, 0.34 mmol) and 2-Bromoethanol (2.5 mL, 35 mmol) were added via a syringe. A white solid precipitated while the suspension was stirred at room temperature for 18 h. The solvent was removed under vaccum before the residue was taken up in ethyl acetate and aqueous HCl (2 M). The water phase was extracted with ethyl acetate and the combined organic phases were washed with a saturated NaCl-solution, dried over $MgSO_4$, filtered and the solvent removed under vacuum. The clear oil was dried under vacuum. (Yield: 8.03 g, 95%)
NMR data of compound **65** corresponded to the reported data from the literature. [152]

5.11.1.3 Synthesis of **66**

To a solution of (2-bromoethoxy)trimethylsilane (2.97 g, 15 mmol) in diethyl ether (30 mL) a deep purple solution of sodium cyclopentadienide (7.5 mL, 2M in THF) was slowly added at -78 °C upon which a white solid precipitates. The solution was stirred at -78 °C for 1 h before it was allowed to warm to room temperature and stirred for further 18 h. Water was added to the suspension and the organic phase was washed with water twice, before it was dried over $MgSO_4$. Removal of the solvent resulted in a brownish liquid. After purification by column chromatography (eluent *n*-hexane/ethyl acetate 1 : 1, v/v) the desired compound was isolated as a clear liquid. (Yield: 880 mg, 32%)
NMR data of compound **66** corresponded to the reported data in the literature. [153]

5.11.1.4 Synthesis of **67**

To a solution of (2-bromoethoxy)(t-butyl)dimethylsilane (4.51 g, 19 mmol) in dichloromethane (100 mL) a deep purple solution of sodium cyclopentadienide (10 mL, 2M in THF) was slowly added at -78 °C upon which a white solid precipitates. The solution was stirred at -78 °C for 1 h before it was warmed to room temperature and stirred for further 18 h. Water was added to the suspension and the organic phase was washed with water twice, before it was dried over $MgSO_4$. Removal of the solvent resulted in a yellow liquid. After purification by column chromatography (eluent *n*-hexane/ethyl acetate 6 : 1, v/v) the desired compound was obtained as a clear colorless liquid. (Yield: 2.03 g, 48%)

MW	224.41 g/mol
Formula	$C_{13}H_{24}OSi$
^{1}H NMR ($CDCl_3$)	δ = 0.04 (s, 3H), 0.04 (s, 3H), 0.90 (s, 9H), 2.60 (m, 2H), 2.94 (m, 2H), 5.98-6.11 (m, 1H), 6.16-6.29 (m, 2H), 6.37-6.48 (m, 2H)
GC-MS	m/z 224

5.11.1.5 Synthesis of **71**

The synthesis of **71** was carried out after a procedure reported by Blum et al. [120]

(3-Bromopropyl)trimethoxysilane (6.6 mL, 35 mmol) was dissolved in THF (60 mL) and a solution of sodium cyclopentadienide (2M in THF, 18 mL) was slowly added at 0 °C. A white precipitate formed and the solution was stirred at room temperature overnight. The solvent was removed under reduced pressure and the residue extracted with *n*-hexane (3 x 15 mL). Removal of the solvent from the yellow solution resulted in a yellow-brown liquid, which was purified by bulb-to-bulb distillation (100 °C, 0.1 mbar). The resulting clear liquid contained two different isomers. (Yield: 4.799 g, 60%)
NMR data of compound **71** corresponds to the reported data in literature. [67b, 154]

MW	228.36 g/mol
Formula	$C1_1H_{20}O_3Si$
^{1}H NMR ($CDCl_3$)	δ = 0.68 (m, 2H), 1.67 (m, 2H), 2.41 (m, 2H), 2.87 (q, *J* = 1.5 Hz, 1H), 2.94 (q, *J* = 1.5 Hz, 1H), 3.56 (s, 9H), 5.99-6.17 (m, 1H), 6.23-6.45 (m, 2H)
^{13}C NMR ($CDCl_3$)	δ = 9.1 (s), 9.2 (s), 22.1 (s), 23.0 (s), 33.2 (s), 34.2 (s), 41.4 (s), 43.3 (s), 50.7 (s), 126.4 (s), 126.8 (s), 130.7 (s), 132.6 (s), 133.8 (s), 134.8 (s), 146.9 (s), 149.6 (s) (two sets of signals for two isomers)
GC-MS	m/z 228 (two isomers)

5.11.2 Synthesis of $Cp^{sub}Co$-complexes

5.11.2.1 Attempted synthesis of **68**

Route (A)

66 (774 mg, 3.4 mmol), $Co_2(CO)_8$ (590 mg, 1.7 mmol) and 3,3-dimethylbut-1-ene (5 mL) are dissolved in dichloromethane (5 mL) and stirred at 40 °C for 24 h. After removal of the solvents the red oil was dried under high vacuum.
NMR and MS analysis did not hint at the formation of the desired complex **68**.

Route (B)

$Co_2(CO)_8$ (150 mg, 0.44 mmol) and iodine (230 mg, 0.44 mmol) were dissolved in THF (30mL) and the green solution stirred at 25 °C for 2 h. Meanwhile **66** (80 mg, 0.44 mmol) and *n*-butyllithium (0.22 mL, 2M) were stirred in THF (5 mL) at -78 °C for 1 h before it was allowed to warm to room temperature. Both solutions were combined and stirred for further 18 h at room temperature. The color of the solution remained green over the entire time suggesting that no reaction had occurred. Removal of the solvent under reduced pressure resulted in a green black slurry.
NMR and MS analysis did not hint at the formation of the desired complex **68**.

Route (C)

$Co_2(CO)_8$ (690 mg, 2 mmol) and iodine (510 mg, 2 mmol) were dissolved in THF (30mL) and the green solution stirred at 25 °C for 2 h. Meanwhile **66** (727 mg, 4 mmol) and sodium sand (90 mg, 4 mmol) were stirred in THF (15 mL) at 25 °C until the gas evolution had ceased. Both solutions were combined and stirred for further 18 h at room temperature. The color of the solution remained green over the entire time suggesting that no reaction had occurred. Removal of the solvent under reduced pressure resulted in a green black slurry.
NMR and MS analysis did not hint at the formation of the desired complex **68**.

5.11.2.2 Attempted synthesis of **69**

Route (A)

67 (774 mg, 3.4 mmol), $Co_2(CO)_8$ (590 mg, 1.7 mmol) and 3,3-dimethylbut-1-ene (5 mL) were dissolved in dichloromethane (5 mL) and stirred at 40 °C for 24 h. After removal of the solvents the red oil was dried under high vacuum.
NMR and MS analysis did not hint at the formation of the desired complex **69**.

Route (C)

$Co_2(CO)_8$ (1 g, 2.9 mmol) and iodine (740 mg, 2.9 mmol) were dissolved in THF (30mL) and the green solution stirred at 25 °C for 2 h. Meanwhile **67** (1.3 g, 5.8 mmol) and sodium sand (133 mg, 5.8 mmol) were stirred in THF (15 mL) at 25 °C until the gas evolution had ceased. Both solutions were combined and stirred for further 18 h at room temperature. The color of the solution remained green over the entire time suggesting that no reaction had occurred. Removal of the solvent under reduced pressure resulted in a green black slurry.
NMR and MS analysis did not hint at the formation of the desired complex **69**.

5.11.2.3 Synthesis of **72**

a) The synthesis was carried out based on a procedure reported by Blum et al. [120]

Compound **71** (1.422 g, 6.2 mmol) and sodium sand (161 mg, 6.2 mmol) were stirred in THF (15 mL) at 25 °C for 24 h until all the sodium had reacted. The clear red solution was stirred for one further hour. Meanwhile $Co_2(CO)_8$ (1.066 g, 3.1 mmol) and iodine (791 mg, 3.1 mmol) were dissolved in THF (40 mL) and stirred for two hours. The sodium cyclopentadienyl solution was added to the green solution at room temperature and stirred for 18 h during which it turned red brown. Upon removal of the solvent the red brown residue was extracted with *n*-hexane (3 x 15 mL), filtered and the solvent reduced. The red oil was dried in high vacuum. (Yield: 591 mg, with 1:1 **71** impurity, 17%)

b) The synthesis was carried out based on a procedure reported by Pang et al. [119a]

Compound **71** (1.2 g, 5.2 mmol), $Co_2(CO)_8$ (899 mg, 2.6 mmol) and 3,3-dimethylbut-1-ene (4 mL) were stirred in dichloromethane (5 mL) at 40 °C for 72 h. All volatiles were removed and the residual red oil was taken up in *n*-pentane and filtered. Upon removal of the solvent the red oil was dried under high vacuum. (Yield: 1.667 g, 93%)

MW	342.31 g/mol
Formula	$C_{13}H_{19}CoO_5Si$

^{1}H NMR (C_6D_6)	δ = 0.60 (t, *J* = 7.8 Hz, 2H), 1.60 (m, 2H), 2.01 (t, *J* = 7.8 Hz, 2H), 3.43 (s, 9H), 4.37 (s, 2H), 4.56 (s, 2H)
^{13}C NMR (C_6D_6)	δ = 9.7 (s), 24.8 (s), 31.5 (s), 50.4 (s), 83.0 (s), 85.2 (s), 107 (s)
CI (isobutane)	m/z 343 [M^+], 315 [M-CO^+], 287 [M-$(CO)_2^+$]
IR	ν_{max} = 450, 541, 562, 616, 802, 1076, 1189, 1457, 1951, 2015, 2054, 2839, 2939 cm^{-1}

5.11.2.4 Synthesis of **73**

Compound **72** (1.242 g, 3.6 mmol) and triethylphosphite (616 µL, 3.6 mmol) were dissolved in THF (1 mL) and stirred at room temperature for 24 h. After addition of the triethylphosphite a gas evolution was visible. Removal of the solvent resulted in a red oil, which was dried under high vacuum. (Yield: 1.28 g, 74%; 26% unreacted [$Cp^{Si}Co(CO)_2$])

MW	480.45 g/mol
Formula	$C_{18}H_{34}CoO_7PSi$
^{1}H NMR (C_6D_6)	δ = 0.75 (m, 2H), 1.1 (t, *J* = 6.9 Hz, 9H), 1.86 (m, 2H), 2.40 (dt, *J* = 1.4 Hz / 7.7 Hz, 2H), 3.45 (s, 9H), 3.99 (dq, *J* = 7.1 Hz / 8.4 Hz, 6H), 4.63 (q, *J* = 1.7 Hz, 2H), 4.84 (t, *J* = 2.1 Hz, 2H)
^{13}C NMR (C_6D_6)	δ = 9.7 (s), 16.4 (d, *J* = 6.4 Hz), 24.7 (s), 31.5 (s), 50.3 (s), 60.5 (s), 83.0 (s), 85.2 (s)
^{31}P NMR (C_6D_6)	δ = 174.1 (bs)
CI (isobutane)	m/z 480 [M^+], 229 [Cp^{Si}+H^+]
IR	ν_{max} = 454, 556, 594, 805, 932, 1024, 1079, 1189, 1387, 1456, 1886, 1928, 2838, 2938 cm^{-1}

5.11.2.5 Synthesis of **74**

Compound **73** (830 mg, 1.73 mmol) and dimethylfumarate (250 mg, 1.73 mmol) were dissolved in THF (6 mL). The solution was irradiated with light under reduced pressure for 24 h before the solvent was removed and the residue taken up in *n*-pentane (5 mL). The solution was filtered to separate the unreacted dimethylfumarate and stored at -78 °C. This led to the

precipitation of an orange solid, which was isolated by filtration and which turned into a deep red oil at room temperature. (Yield: 820 mg, 51%)

MW	596.57 g/mol
Formula	$C_{23}H_{42}CoO_{10}PSi$
^{1}H NMR (C_6D_6)	δ = 0.77 (m, 2H), 1.08 (t, *J* = 7.3 Hz, 9H), 1.87 (quin, *J* = 8.5 Hz, 2H), 2.69 (m, 2H), 3.44 (s, 3H), 3.45 (s, 9H), 3.54 (s, 3H), 3.84 (m, 6H), 4.15 (quin, *J* = 2.0 Hz, 1H), 4.45 (m, 1H), 4.66 (m, 1H), 4.69 (m, 1H)
^{13}C NMR (C_6D_6)	δ = 9.8 (s), 16.2 (d, *J* = 6.8 Hz), 25.1 (s), 31.7 (s), 32.8 (s), 50.4 (s), 50.5 (s), 50.6 (s), 60.5 (s), 82.8 (s), 84.9 (s), 177.2 (s), 177.5 (s)
^{31}P NMR (C_6D_6)	δ = 161.4 (bs)
CI (isobutane)	m/z 597 [M+H$^+$], 452 [M-dimethylfumarate$^+$], 286 [M-dimethylfumarate -P(OEt)$_3^+$]
IR	ν_{max} = 438, 488, 556, 761, 931, 1020, 1080, 1150, 1187, 1252, 1294,1388, 1433, 1693, 1929, 1963, 2839, 2942 cm^{-1}
EA	calc.: C, 46.31%; H, 7.10%; P, 5.19%; Si, 4.71%; found: C, 46.57%; H, 7.07%; P, 5.10%; Si, 4.70%

5.11.2.6 Synthesis of **75**

Compound **71** (620 mg, 3 mmol) and sodium sand (70 mg, 3 mmol) were stirred in THF (12 mL) at 25 °C for 24 h until all the sodium had reacted. **81** (2.643 g, 3 mmol) was dissolved in THF (30 mL) and the red cyclopentadienyl solution was added at room temperature. The complete solution turned immediately red and was stirred for additional 2 h. 1,5-Cyclooctadiene (4 mL, mmol) was added and the solution stirred at 60 °C for additional 18 h. After evaporation of the solvent removal of the triphenylphosphine was accomplished by a method published by Lipshutz and Blomgren.[123] Merrifield's resin ((Chloromethyl)polystyrene, ~5.5 mmol/g Cl loading, obtained from Aldrich; CAS: 55844-94-5) (4 g) and sodium iodide (3 g) were added to the THF (20 mL) solution of the product mixture. After stirring the solution at room temperature for 18 h, the solution was filtered and the solvent removed under reduced pressure. The orange residue was taken up in warm *n*-

hexane and filtered. After removal of the solvent under reduced pressure the complex was obtained as a red oil. (Yield: 907 mg, 77%)

MW	394.47 g/mol
Formula	$C_{19}H_{31}CoO_3Si$
^{1}H NMR (C_6D_6)	δ = 0.72 (m, 2H), 1.73 (d, *J* = 7.8 Hz, 4H), 1.96 (m, 2H), 2.21 (m, 2H), 2.49 (m, 4H), 3.33 (m, 4H), 3.44 (s, 9H), 4.22 (t, *J* = 2.1 Hz, 2H), 4.35 (t, *J* = 2.3 Hz, 2H)
^{13}C NMR (C_6D_6)	δ = 9.9 (s), 24.5 (s), 28.4 (s), 31.3 (s), 32.5 (s), 50.4 (s), 64.6 (s), 83.1 (s), 84.3 (s)
CI (isobutane)	m/z 394 [M^+], 286 [M-cod$^+$]

5.11.3 Synthesis of Sol-Gel-Supported Cp^{sub}Co-complexes

All entrapment experiments were carried out according to a procedure reported by Schumann et al. [120] All aqueous solutions were prepared with degassed and distilled water.

5.11.3.1 Synthesis of SG-(**74**)

Method 1:
HCl (0.01 M, 1.2 mL), $Si(OMe)_4$ (2.5 mL, 17 mmol) and methanol (3.5 mL) were stirred for 15 min at room temperature. The acidic solution was neutralized by the addition of an aqueous solution of NH_4OH (0.1 M, 0.44 mL) and a solution of **74** (500 mg, 0.84 mmol) in THF (2 mL). The red mixture gelled within a few minutes and was left to stand for 1h. The wet gel was dried under high vacuum over night before the coarse red solid was crushed into smaller fragments. The solid was washed four times with hot dichloromethane removing any not entrapped **74**. After sonication in dichloromethane (10 mL) for 30 min the solid was dried under high vacuum over night. (Yield: 1.483 g)

EA	calc.: Co, 2.2%; found: Co, 1.35% (No complete combustion was possible, therefore no exact Co content could be determined)
ICP	calc.: Co, 2.2%; found: Co, 2.0%
IR	ν_{max} = 418, 438, 462, 788, 941, 1053 cm^{-1}

Method 2:

74 (163 mg, 0.30 mmol), HCl (0.01 M, 1.2 mL), $Si(OMe)_4$ (2.5 mL, 17 mmol) and methanol (3.5 mL) were stirred for 15 min at room temperature. The acidic solution was neutralized by the addition of an aqueous solution of NH_4OH (0.1 M, 0.44 mL). The red mixture gelled within a few minutes and was left to stand for 1h. The wet gel was dried under high vacuum over night before the coarse red solid was crushed into smaller fragments. The solid was washed four times with hot dichloromethane removing any not entrapped **74**. After sonication in dichloromethane (10 mL) for 30 min the solid was dried under high vacuum over night. (Yield: 797 mg)

EA	calc.: Co, 2.0%; found: Co, 0.04% (No complete combustion was possible, therefore no exact Co content could be determined)
ICP	calc.: Co, 2.0%; found: Co, 0.5%
IR	ν_{max} = 407, 435, 1053 cm^{-1}

5.11.3.2 Synthesis of SG-(**75**)

Method 1:

HCl (0.01 M, 2.4 mL), $Si(OMe)_4$ (5 mL, 34 mmol) and methanol (7 mL) were stirred for 15 min at room temperature. The acidic solution was neutralized by the addition of an aqueous solution of NH_4OH (0.1 M, 0.88 mL) and a solution of **75** (220 mg, 0.56 mmol) in THF (2 mL). The orange mixture gelled within a few minutes. The wet gel was dried under high vacuum over night before the coarse brown solid was crushed into smaller fragments. The solid was washed twice with hot dichloromethane removing any not entrapped **75**. After sonication in *n*-hexane (6 mL) for 30 min the solid was dried under high vacuum over night. (Yield: 2.5 g)

EA	calc.: Co, 1.32%; found: Co, 0.16% (No complete combustion was possible, therefore no exact Co content could be determined)
ICP	calc.: Co, 1.32%; found: 0.75%

5.11.3.3 Synthesis of SGL-(**74**)

Method 2:

74 (200 mg, 0.37 mmol), HCl (0.01 M, 0.6 mL), 1,4-bis(trimethoxysilylethyl)benzene (2.9 mL, 7.2 mmol) and methanol (2 mL) were stirred for 5 min at room temperature. The acidic solution was neutralized by the addition of an aqueous solution of NH_4OH (0.1 M, 0.22 mL). The red mixture gelled within a few minutes. The wet gel was broken apart with a spatula and washed with acetone and ethanol before it was shortly dried under high vacuum. After sonication in THF (10 mL) for 30 min the red solid was dried under high vacuum over night. (Yield: 2.489 g)

EA	calc.: Co, 0.8%; found: Co, 0.7% (No complete combustion was possible, therefore no exact Co content can be determined)
ICP	calc.: Co, 0.8%; found: Co, 0.3%

5.11.4 Synthesis of Silica-Supported $Cp^{sub}Co$-complexes

5.11.4.1 Synthesis of SiO_2-(**74**)

The supported catalyst was prepared after a reported procedure by Brintzinger et al. [67a] An alternative preparation procedure was reported by Booth et al. [67b]

74 (671 mg, 1.13 mmol) and silica (1 g) were stirred in toluene (10 mL) at 80 °C for 48 h. The solid was separated by filtration and washed with diethyl ether before it was transferred to a Soxhlet thimble and extracted with dichloromethane/diethyl ether (1:1; 100 mL) for 3 h. The pale orange solid was dried under vacuum to yield the desired supported complex. (Yield: 1.01 g)

EA	calc.: Co, 3.2%, P, 1.7%; found: Co, 1.4%, P, 0.7%
ICP	calc.: Co, 3.2%, P, 1.7%; found: Co, 2.0%, P, 0.8%
IR	ν_{max} = 448, 794, 1051 cm^{-1}

5.11.5 Catalytic Screening of the Solid-Supported Complexes

5.11.5.1 General Experimental Setup for the Screening of SG-(**74**), SG-(**75**), SGL-(**74**) and SiO_2-(**74**)

(A) Thermal Conditions

1,6-Heptadiyne (228 µL, 2 mmol), benzonitrile (1 mL, 10 mmol) and the solid supported cobalt complex were dissolved in toluene (3 mL). The solution was stirred at 100 °C for 24 h. After filtration and thorough washing with THF the combined solutions were evaporated under reduced pressure yielding a yellow oil. Purification through column chromatography (*n*-hexane/ethyl acetate, 6 : 1 v/v) yielded the desired product as a white solid. The catalyst was dried under high vacuum before it was reused in the next cycle.

(B) Microwave Conditions

1,6-Heptadiyne (114 µL, 1 mmol), benzonitrile (512 µL, 5 mmol) and the solid-supported cobalt complex were dissolved in DMF (2 mL). The solution was heated to 200 °C for 30 min. After filtration and thorough washing with THF the combined solutions were evaporated under reduced pressure yielding a yellow oil. Purification through column chromatography (*n*-hexane/ethyl acetate, 6 : 1 v/v) yielded the desired product as a white solid. The catalyst was dried under high vacuum before it was reused in the next cycle.

(C) Photochemical Conditions

1,6-Heptadiyne (228 µL, 2 mmol), benzonitrile (1 mL, 10 mmol) and the solid supported cobalt complex were dissolved in THF (6 mL). The solution was irradiated with light at room temperature for 24 h. After filtration and thorough washing with THF the combined solutions were evaporated under reduced pressure yielding a yellow oil. Purification through column chromatography (*n*-hexane/ethyl acetate, 6 : 1 v/v) yielded the desired product as a white solid. The catalyst was dried under high vacuum before it was reused in the next cycle.

5.12 Crystallographic Data

Table 15: Crystallographic data for **17**, **18** and **22**

	18	**22**	**31**
Empirical formula	$C_{41}H_{35}CoO_6P_2$	$C_{47}H_{29}CoF_{18}O_6P_2$	$C_{16}H_{16}CoO_4P$
Formula weight [g/mol]	744.56	1152.57	362.19
Color	yellow	yellow	orange
Crystal system	Monoclinic	Triclinic	Monoclinic
Space group	$P2_1/n$	$P\bar{1}$	$P2_{(1)}/_n$
Unit cell dimensions:			
a [Å]	10.6388(2)	12.6268(3)	6.2701(1)
b [Å]	8.0790(1)	13.1546(3)	9.8494(2)
c [Å]	40.5718(8)	14.8518(4)	24.7933(5)
α [°]	90	73.1950(10)	90
β [°]	92.796(1)	78.0650(10)	91.4320(1)
γ [°]	90	85.237(2)	90
Cell volume [$Å^3$]	3483.03(10)	2309.78(10)	1530.75(5)
Z	4	2	4
Calculated density [g/cm^{-3}]	1.420	1.657	1.572
Temperature [K]	150(2)	150(2)	150(2)
μ (Mo K α) [mm^{-1}]	0.634	0.564	1.240
Reflections collected	43961	92581	3694
Reflections unique	6550	10619	3224
Parameters	451	807	353
Goodness-of-fit (F^2)	0.945	1.041	1.038
R_1 ($I>2\sigma(I)$)	0.0257	0.0425	0.0370
wR_2 (all data)	0.0667	0.1196	0.0688
CCDC #	879909	879908	---

Table 16: Crystallographic data for **25** and **26**

	25	**26**
Empirical formula	$C_{17}H_{28}CoO_7P$	$C_{29}H_{28}CoO_7P$
Formula weight [g/mol]	434.29	578.41
Color	orange	red
Crystal system	Orthorombic	Monoclinic
Space group	$Pca2_{(1)}$	P2(1)/n
Unit cell dimensions:		
a [Å]	14.3800(7)	9.8124(2)
b [Å]	8.7254(5)	27.5055(6)
c [Å]	15.5859(7)	9.9190(2)
α [°]	90	90
β [°]	90	100.519(1)
γ [°]	90	90
Cell volume [$Å^3$]	1955.58(17)	2632.10(9)
Z	4	4
Calculated density [g/cm^{-3}]	1.475	1.460
Temperature [K]	150(2)	150(2)
μ (Mo K α) [mm^{-1}]	0.994	0.760
Reflections collected	4301	86796
Reflections unique	3731	6526
Parameters	353	353
Goodness-of-fit (F^2)	1.011	1.049
R_1 ($I>2\sigma(I)$)	0.0418	0.0260
wR_2 (all data)	0.0623	0.0650
CCDC #	928416	928415

5.13 Molecule Catalogue

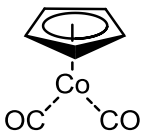

1

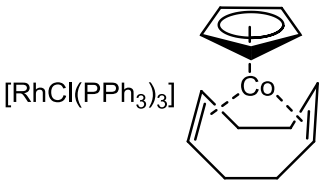

2 **3**

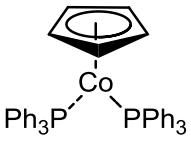

4

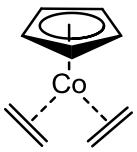

5

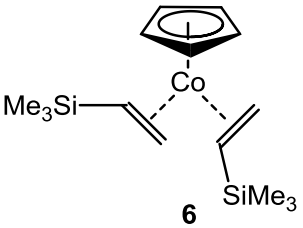

6

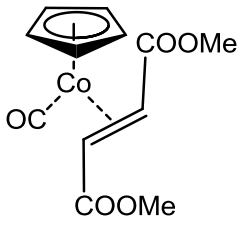

7

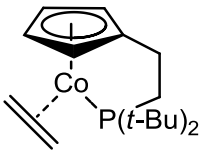

8

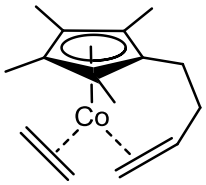

9

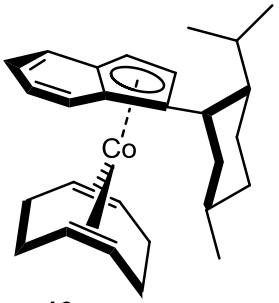

10

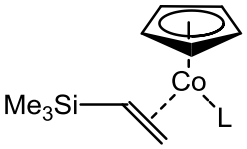

11 L = $P(OPh)_3$
12 L = $P(OCH_2CF_3)_3$
13 L = $P(OC_6H_4\text{-}p\text{-}CF_3)_3$
14 L = $P(OEt)_3$
15 L = $P(OiPr)_3$
16 L = cyclo-PO

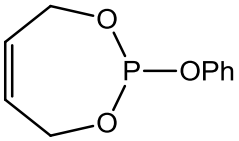

17

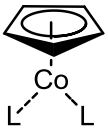

18 L = $P(OPh)_3$
19 L = $P(OEt)_3$
20 L = $P(OiPr)_3$
21 L = $P(OCH_2CF_3)_3$
22 L = $P(OC_6H_4\text{-}p\text{-}CF_3)_3$

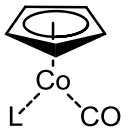

23 L = $P(OEt)_3$
24 L = $P(OPh)_3$

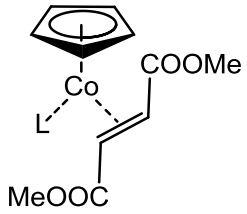

25 L = $P(OEt)_3$
26 L = $P(OPh)_3$

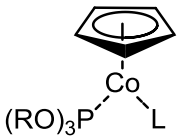

27 R = Et, L = coe
28 R = Ph, L = coe
29 R = Et, L = dimethylmaleate

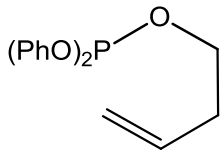

30

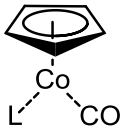

31 L = **17**
32 L = **30**

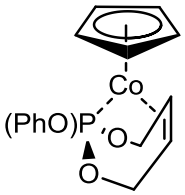

33

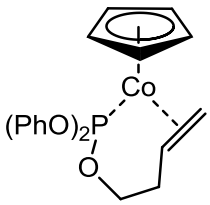

34

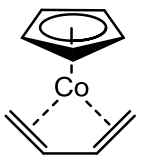

35

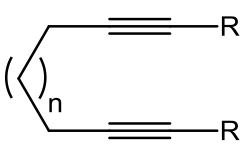

36 n = 1, R = H
37 n = 2, R = H
38 n = 3, R = H
39 n = 1, R = *n*-Pr

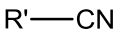

40 R' = Ph
41 R' = *i*-Pr
42 R' = *t*-Bu

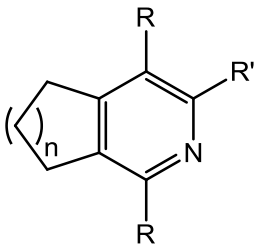

43 n = 1, R = H, R' = Ph
44 n = 1, R = H, R' = *i*-Pr
45 n = 1, R = H, R' = *t*-Bu
46 n = 2, R = H, R' = Ph
47 n = 2, R = H, R' = *i*-Pr
48 n = 2, R = H, R' = *t*-Bu
49 n = 3, R = H, R' = Ph
50 n = 1, R = *n*-Pr, R' = Ph

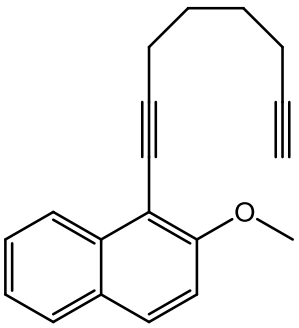

51

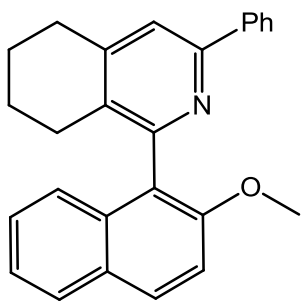

52

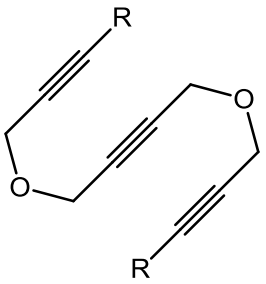

53 R = H
54 R = Ph

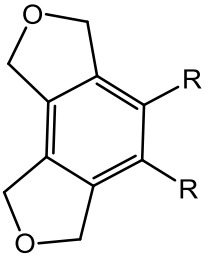

55 R = H
56 R = Ph

57 R = Et, R' = Et
58 R = Ph, R' = H

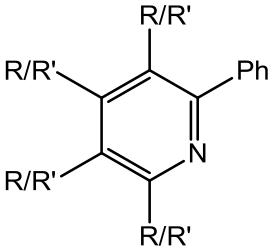

59 R = Et, R' = Et
60 R = Ph, R' = H

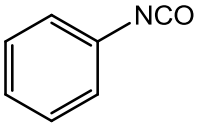

61

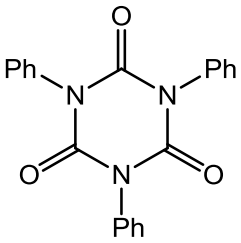

62

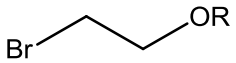

63 R = H
64 R = TMS
65 R = TBS

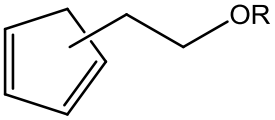

66 R = TMS
67 R = TBS

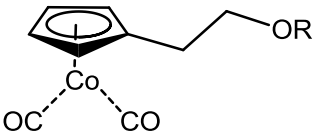

68 R = TMS
69 R = TBS

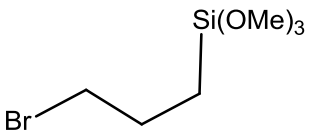

70

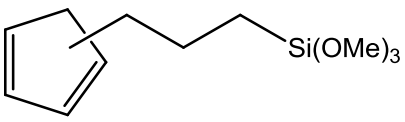

71

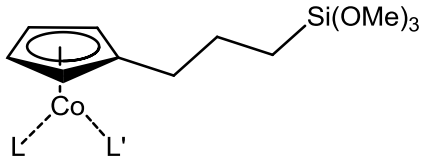

72 L = CO, L' = CO
73 L = CO, L' = $P(OEt)_3$
74 L = dimethylfumarate, L' = $P(OEt)_3$
75 L/L' = cod

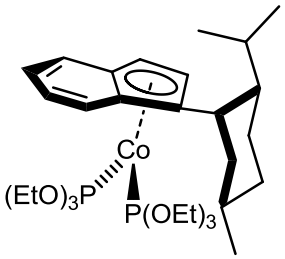

76

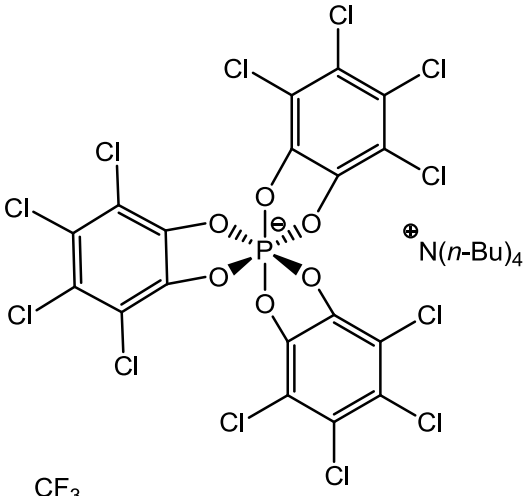

77

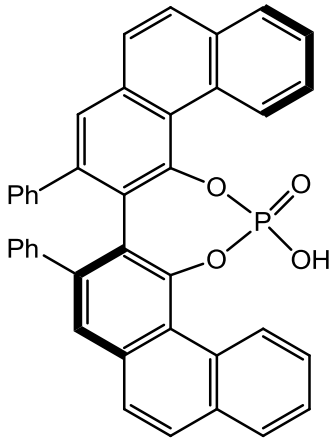

78

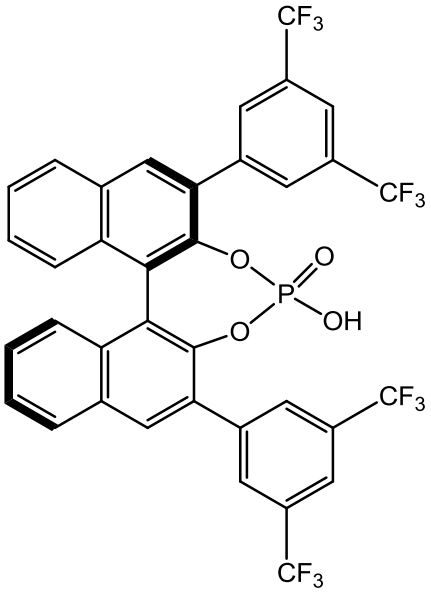

79

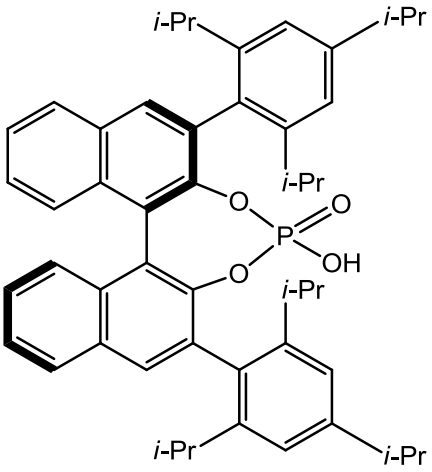

80

[CoCl(PPh$_3$)$_3$]

81

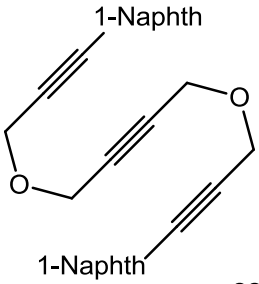

82

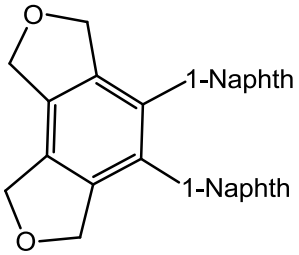

83

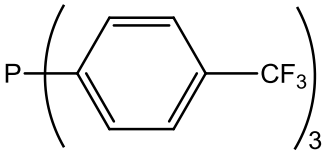

84

6. REFERENCES

[1] http://dictionary.reference.com/browse/catalysis, **2013**, June 16th; 15:49pm.

[2] a) J. J. Berzelius, *Annls. Chim. Phys.* **1836**, *61*, 146; b) A. J. B. Robertson, *Plat. Metals Rev.* **1975**, *19*, 64-69.

[3] *Vol.: DE235421 (C)* (Ed.: BASF), **1908**.

[4] a) P. H. Emmett, *CRC Crit. Rev. Solid State Sci.* **1973**, *4*, 127-150; b) J. K. Smith, in *Encyclopedia of Catalysis*, John Wiley & Sons, **2002**; c) G. A. Somorjai, K. McCrea, *Appl. Catal. A* **2001**, *222*, 3-18.

[5] G. Bringmann, Y. Reichert, V. V. Kane, *Tetrahedron* **2004**, *60*, 3539-3574.

[6] a) J. B. Tarr, J. Arditti, *Plant Physiol.* **1982**, *69*, 553-556; b) J. B. Tarr, J. Arditti, *Am. J. Bot.* **1979**, *66*, 1105-1113.

[7] A. Sakai, M. Kita, Y. Tani, *J. Nutr. Sci. Vitaminol.* **2004**, *50*, 69-77.

[8] A. E. Tschitschibabin, *J. Prak. Chem.* **1924**, *107*, 122-128.

[9] A. Hantzsch, *Justus Liebigs Ann. Chem.* **1882**, *215*, 1-82.

[10] F. Bohlmann, D. Rahtz, *Chem. Ber.* **1957**, *90*, 2265-2272.

[11] a) K. Yoshida, F. Kawagoe, N. Iwadate, H. Takahashi, T. Imamoto, *Chem. Asian J.* **2006**, *1*, 611-613; b) H. Takahashi, K. Yoshida, A. Yanagisawa, *J. Org. Chem.* **2009**, *74*, 3632-3640; c) K. Yoshida, H. Takahashi, T. Imamoto, *Chem. Eur. J.* **2008**, *14*, 8246-8261; d) K. Yoshida, S. Horiuchi, N. Iwadate, F. Kawagoe, T. Imamoto, *Synlett* **2007**, 1561-1564.

[12] Y. Wei, N. Yoshikai, *J. Am. Chem. Soc.* **2013**, *135*, 3756–3759.

[13] J. M. Neely, T. Rovis, *J. Am. Chem. Soc.* **2013**, *135*, 66-69.

[14] K. P. C. Vollhardt, *Angew. Chem., Int. Ed. Engl.* **1984**, *23*, 539-556.

[15] M. J. Eichberg, R. L. Dorta, K. Lamottke, K. P. C. Vollhardt, *Org. Lett.* **2000**, *2*, 2479-2481.

[16] a) R. L. Funk, K. P. C. Vollhardt, *J. Am. Chem. Soc.* **1977**, *99*, 5483-5484; b) R. L. Funk, K. P. C. Vollhardt, *J. Am. Chem. Soc.* **1980**, *102*, 5253-5261.

[17] a) S. J. Neeson, P. J. Stevenson, *Tetrahedron* **1989**, *45*, 6239-6248; b) B. Witulski, A. Zimmermann, N. D. Gowans, *Chem. Commun.* **2002**, 2984-2985.

[18] E. A. Anderson, E. J. Alexanian, E. J. Sorensen, *Angew. Chem., Int. Ed.* **2004**, *43*, 1998-2001.

[19] A. Gutnov, V. Abaev, D. Redkin, C. Fischer, W. Bonrath, B. Heller, *Synlett* **2005**, 1188-1190.

[20] R. B. Woodward, R. Hoffmann, *The Conservation of Orbital Symmetry*, Academic Press, New York, **1970**.

[21] S. W. Benson, *Thermodynamic Kinetics*, Wiley, New York, **1976**.

[22] a) K. N. Houk, R. W. Gandour, R. W. Strozier, N. G. Rondan, L. A. Paquette, *J. Am. Chem. Soc.* **1979**, *101*, 6797-6802; b) W. V. Dower, K. P. C. Vollhardt, *J. Am. Chem. Soc.* **1982**, *104*, 6878-6879; c) R. C. Bingham, M. J. S. Dewar, D. H. Lo, *J. Am. Chem. Soc.* **1975**, *97*, 1294-1301.

[23] a) D. B. Grotjahn, *Comprehensive Organometallic Chemistry II, Vol. 12*, Pergamon, Oxford, **1995**; b) H. Bönnemann, W. Brijoux, *Transition Metals for Organic Synthesis, Vol. 1*, Wiley-VCH, Weinheim, **1998**; c) J. P. Collman, L. S. Hegedus, J. R. Norton, R. G. Finke, *Principles and Applications of Organotransition Metal Chemistry*, Oxford University Press, Oxford, **1987**; d) N. E. Schore, *Chem. Rev.* **1988**, *88*, 1081-1119; e) J. A. Varela, C. Saá, *Chem. Rev.* **2003**, *103*, 3787-3802; f) S. Kotha, E. Brahmachary, K. Lahiri, *Eur. J. Org. Chem.* **2005**, 4741-4767; g) J. Louie, *Curr.*

Org. Chem. **2005**, *9*, 605-623; h) P. R. Chopade, J. Louie, *Adv. Synth. Catal.* **2006**, *348*, 2307-2327; i) B. R. Galan, T. Rovis, *Angew. Chem. Int. Ed.* **2009**, *48*, 2830-2834; j) P. A. Inglesby, P. A. Evans, *Chem. Soc. Rev.* **2010**, *39*, 2791-2805.

[24] a) J. Louie, J. E. Gibby, M. V. Farnworth, T. N. Tekavec, *J. Am. Chem. Soc.* **2002**, *124*, 15188-15189; b) M. M. McCormick, H. A. Duong, G. Zuo, J. Louie, *J. Am. Chem. Soc.* **2005**, *127*, 5030-5031; c) R. M. Stolley, H. A. Duong, D. R. Thomas, J. Louie, *J. Am. Chem. Soc.* **2012**, *134*, 15154–15162; d) T. N. Tekavec, A. M. Arif, J. Louie, *Tetrahedron* **2004**, *60*, 7431-7437; e) T. N. Tekavec, G. Zuo, K. Simon, J. Louie, *J. Org. Chem.* **2006**, *71*, 5834-5836.

[25] a) B. R. D'Souza, T. K. Lane, J. Louie, *Org. Lett.* **2011**, *13*, 2936-2939; b) C. Wang, D. Wang, F. Xu, B. Pan, B. Wan, *J. Org. Chem.* **2013**, *78*, 3065–3072.

[26] a) Y. Wakatsuki, H. Yamazaki, *J. Chem. Soc., Chem. Commun.* **1973**, 280a-280a; b) U. M. Dzhemilev, F. A. Selimov, G. A. Tolstikov, *ARKIVOC* **2001**, *9*, 85-116; c) H. Bönnemann, *Angew. Chem., Int. Ed. Engl.* **1985**, *24*, 248-262; d) B. Heller, M. Hapke, *Chem. Soc. Rev.* **2007**, *36*, 1085-1094; e) B. Heller, G. Oehme, *J. Chem. Soc., Chem. Commun.* **1995**, 179-180; f) S. Okamoto, Y.-k. Sugiyama, *Synlett* **2013**, 1044-1060.

[27] a) P. Diversi, L. Ermini, G. Ingrosso, A. Lucherini, *J. Organomet. Chem.* **1993**, *447*, 291-298; b) P. Diversi, G. Ingrosso, A. Lucherini, A. Minutillo, *J. Mol. Catal.* **1987**, *40*, 359-377.

[28] a) G. Onodera, Y. Shimizu, J.-n. Kimura, J. Kobayashi, Y. Ebihara, K. Kondo, K. Sakata, R. Takeuchi, *J. Am. Chem. Soc.* **2012**, *134*, 10515–10531; b) G. Onodera, M. Suto, R. Takeuchi, *J. Org. Chem.* **2011**, *77*, 908–920; c) T. Shibata, Y. Arai, K. Takami, K. Tsuchikama, T. Fujimoto, S. Takebayashi, K. Takagi, *Adv. Synth. Catal.* **2006**, *348*, 2475-2483; d) T. Shibata, T. Fujimoto, K. Yokota, K. Takagi, *J. Am. Chem. Soc.* **2004**, *126*, 8382-8383; e) T. Shibata, S. Yoshida, Y. Arai, M. Otsuka, K. Endo, *Tetrahedron* **2008**, *64*, 821-830.

[29] T. Hosokawa, N. Shimo, K. Maeda, A. Sonoda, S. I. Murahashi, *Tetrahedron Lett.* **1976**, *17*, 383-386.

[30] Y. Yamamoto, R. Ogawa, K. Itoh, *J. Am. Chem. Soc.* **2001**, *123*, 6189-6190.

[31] a) Y. Satoh, Y. Obora, *J. Org. Chem.* **2011**, *76*, 8569-8573; b) Y. Satoh, K. Yasuda, Y. Obora, *Organometallics* **2012**, *31*, 5235-5238; c) Y. Satoh, Y. Obora, *J. Org. Chem.* **2013**, *78*, 7771-7776.

[32] D. Suzuki, R. Tanaka, H. Urabe, S. Sato, *J. Am. Chem. Soc.* **2002**, *124*, 3518-3519.

[33] a) T. Takahashi, F. Y. Tsai, M. Kotora, *J. Am. Chem. Soc.* **2000**, *122*, 4994-4995; b) T. Takahashi, F. Y. Tsai, Y. Li, H. Wang, Y. Kondo, M. Yamanaka, K. Nakajima, M. Kotora, *J. Am. Chem. Soc.* **2002**, *124*, 5059-5067.

[34] a) N. Weding, M. Hapke, *Chem. Soc. Rev.* **2011**, *40*, 4525-4538; b) K. Tanaka, *Heterocycles* **2012**, *85*, 1017-1043.

[35] a) M. Berthelot, *C. R. Hebd. Seances Acad. Sci.* **1866**, *63*, 905-909; b) A. Henninger, *Ber. Dtsch. Chem. Ges.* **1877**, *10*, 727-737.

[36] W. Ramsay, *Phil. Mag.* **1876**, *2*, 269-281.

[37] a) W. Reppe, O. Schlichting, K. Klager, T. Toepel, *Justus Liebigs Ann. Chem.* **1948**, *560*, 1-92; b) W. Reppe, W. J. Schweckendiek, *Justus Liebigs Ann. Chem.* **1948**, *560*, 104-116.

[38] a) G. Dazinger, M. Torres-Rodrigues, K. Kirchner, M. J. Calhorda, P. J. Costa, *J. Organomet. Chem.* **2006**, *691*, 4434-4445; b) N. Saino, D. Kogure, K. Kase, S. Okamoto, *J. Organomet. Chem.* **2006**, *691*, 3129-3136; c) M. A. Bennett, E. Wenger, *Organometallics* **1995**, *14*, 1267-1277.

[39] a) A. A. Dahy, N. Koga, *J. Organomet. Chem.* **2010**, *695*, 2240-2250; b) A. A. Dahy, K. Yamada, N. Koga, *Organometallics* **2009**, *28*, 3636-3649; c) D. R. McAlister, J. E.

Bercaw, R. G. Bergman, *J. Am. Chem. Soc.* **1977**, *99*, 1666-1668; d) R. Diercks, B. E. Eaton, S. Gürtzgen, S. Jalisatgi, A. J. Matzger, R. H. Radde, K. P. C. Vollhardt, *J. Am. Chem. Soc.* **1998**, *120*, 8247-8248.

[40] a) J. P. Collman, J. W. Kang, W. F. Little, M. F. Sullivan, *Inorg. Chem.* **1968**, *7*, 1298-1303; b) H. Yamazaki, N. Hagihara, *J. Organomet. Chem.* **1970**, *21*, 431-443; c) H. Yamazaki, N. Hagihara, *J. Organomet. Chem.* **1967**, *7*, P22-P23.

[41] Y. Wakatsuki, H. Yamazaki, *Tetrahedron Lett.* **1973**, *14*, 3383-3384.

[42] H. Bönnemann, *Angew. Chem., Int. Ed. Engl.* **1978**, *17*, 505-515.

[43] Y. Wakatsuki, T. Kuramitsu, H. Yamazaki, *Tetrahedron Lett.* **1974**, *15*, 4549-4552.

[44] J. P. Lomont, S. C. Nguyen, M. C. Zoerb, A. D. Hill, J. P. Schlegel, C. B. Harris, *Organometallics* **2012**, *31*, 3582-3587.

[45] N. Agenet, V. Gandon, K. P. C. Vollhardt, M. Malacria, C. Aubert, *J. Am. Chem. Soc.* **2007**, *129*, 8860-8871.

[46] N. Weding, R. Jackstell, H. Jiao, A. Spannenberg, M. Hapke, *Adv. Synth. Catal.* **2011**, *353*, 3423-3433.

[47] R. Benn, K. Cibura, P. Hofmann, K. Jonas, A. Rufinska, *Organometallics* **1985**, *4*, 2214-2221.

[48] H. Bönnemann, W. Brijoux, R. Brinkmann, W. Meurers, R. Mynott, W. von Philipsborn, T. Egolf, *J. Organomet. Chem.* **1984**, *272*, 231-249.

[49] B. Heller, B. Sundermann, H. Buschmann, H.-J. Drexler, J. You, U. Holzgrabe, E. Heller, G. Oehme, *J. Org. Chem.* **2002**, *67*, 4414-4422.

[50] K. Jonas, E. Deffense, D. Habermann, *Angew. Chem., Int. Ed. Engl.* **1983**, *22*, 716-717.

[51] M. Hapke, N. Weding, A. Spannenberg, *Organometallics* **2010**, *29*, 4298-4304.

[52] A. Geny, N. Agenet, L. Iannazzo, M. Malacria, C. Aubert, V. Gandon, *Angew. Chem. Int. Ed.* **2009**, *48*, 1810-1813.

[53] a) J. Foerstner, R. Kettenbach, R. Goddard, H. Butenschön, *Chem. Ber.* **1996**, *129*, 319-325; b) H. Butenschön, R. T. Kettenbach, C. Krüger, *Angew. Chem., Int. Ed. Engl.* **1992**, *31*, 1066-1068; c) R. T. Kettenbach, W. Bonrath, H. Butenschön, *Chem. Ber.* **1993**, *126*, 1657-1669; d) J. Okuda, K. H. Zimmermann, E. Herdtweck, *Angew. Chem., Int. Ed. Engl.* **1991**, *30*, 430-431; e) J. Okuda, K. H. Zimmermann, *Chem. Ber.* **1992**, *125*, 637-641.

[54] J. A. Klang, D. B. Collum, *Organometallics* **1988**, *7*, 1532-1537.

[55] K. P. Angermund, P. Betz, H. Butenschön, *Chem. Ber.* **1993**, *126*, 713-724.

[56] A. Spencer, H. Werner, *J. Organomet. Chem.* **1979**, *171*, 219-228.

[57] L. Hofmann, H. Werner, *J. Organomet. Chem.* **1985**, *289*, 141-155.

[58] H. Werner, B. Juthani, *J. Organomet. Chem.* **1981**, *209*, 211-218.

[59] P. Hong, Y. Yamamoto, H. Yamazaki, *J. Organomet. Chem.* **1982**, *232*, 71-79.

[60] D. W. Macomber, R. D. Rogers, *Organometallics* **1985**, *4*, 1485-1487.

[61] a) C. L. Vélez, P. R. L. Markwick, R. L. Holland, A. G. DiPasquale, A. L. Rheingold, J. M. O'Connor, *Organometallics* **2010**, *29*, 6695-6702; b) E. Fooladi, B. Dalhus, M. Tilset, *Dalton Trans.* **2004**, 3909-3917.

[62] M. E. Rerek, F. Basolo, *Organometallics* **1983**, *2*, 372-376.

[63] C. C. Leznoff, *Chem. Soc. Rev.* **1974**, *3*, 65-85.

[64] a) D. C. Bailey, S. H. Langer, *Chem. Rev.* **1981**, *81*, 109-148; b) F. R. Hartley, P. N. Vezey, in *Advances Organometallic Chemistry, Vol. 15* (Eds.: F. G. A. Stone, R. West), Academic Press Inc., London, **1977**, 189-234.

[65] Y.-Y. Lin, S.-C. Tsai, S. J. Yu, *J. Org. Chem.* **2008**, *73*, 4920-4928.

[66] a) R. van Heerbeek, P. C. J. Kamer, P. W. N. M. van Leeuwen, J. N. H. Reek, *Chem. Rev.* **2002**, *102*, 3717-3756; b) L. Garcia, A. Roglans, R. Laurent, J.-P. Majoral, A. Pla-Quintana, A.-M. Caminade, *Chem. Commun.* **2012**, *48*, 9248-9250.
[67] a) F. R. W. P. Wild, G. Gubitosa, H. H. Brintzinger, *J. Organomet. Chem.* **1978**, *148*, 73-80; b) B. L. Booth, G. C. Ofunne, C. Stacey, P. J. T. Tait, *J. Organomet. Chem.* **1986**, *315*, 143-156.
[68] E. Serrano, N. Linares, J. Garcia-Martinez, J. R. Berenguer, *ChemCatChem* **2013**, *5*, 844-860.
[69] a) N. E. Leadbeater, *Tetrahedron Lett.* **2002**, *43*, 691-693; b) W. D. Bonds, C. H. Brubaker, E. S. Chandrasekaran, C. Gibbons, R. H. Grubbs, L. C. Kroll, *J. Am. Chem. Soc.* **1975**, *97*, 2128-2132; c) C. Ayats, A. H. Henseler, M. A. Pericàs, *ChemSusChem* **2012**, *5*, 320-325; d) S. Islam, M. Mobarok, P. Mondal, A. Roy, N. Salam, D. Hossain, S. Mondal, *Transition Met. Chem.* **2012**, *37*, 97-107.
[70] a) Z. Zhang, S. D. Lepore, *Tetrahedron Lett.* **2002**, *43*, 7357-7360; b) K. Heinze, M. Beckmann, K. Hempel, *Chem. Eur. J.* **2008**, *14*, 9468-9480; c) Z. M. Michalska, D. E. Webster, *Plat. Metals Rev.* **1974**, *18*, 65-73.
[71] V. Conte, E. Elakkari, B. Floris, V. Mirruzzo, P. Tagliatesta, *Chem. Commun.* **2005**, 1587-1588.
[72] I. González, S. Bouquillon, A. Roglans, J. Muzart, *Tetrahedron Lett.* **2007**, *48*, 6425-6428.
[73] Y.-H. Wang, S.-H. Huang, T.-C. Lin, F.-Y. Tsai, *Tetrahedron* **2010**, *66*, 7136-7141.
[74] P. Perkins, K. P. C. Vollhardt, *J. Am. Chem. Soc.* **1979**, *101*, 3985-3987.
[75] Y. Wakatsuki, H. Yamazaki, *Synthesis* **1976**, 26-28.
[76] K. Tanaka, *Synlett* **2007**, 1977-1993.
[77] D. D. Young, A. Deiters, *Angew. Chem. Int. Ed.* **2007**, *46*, 5187-5190.
[78] T. Shibata, H. Kurokawa, K. Kanda, *J. Org. Chem.* **2007**, *72*, 6521-6525.
[79] T. Shibata, K. Tsuchikama, M. Otsuka, *Tetrahedron: Asymmetry* **2006**, *17*, 614-619.
[80] T. Shibata, K. Tsuchikama, *Org. Biomol. Chem.* **2008**, *6*, 1317-1323.
[81] K. Tanaka, G. Nishida, A. Wada, K. Noguchi, *Angew. Chem., Int. Ed.* **2004**, *43*, 6510-6512.
[82] K. Tanaka, G. Nishida, M. Ogino, M. Hirano, K. Noguchi, *Org. Lett.* **2005**, *7*, 3119-3121.
[83] G. Nishida, N. Suzuki, K. Noguchi, K. Tanaka, *Org. Lett.* **2006**, *8*, 3489-3492.
[84] K. Tanaka, A. Wada, K. Noguchi, *Org. Lett.* **2005**, *7*, 4737-4739.
[85] T. Araki, K. Noguchi, K. Tanaka, *Angew. Chem., Int. Ed.* **2013**, *52*, 5617-5621.
[86] M. Amatore, D. Lebœuf, M. Malacria, V. Gandon, C. Aubert, *J. Am. Chem. Soc.* **2013**, *135*, 4576–4579.
[87] A. Gutnov, H.-J. Drexler, A. Spannenberg, G. Oehme, B. Heller, *Organometallics* **2004**, *23*, 1002-1009.
[88] A. Gutnov, B. Heller, C. Fischer, H.-J. Drexler, A. Spannenberg, B. Sundermann, C. Sundermann, *Angew. Chem., Int. Ed.* **2004**, *43*, 3795-3797.
[89] M. Hapke, K. Kral, C. Fischer, A. Spannenberg, A. Gutnov, D. Redkin, B. Heller, *J. Org. Chem.* **2010**, *75*, 3993-4003.
[90] F. Fischer, P. Jungk, N. Weding, A. Spannenberg, H. Ott, M. Hapke, *Eur. J. Org. Chem.* **2012**, 5828-5838.
[91] J. F. Hartwig, in *Organotransition Metal Chemistry*, University Science Books, Sausalito, **2010**.
[92] a) P. Diversi, A. Giusti, G. Ingrosso, A. Lucherini, *J. Organomet. Chem.* **1981**, *205*, 239-246; b) V. Harder, J. Müller, H. Werner, *Helv. Chim. Acta* **1971**, *54*, 1-6; c) R. J. McKinney, *Inorg. Chem.* **1982**, *21*, 2051-2056.

[93] a) C. P. Lenges, P. S. White, M. Brookhart, *J. Am. Chem. Soc.* **1998**, *120*, 6965-6979; b) C. P. Lenges, M. Brookhart, B. E. Grant, *J. Organomet. Chem.* **1997**, *528*, 199-203.
[94] C. P. Lenges, P. S. White, W. J. Marshall, M. Brookhart, *Organometallics* **2000**, *19*, 1247-1254.
[95] M. Hapke, A. Spannenberg, *Acta Cryst.* **2009**, *E65*.
[96] H. G. Schuster-Woldan, F. Basolo, *J. Am. Chem. Soc.* **1966**, *88*, 1657-1663.
[97] K. Huang, C.-L. Sun, Z.-J. Shi, *Chem. Soc. Rev.* **2011**, *40*, 2435-2452.
[98] a) J. L. Templeton, P. B. Winston, B. C. Ward, *J. Am. Chem. Soc.* **1981**, *103*, 7713-7721; b) W. D. Jones, F. J. Feher, *Acc. Chem. Res.* **1989**, *22*, 91-100.
[99] a) R. A. Kadyrov, I. K. Shakirov, R. P. Arshinova, S. G. Gnevashev, R. R. Shagidullin, B. A. Arbuzov, *Rus. Chem. Bull.* **1989**, *38*, 964-971; b) B. A. Arbuzov, A. V. Aganov, V. V. Klochkov, *Izv. Akad. Nauk SSSR, Ser. Khim.* **1982**, *5*, 1195; c) S. G. A. van Assema, A. W. Ehlers, F. J. J. de Kanter, M. Schakel, A. L. Spek, M. Lutz, K. Lammertsma, *Chem. Eur. J.* **2006**, *12*, 4333-4340; d) I. Morita, K. Kunimoto, M. Tsuda, S.-I. Tada, M. Kise, K. Kimura, *Chem. Pharm. Bull.* **1987**, *35*, 4144-4154; e) H. Ingenuin, P. C. William, F. C. Lanoue, *Vol.: US2834798*, (Ed.: C. SHEA CHEMICAL CORP), **1958**.
[100] R. L. Pruett, W. R. Myers, *Vol.: 3,159,659*, (Ed.: U. C. Corporation), **1964**.
[101] W. H. Hersh, F. J. Hollander, R. G. Bergman, *J. Am. Chem. Soc.* **1983**, *105*, 5834-5846.
[102] K. K. Baldridge, J. M. O'Connor, M.-C. Chen, J. S. Siegel, *J. Phys. Chem. A* **1999**, *103*, 10126-10131.
[103] B. Eaton, J. A. King, K. P. C. Vollhardt, *J. Am. Chem. Soc.* **1986**, *108*, 1359-1360.
[104] T. L. Cottrell, *The Strengths of Chemical Bonds*, 2nd ed., Butterworths Scientific Publications, London, **1958**.
[105] J. K. McDonald, J. A. Merritt, A. E. Stanley, *Vol.: 4,529,489*, (Ed.: T. U. S. o. A. a. r. b. t. S. o. t. Army), **1985**.
[106] R. Lal De, K. Maiti, *Indian J. Chem.* **2001**, *40A*, 1097-1100.
[107] Y. Taguchi, I. Shibuya, M. Yasumoto, T. Tsuchiya, K. Yonemoto, *Bull. Chem. Soc. Jpn.* **1990**, *63*, 3486-3489.
[108] Y. Yamamoto, K. Kinpara, R. Ogawa, H. Nishiyama, K. Itoh, *Chem. Eur. J.* **2006**, *12*, 5618-5631.
[109] K. A. M. Ampt, S. Burling, S. M. A. Donald, S. Douglas, S. B. Duckett, S. A. Macgregor, R. N. Perutz, M. K. Whittlesey, *J. Am. Chem. Soc.* **2006**, *128*, 7452-7453.
[110] J. C. Linehan, S. L. Wallen, C. R. Yonker, T. E. Bitterwolf, J. T. Bays, *J. Am. Chem. Soc.* **1997**, *119*, 10170-10177.
[111] B. D. Rossenaar, D. J. Stufkens, A. Oskam, J. Fraanje, K. Goubitz, *Inorg. Chim. Acta* **1996**, *247*, 215-229.
[112] a) K. M. Tait, J. A. Parkinson, S. P. Bates, W. J. Ebenezer, A. C. Jones, *J. Photochem. Photobio. A* **2003**, *154*, 179-188; b) N. Wazzan, The University of Edinburgh, PhD Thesis (Edinburgh), **2009**; c) D. Gibson, The University of Edinburgh, PhD Thesis (Edinburgh), **2007**.
[113] G. E. Ball, in *Spectroscopic Properties of Inorganic and Organometallic Compounds Vol. 41* (Eds.: J. Yarwood, R. Douthwaite, S. Duckett), The Royal Society of Chemistry, **2010**, pp. 262-287.
[114] G. Walther, A. Köckritz, A. Martin, D. Selent, *Vol.: DE102011007527 (A1)*, (Ed.: **2011**.
[115] a) R. H. Grubbs, C. Gibbons, L. C. Kroll, W. D. Bonds, C. H. Brubaker, *J. Am. Chem. Soc.* **1973**, *95*, 2373-2375; b) E. S. Chandrasekaran, R. H. Grubbs, C. H. Brubaker Jr., *J. Organomet. Chem.* **1976**, *120*, 49-63.

[116] a) B. H. Chang, R. H. Grubbs, C. H. Brubaker Jr., *J. Organomet. Chem.* **1979**, *172*, 81-89; b) K. G. Allum, R. D. Hancock, I. V. Howell, R. C. Pitkethly, P. J. Robinson, *J. Organomet. Chem.* **1975**, *87*, 189-201.
[117] a) A. Sekiya, J. K. Stille, *J. Am. Chem. Soc.* **1981**, *103*, 5096-5100; b) D. A. Annis, E. N. Jacobsen, *J. Am. Chem. Soc.* **1999**, *121*, 4147-4154.
[118] G. Gubitosa, M. Boldt, H. H. Brintzinger, *J. Am. Chem. Soc.* **1977**, *99*, 5174-5175.
[119] a) L. Li, S. Han, Q. Li, Z. Chen, Z. Pang, *Eur. J. Inorg. Chem.* **2007**, 5127-5137; b) W. S. Rees Jr, U. W. Lay, K. A. Dippel, *J. Organomet. Chem.* **1994**, *483*, 27-31; c) A. Trifonov, F. Ferri, J. Collin, *J. Organomet. Chem.* **1999**, *582*, 211-217; d) W. P. Hart, D. Shihua, M. D. Rausch, *J. Organomet. Chem.* **1985**, *282*, 111-121; e) P.-H. Yeh, Z. Pang, R. F. Johnston, *J. Organomet. Chem.* **1996**, *509*, 123-129; f) G. Rubner, K. Bensdorf, A. Wellner, S. Bergemann, I. Ott, R. Gust, *Eur. J. Med. Chem.* **2010**, *45*, 5157-5163.
[120] H. Schumann, M. Hasan, F. Gelman, D. Avnir, J. Blum, *Inorg. Chim. Acta* **1998**, *280*, 21-25.
[121] T. E. Bitterwolf, T. L. Hubler, A. L. Rheingold, *J. Organomet. Chem.* **1992**, *431*, 199-214.
[122] a) L.-C. Song, P.-C. Liu, Q.-M. Hu, G.-L. Lu, G.-F. Wang, *J. Organomet. Chem.* **2003**, *681*, 264-268; b) Y. Wakatsuki, H. Yamazaki, *Bull. Chem. Soc. Jpn.* **1985**, *58*, 2715-2716; c) X. Hou, Z. Pang, Z. Huang, R. Cai, X. Zhou, *Synth. React. Inorg. Met.-Org. Chem.* **1998**, *28*, 1505-1520; d) H. Komatsu, H. Yamazaki, *J. Organomet. Chem.* **2001**, *634*, 109-121; e) M. Costa, E. Dalcanale, F. S. Dias, C. Graiff, A. Tiripicchio, L. Bigliardi, *J. Organomet. Chem.* **2001**, *619*, 179-193.
[123] B. H. Lipshutz, P. A. Blomgren, *Org. Lett.* **2001**, *3*, 1869-1871.
[124] a) V. Polshettiwar, Á. Molnár, *Tetrahedron* **2007**, *63*, 6949-6976; b) V. Polshettiwar, C. Len, A. Fihri, *Coord. Chem. Rev.* **2009**, *253*, 2599-2626.
[125] a) S. C. Bourque, F. Maltais, W.-J. Xiao, O. Tardif, H. Alper, P. Arya, L. E. Manzer, *J. Am. Chem. Soc.* **1999**, *121*, 3035-3038; b) J. P. K. Reynhardt, Y. Yang, A. Sayari, H. Alper, *Chem. Mater.* **2004**, *16*, 4095-4102.
[126] J.-M. Collinson, J. D. E. T. Wilton-Ely, S. Diez-Gonzalez, *Chem. Commun.* **2013**, DOI: 10.1039/C1033CC44371J.
[127] a) B. Heller, M. Hapke, C. Fischer, A. Andronova, I. Starý, I. G. Stará, *J. Organomet. Chem.* **2013**, *723*, 98-102; b) B. Heller, A. Gutnov, C. Fischer, H.-J. Drexler, A. Spannenberg, D. Redkin, C. Sundermann, B. Sundermann, *Chem. Eur. J.* **2007**, *13*, 1117-1128.
[128] K. Kral, Universität Rostock, PhD Thesis (Rostock), **2012**.
[129] a) M. Mahlau, B. List, *Angew. Chem. Int. Ed.* **2013**, *52*, 518-533; b) E. P. Ávila, G. W. Amarante, *ChemCatChem* **2012**, *4*, 1713-1721; c) M. Mahlau, B. List, *Isr. J. Chem.* **2012**, *52*, 630-638; d) S. Mayer, B. List, *Angew. Chem. Int. Ed.* **2006**, *45*, 4193-4195; e) R. J. Phipps, G. L. Hamilton, F. D. Toste, *Nat. Chem.* **2012**, *4*, 603-614.
[130] J. Lacour, D. Moraleda, *Chem. Comm.* **2009**, 7073-7089.
[131] J. R. Zbieg, E. Yamaguchi, E. L. McInturff, M. J. Krische, *Science* **2012**, *336*, 324-327.
[132] S. Liao, B. List, *Angew. Chem. Int. Ed.* **2010**, *49*, 628-631.
[133] G. L. Hamilton, E. J. Kang, M. Mba, F. D. Toste, *Science* **2007**, *317*, 496-499.
[134] a) K. Kiyoshi, M. Tsutomu, O. Atsumu, *J. Mol. Catal.* **1979**, *5*, 175-187; b) H. Kanai, Y. Watabe, T. Nakayama, *Bull. Chem. Soc. Jpn.* **1986**, *59*, 1277-1278.
[135] a) K. Kawakami, T. Mizoroki, A. Ozaki, *Bull. Chem. Soc. Jpn.* **1978**, *51*, 21-24; b) K. Kawakami, T. Mizoroki, A. Ozaki, *Chem. Lett.* **1975**, *4*, 903-904.

[136] a) H. Kanai, K. Ishi, *Bull. Chem. Soc. Jpn.* **1981**, *54*, 1015-1018; b) H. Kanai, M. Okada, *Chem. Lett.* **1975**, *4*, 167-168.
[137] M. A. Cairns, J. F. Nixon, *J. Organomet. Chem.* **1974**, *64*, C19-C21.
[138] H.-Y. Rhyoo, B. Y. Lee, H. K. Bae Yu, Y. K. Chung, *J. Mol. Catal.* **1994**, *92*, 41-49.
[139] G. Hilt, W. Hess, T. Vogler, C. Hengst, *J. Organomet. Chem.* **2005**, *690*, 5170-5181.
[140] M. Barbazanges, M. Augé, J. Moussa, H. Amouri, C. Aubert, C. Desmarets, L. Fensterbank, V. Gandon, M. Malacria, C. Ollivier, *Chem. Eur. J.* **2011**, *17*, 13789-13794.
[141] a) J. Oppenheimer, W. L. Johnson, M. R. Tracey, R. P. Hsung, P.-Y. Yao, R. Liu, K. Zhao, *Org. Lett.* **2007**, *9*, 2361-2364; b) S. Shoai, P. Bichler, B. Kang, H. Buckley, J. A. Love, *Organometallics* **2007**, *26*, 5778-5781; c) A. Dachs, S. l. Osuna, A. Roglans, M. Solà, *Organometallics* **2010**, *29*, 562-569; d) L. Garcia, A. Pla-Quintana, A. Roglans, T. Parella, *Eur. J. Org. Chem.* **2010**, 3407-3415.
[142] a) A. Dachs, A. Torrent, A. Pla-Quintana, A. Roglans, A. Jutand, *Organometallics* **2009**, *28*, 6036-6043; b) R. Grigg, R. Scott, P. Stevenson, *J. Chem. Soc., Perkin Trans. 1* **1988**, 1357-1364.
[143] F. E. McDonald, H. Y. H. Zhu, C. R. Holmquist, *J. Am. Chem. Soc.* **1995**, *117*, 6605-6606.
[144] M. Auge, M. Barbazanges, A. T. Tran, A. Simonneau, P. Elley, H. Amouri, C. Aubert, L. Fensterbank, V. Gandon, M. Malacria, J. Moussa, C. Ollivier, *Chem. Commun.* **2013**, DOI:10.1039/C1033CC43188F.
[145] G. M. Sheldrick, *Acta Crystallogr.* **2008**, *A64*, 112-122.
[146] R. Beckert, E. Fanghänel, W. D. Habicher, P. Metz, D. Pavel, K. Schwetlick, *Organikum*, 22. ed., Wiley-VCH, Weinheim, **2004**.
[147] C. J. Cobley, P. G. Pringle, *Inorg. Chim. Acta* **1997**, *265*, 107-115.
[148] M. Oba, Y. Okada, K. Nishiyama, W. Ando, *Org. Lett.* **2009**, *11*, 1879-1881.
[149] a) M. Aresta, M. Rossi, A. Sacco, *Inorg. Chim. Acta* **1969**, *3*, 227-231; b) Y. Wakatsuki, H. Yamazaki, E. Lindner, A. Bosamle, *Inorg. Synth.* **2007**, *15*, 189-200.
[150] L. Thunberg, S. Allenmark, *Tetrahedron: Asymmetry* **2003**, *14*, 1317-1322.
[151] I. Thiel, H. Jiao, A. Spannenberg, M. Hapke, *Chem. Eur. J.* **2013**, *19*, 2548-2554.
[152] G. Dannhardt, S. Plutizki, C. Ganser, E. Lauermann, *Vol.: WO2012/84683 A1*, (Ed.: J. G.-U. Mainz), **2012**.
[153] A. M.-E. Lafuente, G. H. Llinas, *Vol.: US6114555 A*, (Ed.: R. Q. S.A.), **2000**.
[154] a) J. A. Adeleke, B. L. Booth, *J. Organomet. Chem.* **1988**, *339*, 223-230; b) J. Zhao, A. Sakthivel, A. M. Santos, F. E. Kühn, *Inorg. Chim. Acta* **2005**, *358*, 4201-4207.

Declaration

Ich versichere hiermit an Eides statt, dass ich die vorliegende Arbeit selbstständig angefertigt und ohne fremde Hilfe verfasst habe, keine außer den von mir angegebenen Hilfsmitteln und Quellen dazu verwendet habe und die den benutzten Werken inhaltlich und wörtlich entnommenen Stellen als solche kenntlich gemacht habe.

Diese Dissertation wurde bisher an keiner anderen Hochschule oder Universität vorgelegt.

Rostock, September 13th 2013

Indre Thiel